

Environmental electrochemistry of organic compounds at metal oxide electrodes

By

Mosidi Elizabeth Makgae

Dissertation presented for the degree of

Doctor of Philosophy

(Chemistry)

at the

University of Stellenbosch

Promoter: Prof. A.M. Crouch

Stellenbosch

December 2004

DECLARATION

I, the undersigned, hereby declare that the work contained in this dissertation is my own original work and has not previously in its entirety or in part been submitted to any university for a degree

Signed _____

Date: 25 November 2004

ABSTRACT

This study investigates the electrochemical oxidation of phenol. Phenol is a major toxin and water pollutant. In addition, during water treatment it reacts with chlorine to produce carcinogenic chlorophenols. Its treatment down to trace levels is therefore of increasing concern.

For this purpose, dynamically stable anodes for the breakdown of phenols to carbon dioxide or other less harmful substances were developed and characterized. The anodes were prepared from mixed oxides of tin (Sn) and the precious metals ruthenium (Ru), tantalum (Ta) and iridium (Ir), which in turn were prepared using sol-gel techniques. This involved dip-coating the aqueous salts of the respective metals onto titanium substrates and heating to temperatures of several hundreds of degree Celsius.

The properties of these mixed oxide thin films were investigated and characterized using thermal gravimetric analysis (TGA), scanning electron microscopy (SEM), atomic force microscopy (AFM), elemental dispersive energy X-ray analysis (EDX), X-ray diffraction (XRD), Rutherford backscattering spectrometry (RBS), particle induced X-ray emission (PIXE) and electrochemical measurements.

A variety of different electrode materials including Ti/ SnO₂-RuO₂-IrO₂, Ti/Ta₂O₅-IrO₂ and Ti/RhO_x-IrO₂ were developed and tested for their potential as oxidation catalysts for organic pollutants in wastewaters. Depending on the anode type, phenol was found to be

II

electrochemically degraded, to different extents, on these surfaces during electrolysis. It was however found that the oxidation rate not only depended on the chemical composition but also on the oxide morphology revealed, resulting from the preparation procedure. The Ti/SnO₂-RuO₂-IrO₂ film was found to be the most efficient surface for the electrolytic breakdown of phenol. This film oxidized phenol at a potential of 200 mV vs Ag/AgCl.

Abstract

The activity of the catalytic systems was evaluated both on the basis of phenol removal efficiency as well as the kinetics of these reactions. Phenol removal efficiency was more than 90% for all the film surfaces prepared and the rate of the reaction followed first order kinetics. A pathway for the electrochemical degradation of phenol was derived using techniques such as HPLC to identify the breakdown products. These pathway products included the formation of benzoquinone and the further oxidation of benzoquinone to the carboxylic acids malic, malonic and oxalic.

OPSOMMING

Die onderwerp van hierdie studie is die elektrochemiese oksidasie van fenol deur nuwe gemengde-oksied elektrodes. Fenol is 'n belangrike gifstof en besoedelingsmiddel in water. Daarbenewens kan fenol ook met chloor reageer tydens waterbehandeling om sodoende karsinogeniese chlorofenole te vorm. Dit is dus belangrik dat metodes ondersoek word wat die konsentrasie van fenol in water verminder.

Hierdie studie behels die bereiding en karakterisering van nuwe dinamiese stabiele anodes (DSA) vir die afbreek van fenol tot koolstofdioksied en ander minder gevaarlike verbindings. Hierdie nuwe anodes is berei vanaf die gemengde-okside van die edelmetale tin (Sn), ruthenium (Ru), tantalum (Ta) en iridium (Ir), met behulp van sol-gel tegnieke. Die finale stap in die bereiding behels kalsinering van die oksides by temperature van 'n paar honderd grade Celsius. Hierdie nuwe elektrodes is later gebruik om die oksidasie van fenol te evalueer.

Die gemengde-oksied dunlae/anodes is d.m.v. die volgende analitiesetegnieke gekarakteriseer: termiese-gravimetriese analise (TGA), skandeerelektronmikroskopie (SEM), atoomkragmikroskopie (AFM), elementverstrooiingsenergie-X-straalanalise (EDX), X-straaldiffraksie (XRD), Rutherford terug-verstrooiingspektroskopie (RBS), partikel-geïnduseerde X-straal emissie (PIXE), en elektrochemiese metings.

IV

'n Verskeidenheid elektrodes van verskillende materiale is berei en hul potensiaal as oksidasie-kataliste vir organiese besoedelingsmiddels in afloopwater bepaal. Hierdie elektrodes het die volgende ingesluit: $\text{Ti/SnO}_2\text{-RuO}_2\text{-IrO}_2$, $\text{Ti/Ta}_2\text{O}_5\text{-IrO}_2$ en $\text{Ti/RhO}_x\text{-IrO}_2$.

Gedurende elektrolise is fenol elektrochemies afgebreek tot verskillende vlakke, afhangende van die tipe elektrode. Die oksidasietempo het egter nie alleen van die chemiese samestelling van die elektrode afgehang nie, maar ook van die morfologie van die okside, wat op hulle beurt van die voorbereidingsprosedure afgehang het.

Daar is bevind dat die $\text{Ti/SnO}_2\text{-RuO}_2\text{-IrO}_2$ elektrode die mees effektiewe oppervlakke vir die afbreek van fenol is. Hier het die oksidasie van fenol by 'n potensiaal van 200 mV plaasgevind.

Die aktiwiteite van die katalitiese sisteme is bepaal op grond van hulle fenolverwyderingsdoeltreffendheid. Die kinetika van die reaksies is ook bepaal. Al die elektrodes het >90% fenolverwyderingsdoeltreffendheid getoon en die reaksietempos was van die eerste-orde.

Deur van analitiese tegnieke soos hoëdrukvlloeistofchromatografie (HPLC) gebruik te maak is die afbreekprodukte van fenol geïdentifiseer en 'n skema vir die elektrochemiese afbreek van fenol uitgewerk. Daar is bevind dat bensokinoon gevorm het, wat later oksidasie ondergaan het om karboksielsure te vorm.

ACKNOWLEDGEMENTS

I sincerely thank my advisor Prof A.M. Crouch for his support, inspiring enthusiasm and valuable guidance throughout the study.

I also thank the iThemba LABS staff for X-ray Diffraction (XRD), Rutherford Backscattering Spectrometry (RBS) and Particle Induced X-ray Emission (PIXE) analyses, for without their support I would not have been able to characterize the thin film electrode surfaces.

I thank Miranda Waldron from the University of Cape Town for helping me with the cross-sectional surface analysis of the thin film electrode surfaces.

I would also like to thank the Geology Department of the University of Stellenbosch for the use of their Scanning Electron Microscope (SEM). The Division of Polymer Science, Department of Chemistry, is thanked, particularly Dorothea Van Vuuren and Derek McAuley, for Thermal Gravimetric Analysis (TGA) and Atomic Force Microscope (AFM). I thank our technical staff, Johannes Stuurman and Moebarick Bickerstaff for their willingness to help whenever I needed them, and my colleagues for being there.

The financial support from National Research Foundation (NRF) and Eskom is gratefully acknowledged.

I am indebted to my mom and my daughter Tshiamo for their support and encouragement throughout the years.

To my late father: Rapula Alfred Makgae

TABLE OF CONTENTS

Abstract

Opsomming

Acknowledgements

Abbreviations and symbols

List of Figures

List of Tables

1.	Introduction	1
2.	Theoretical background	19
3.	Experimental	35
4.	Preparation, characterization and electrochemical evaluation of the Ti/ SnO₂-RuO₂-IrO₂ thin film as an electrode material for the oxidation of phenol	46
5.	Preparation, characterization and electrochemical evaluation of the binary oxide electrode Ti/Ta₂O₅-IrO₂ for the oxidation for phenol	62

VII

6.	Preparation, characterization and electrochemical evaluation of the Ti/RhO_x-IrO₂ electrode for the oxidation of phenol	78
7.	Further mechanistic study of the mixed metal oxide surfaces using rotating disk electrodes	91
8.	Degradation of phenol by bulk electrolysis in a batch system using metal oxides electrodes.	109
9.	Conclusions and recommendations for further studies.	129

ABBREVIATIONS AND SYMBOLS

A	Amperes
A	Electrode surface area
AFM	Atomic force microscopy
BAS	Bio-analytical system
C	Final concentration
C_0	Initial concentration
CV	Cyclic voltammetry
D_0	Diffusion coefficient
DSA	Dynamically stable anode
E	Potential
EDX	Elemental dispersive X-ray analyser
F	Faraday's constant
HPLC	High performance liquid chromatography
i	Current
I_{lim}	Limiting current
j_k	Kinetic current
K	Kelvin
kV	Kilovolts
mM	Millimolar
MeV	Millivolts
n	Number of moles

IX

nm	Nanometer
PIXE	Particle induced X-ray emission
PDA	Photo diode array
ppm	Parts per million
Q	Charge
RBS	Rutherford backscattering spectrometry
RDE	Rotating disk electrode
SEM	Scanning electron microscopy
SPM	Scanning probe microscopy
STM	Scanning tunnelling microscopy
TGA	Thermal gravimetric analysis
TOC	Total organic carbon
UV	Ultraviolet
XRD	X-ray diffraction
ω	Rotation speed
ν	Kinematic viscosity
μm	Micrometers
μl	Microliter
μC	Microcharge
λ	Wavelength

LIST OF FIGURES

- Figure 4.1 Thermograms of the respective hydrated SnCl_2 , RuCl_2 and IrCl_2 precursors and mixed metal chlorides (Sn/Ru/Ir) with high Ru content (40%).
- Figure 4.2 The microstructure of the $\text{Ti/SnO}_2\text{-RuO}_2\text{-IrO}_2$ electrode.
- Figure 4.3 XRD patterns of the $\text{Ti/SnO}_2\text{-RuO}_2\text{-IrO}_2$ electrode.
- Figure 4.4 RBS simulated spectrum of the $\text{Ti/SnO}_2\text{-RuO}_2\text{-IrO}_2$ electrode.
- Figure 4.5 Fitted PIXE spectrum of the $\text{Ti/SnO}_2\text{-RuO}_2\text{-IrO}_2$ electrode.
- Figure 4.6 Cyclic voltammograms of phenol oxidation at (a) platinum and (b) $\text{Ti/SnO}_2\text{-RuO}_2\text{-IrO}_2$ electrodes.
- Figure 5.1 Thermograms of the TaCl_5 , IrCl_3 precursors and Ta/Ir mixed precursors.
- Figure 5.2 The microstructure of the $\text{Ti/IrO}_2\text{-Ta}_2\text{O}_5$ electrode.
- Figure 5.3 XRD patterns of the $\text{Ti/IrO}_2\text{-Ta}_2\text{O}_5$ electrode.

XI

- Figure 5.4 RBS simulated spectrum of the Ti/IrO₂-Ta₂O₅ electrode.
- Figure 5.5 Fitted PIXE spectrum of the Ti/IrO₂-Ta₂O₅ electrode.
- Figure 5.6 Cyclic voltammograms of phenol at (a) Ti/IrO₂-Ta₂O₅ and (b) Pt electrodes.
- Figure 6.1 TGA curves of the hydrated RhCl₃ and IrCl₃ precursors respectively.
- Figure 6.2 TGA curves of Rh-Ir oxide precursors.
- Figure 6.3 The microstructure of a Ti/RhO_x-IrO₂ electrode.
- Figure 6.4 XRD patterns of a RhO_x-IrO₂ electrode.
- Figure 6.5 RBS simulated spectrum of a RhO_x-IrO₂ electrode.
- Figure 6.6 Cyclic voltammograms of phenol at a RhO_x-IrO₂ electrode.
- Figure 7.1 RDE voltammograms of phenol oxidation at Ti/SnO₂-RuO₂-IrO₂ electrode (a) under diffusion-controlled conditions (b) at a rotation speed of 1000 rpm.

XII

Figure 7.2 RDE voltammograms of phenol oxidation at Ti/Ta₂O₅-IrO₂ electrode (a) under diffusion-controlled conditions (b) at a rotation speed of 1000 rpm.

Figure 7.3 RDE voltammograms of phenol oxidation at Ti/RhO_x-IrO₂ electrode (a) under diffusion-controlled conditions (b) at a rotation speed of 1000 rpm.

Figure 7.4 Levich plot of a Ti/SnO₂-RuO₂-IrO₂ electrode.

Figure 7.5 Levich plot of a Ti/IrO₂-Ta₂O₅ electrode.

Figure 7.6 Levich plot of a RhO_x-IrO₂ electrode.

Figure 8.1 HPLC chromatogram showing phenol and its aromatic by-products.

Figure 8.2 The breakdown of phenol into by-products during electrolysis using the Sn/Ru/Ir system as determined by HPLC and PDA.

Figure 8.3 The breakdown of phenol into by-products during electrolysis using the Ta/Ir system as determined by HPLC and PDA.

Figure 8.4 The breakdown of phenol into by-products during electrolysis using the Rh/Ir system as determined by HPLC and PDA.

XIII

Figure 8.5 HPLC chromatogram showing carboxylic acids as by-products of phenol oxidation.

Figure 8.6 Cyclic voltammogram of oxalic acid at the Ti/SnO₂-RuO₂-IrO₂ electrode.

Figure 8.7 A plot of $\ln(C_0/C)$ as a function of time using different pH media for the Sn/Ru/Ir system, where C is the final and C₀ is the initial concentration.

Figure 8.8 A plot of $\ln(C_0/C)$ as a function of time using different pH media for the Ta/Ir system, where C is the final and C₀ is the initial concentration.

Figure 8.9 A plot of $\ln(C_0/C)$ as a function of time using different pH media for the Rh/Ir system, where C is the final and C₀ is the initial concentration.

LIST OF TABLES

- Table 3.1 The reagent compositions of the prepared metal oxides electrodes (% mol/mol)
- Table 3.2 Different metal oxides at their respective annealing temperatures and times
- Table 8.1 The % of removal/conversion and rate constants of the phenol oxidation process on the Ti/SnO₂-RuO₂-IrO₂, Ti/Ta₂O₅-IrO₂ and Ti/RhO_x-IrO₂ surfaces at various pHs.

1 General introduction

1.1 Environmental Electrochemistry

For decades, electrochemical technology has contributed successfully to environmental protection. Examples include the generation of energy using batteries and fuel cells [1], selective synthesis of organic chemicals [2], removal of impurities from process air, liquids and soil, recycling of process streams and development of sensors. Environmental electrochemistry is capable of making even greater contributions in future by the application and improvement of existing technologies, and the research, development and implementation of new technologies [3].

The applications of electrochemistry for the protection of the environment have already been the topic of many books and reviews [4-6]. Environmental electrochemistry involves electrochemical techniques or methods that can be used to remove impurities from gases, liquids and soil in order to prevent or to minimise environmental pollution. It is particularly emissions to the atmosphere, discharges of pollutants into waters and the disposal of solids to land sites that have to be minimised. The best way to tackle pollution problems is at their source, namely, the main processes in the chemical and related industries.

1.2 What is electrochemistry?

Electrochemistry is a link between physical chemistry and electronic science. It has proved to be a clean, versatile and powerful tool for the development of new advanced methods for water purification [7-10]. Electrochemistry, as a branch of physical chemistry, plays an important role in most areas of science and technology. Furthermore, it is increasingly acknowledged as a significant means of handling environmental and energy problems facing mankind today, and in the near future [11].

A key feature of dynamic electrochemistry is that the current response is governed by the flux of reactants at the electrode/solution interface, which is a direct measure of the interfacial reaction rate. There are innumerable voltammetric techniques in which mass transport is controllable and calculable. Simple methods such as linear sweep and cyclic voltammetry in quiescent solution result in well-defined diffusion fields adjacent to the working electrode [12].

1.3 The development of electrochemistry

Electrochemistry, now a mature and distinguished science, has undergone tremendous transformations during the last three decades. The transformation of electrochemistry into a modern and interdisciplinary science integrates the measurements of current, or potential, with modern spectroscopic, diffraction and imaging techniques. Electrochemical science is now able to provide molecular-level descriptions of charge or potential-driven phenomena.

A few developments have revolutionized electrochemistry: (1) sample miniaturization, (2) availability of modern spectroscopic techniques, (3) development of scanning probe microscopies (SPM), such as scanning tunnelling microscopy (STM) and atomic force microscopy (AFM) and (4) progress in scientific instrumentation that allows nanosecond time gating and the measurement of current in the pico ampere range.

Electrode reactions are heterogeneous processes and their rates and mechanisms depend on the structure and composition of the electrode-solution interface [12]. The interfacial phenomena at the electrified solid-solution interface are the objectives of study in surface electrochemistry. Electrochemistry provides surface science with a 'joystick' that can be used to force ions and molecules to adsorb or desorb, to form ordered or disordered layers, change their surface orientation, spread them into a uniform film or group them together into surface aggregates.

Surface electrochemistry makes significant inroads into other disciplines such as material science, surface science, etc. The methodological progress has spawned new disciplines such as electrochemical nano-technology. One interesting development in electrochemical nano-technology is the demonstration that nano-wires may be used as electrochemical sensors [13].

There are many other important areas of electrochemistry that are in the process of methodological and scientific changes. They include dramatic progress in batteries and fuel cell research, solar energy conversion, development of sensors, biosensors and molecular recognition devices [13].

Environmental and ecological demands have given birth to the relatively new branch of environmental electrochemistry with the promise of rapid growth in pollution control. Typical subject areas are the electrochemical oxidation of organic compounds in water, pollutant sensors, photo electrochemical/semiconductor techniques, magnetic field effects, etc.

On the map of science, electrochemistry is located at the crossroad of many disciplines. The knowledge gained from electrochemical studies is relevant to other fields such as analytical chemistry, energy storage and conversion, biology and medicine, material science and microelectronics [13].

1.4 Why the use of mixed metal oxides as thin films?

Metal oxides constitute a diverse and fascinating class of materials whose properties range from those of metals to semi-conductors and insulators. Binary oxides contain a metal and oxygen, as in TiO_2 or Fe_2O_3 . The range of such compounds is quite large, but is extended even further by considering ternary and yet more complex compounds, where additional metallic elements are present [14-16].

During the 1960s investigators in the field of electrochemistry began to turn their attention from Pt coated anodes to the oxides of Pt group metals [10]. One of the unique properties of many of the oxides of these metals is their ability to show near metallic conductivities. As research progressed, it was found that mixtures of these metal oxides showed even more unique properties with regard to electrochemical requirements, such as potential and low consumption rate. The term mixed metal oxide became a by-word when referring to this technology [17].

Transition metal oxides, owing to their ability to switch between different valence states, possess appreciable catalytic and electrocatalytic activity, which make them versatile materials for chemical and electrochemical reactions [17]. For the same reasons, these oxides exhibit remarkable stability toward chemical and electrochemical attack under appropriate conditions [17]. The term ‘insoluble oxide electrodes’ is often used when referring to these properties. But the term most well known for describing activated oxide electrodes is DSA (dimensionally stable anodes), related to the origins of the introduction into the electrochemical field [17].

Physically, the mixed metal oxides referred to above have little strength or structural integrity of their own. In order for them to be useful, they must reside on a suitable metal substrate [18]. Earlier technology had shown “film forming metals” such as titanium to be an ideal candidate as a base for the mixed metal oxides [4].

A thin, tightly adherent oxide film naturally protects pure titanium, which is acid tolerant and resistant to the passage of current in the anode direction. Expressing this differently, in order for titanium to behave as an anode, considerable applied voltage is required on its surface in order for it to pass a significant amount of current. This property has earned titanium the title as one of the “electrochemical valve metals” [10].

Some of the oxides of ruthenium, iridium, tantalum, etc. have the ability to form a solid solution with the oxide film on titanium and render it conductive [10, 19-20]. Composite anodes which consist of an inert conductive oxide coating on a “valve metal” titanium base can be formed. The electrochemical characteristics of such an anode rest within the mixed metal oxide coating and the anode strength resides within the titanium substrate.

An advantage of using titanium as a coating base for the mixed metal oxides is its “self healing” property. If there is a defect in the conductive coating, then the valve metal immediately forms its protective oxide over the exposed area. Current from the anode continues to come from the surface covered by the mixed metal coating.

The mixed oxides are formed by spraying, brushing or dip coating aqueous salts of the metals on the titanium substrate and then heating the titanium to temperatures of several hundreds of degrees Celsius [4]. The metal oxide electrodes are sometimes referred to as dynamically stable anodes (DSA).

1.5 Some advantages of electrochemical processes

These include:

- Versatility – direct or indirect oxidation and reduction, phase separation, concentration or dilution, biocide functionality, applicability to a variety of media and pollutants in gases, liquids and solids, and treatment of small to large volumes from micro litres up to millions of litres.
- Energy efficiency – electrochemical processes generally have lower temperature requirements than their equivalent non-electrochemical counterparts, for example, thermal incineration. Electrodes and cells can be designed to minimise power losses caused by inhomogeneous current distribution, voltage drop and side reactions.
- Amenability to automation – the system inherent variables of electrochemical processes, for example, electrode potential and cell current, are particularly suitable for facilitating process automation.
- Cost effectiveness – cell constructions and peripheral equipment is generally simple and, if properly designed, also inexpensive.

Despite these advantages, electrochemical processes are of a heterogeneous nature, which means that the reactions take place at the interface of an electrode and the electrolyte. This implies that the performance of the electrochemical processes may suffer from limitations of mass transfer and the size of the specific electrode area. Another crucial

point is the chemical stability of the cell components in contact with an aggressive medium and in particular the long term stability and activity of the electrode material.

1.6 Motivation for the research

The growth of numerous industries has resulted in an increase in the volume of industrial wastewater discharged and in the kinds of chemical substances entering water supplies. Many industrial wastewater streams, for example those from petrochemical refineries, and pulp and paper mills, contain toxic organic compounds such as phenols and quinones, and their treatment down to trace levels of pollutants is of increasing concern [21].

There are several methods for treating wastewater containing organic pollutants, including incineration, adsorption, biological treatment and chemical and electrochemical oxidation [7]. The choice of treatment depends on the economics as well as ease of process control, reliability and treatment efficiency [22].

Biological methods, widely applied to many types of wastewaters, are generally impractical or do not provide the necessary quality of treatment for wastes containing bio-resistant substances. Therefore, in recent years, combined treatment methods have been increasingly used; particularly physio-chemical treatment with subsequent biological treatment, and physio-chemical processes employed as tertiary treatment after biological treatment.

Physio-chemical treatment processes with chemical addition often involves the use of high chemical doses and causes the secondary pollution of liquids, that is, an increase in salt concentration. In recent years, wastewater treatment without the addition of chemicals has become popular [9, 21-22]. Therefore, the development and the implementation of electrochemical methods is an advanced trend in the technology of wastewater treatment [23]. Electrochemical methods usually do not lead to an increase in the salt content of treated effluent and, in many cases, eliminate sludge formation or substantially reduce the volume of sludge.

The use of high oxygen overvoltage anodes for the direct oxidation of refractory organic chemicals, and for the generation of strong oxidants such as ozone, is of great potential value in wastewater treatment. However, an adverse effect of utilizing an electrochemical oxidation approach is the low ionic conductivity of many types of wastewaters. The electrochemical method for wastewater treatment has attracted a great deal of attention recently [8, 9, 22, 24], mainly because of the ease of control and increased efficiencies provided by the use of compact bipolar electrochemical reactors and by the large surface area of three-dimensional electrodes.

In this study an electrochemical oxidation or combustion of phenol, which is often used as a standard contaminant of hazardous organic compounds in water, is investigated. Phenol is listed as a priority pollutant by most of the environmental protection agencies and is considered to be one of the major water pollutants that need to be recovered, removed or destroyed [25]. It reacts with chlorine during water treatment and produces

chlorophenols, which are carcinogenic. Even at low concentrations, phenol causes the taste and odour of fish, and it has deleterious effects on bacteria, algae, mammals and human beings [26-27].

1.7 Objectives

The main objective of this study is to develop and characterize dynamically stable anodes that could be applied to break down phenol to carbon dioxide or to other less harmful substances/compounds. The metal oxide surfaces will be prepared by using sol-gel technique. The techniques that will be used for characterization are:

- Scanning electron microscope (SEM)
- Atomic force microscopy (AFM)
- Energy dispersive X-ray analysis (EDX)
- X-ray diffraction (XRD)
- Rutherford backscattering spectrometry (RBS)
- Particle induced X ray emission (PIXE) and
- Electrochemical measurements

Although this process was demonstrated before [7, 11, 25, 27-28], there is still considerable controversy about the reaction mechanism of this anodic oxidation process [26]. Furthermore, the development of non-toxic anode materials, as well as anodes exhibiting good efficiencies for the oxidation of organic compounds down to low concentration, is needed. Currently, promising materials are doped tin oxide and doped

lead oxide as thin films on titanium, which seem to allow the complete oxidation of many organics [7, 23]. They are however prone to fouling due to the presence of the intermediate degradation products formed. Stability of these electrodes over a long period has also not been proven conclusively.

1.8 Project outline

The project is outlined in such a way that it gives an introduction on environmental electrochemistry, the definition of electrochemistry, its development today and the potential applications thereof. The use of mixed metal oxides as thin films electrodes is explained. To achieve the objectives of this study, there were several tasks that had to be undertaken.

Firstly, the preparation of mixed metal oxide thin film electrodes by sol-gel technique is outlined. Secondly, the techniques used to characterize these thin film electrodes were also outlined. These include:

- SEM, AFM and EDX for the morphology and physical properties of the thin films.
- RBS and PIXE to determine the surface properties.
- TGA, XRD, CV, RDE and bulk electrolysis were used to determine the bulk properties.

The layout of the thesis comprises of:

- Chapter 1** which gives the general introduction to the study.

- Chapter 2** which deals with the theoretical background of the techniques used in this project.
- Chapter 3** that deals with the technical aspects of the experimental methods.
- Chapter 4** which gives the preparation, characterization and electrochemical evaluation of the Ti/SnO₂-RuO₂-IrO₂ thin films as electrode materials for the oxidation of phenol.
- Chapter 5** which deals with the preparation, characterization and electrochemical evaluation of the binary electrode Ti/Ta₂O₅-IrO₂ for the oxidation of phenol.
- Chapter 6** which deals with the preparation, characterization and electrochemical evaluation of the Ti/RhO_x-IrO₂ electrode for the oxidation of phenol.
- Chapter 7** that gives a further mechanistic study of these mixed metal oxides surfaces using rotating disk electrodes.
- Chapter 8** that deals with the degradation of phenol by bulk electrolysis in a batch system using mixed metal oxide electrodes.
- Chapter 9** which deals with the conclusions and recommendations for further study.

REFERENCES

1. Janssen, M.M.P., Moolhuysen, J. *Electrochimica Acta*. **1976**, 21, 1861.
2. Teterycz, H., Klimkiewicz, R., Licznarski, B.W. *Applied Catalysis A: General*. **2001**, 214 (2) 243.
3. Janssen, L.J.J., Koene, L. *Chemical Engineering Journal*. **2002**, 85, 137.
4. Trasatti, S. *Journal of Applied Electrochemistry*. **1991**, 21, 335.
5. Pletcher, D., Walsh F. C. *Industrial Electrochemistry*; 2nd Edition, Chapman and Hall: London, 1990.
6. Brett, M.A., Brett, M.O. *Electrochemistry: Principles, Methods and Applications*; Oxford Science Publications, New York, 1993.
7. Grimm, J., Bessarabov, D., Sanderson, R. *Desalination*. **1998**, 115, 285.
8. Murphy, O.J., Hutchins, G.D., Kaba, L., Verostko, C.E. *Water Research*. **1992**, 26 (4) 443.
9. Sharifian, H., Kirk, D. W. *Journal of Electrochem. Society*. **1986**, 133 (5) 921.
10. Comninellis, C., Vercesi, G.P. *Journal of Applied Electrochemistry*. **1991**, 21, 335.
11. Trasatti, S. *Electrochimica Acta*. **2000**, 45, 2377.
12. Unwin, P.R. *Journal of Chem. Society, Faraday Trans*. **1998**, 94, 3183.

13. Lipkowi, J. *Canadian Chemical News: Challenges and Opportunities of Modern Electrochemistry*, (2000), 12.
14. Cox, P. A. *Transition metal oxides*, Clarendon Press, Oxford, 1995.
15. Goodenough, J.B. *Prog. Solid State Chemistry*, **1971**, 5, 145.
16. Greenwood, N.N., Earushaw, A. *Chemistry of elements*, Pergamon, Oxford, 1984.
17. Trasatti, S. *Electrodes of Conductive Metallic Oxides: Part B*, Elsevier Scientific Publishing, New York, 1981.
18. Piccirillo, C., Daolio, S., Kristof, J., Mihaly, J., Facchin, B., Fabrixio, M. *International Journal of Mass Spec. and Ion Processes*. **1997**, 161, 141.
19. Lasalli, T.A.F., Boodts, J.F.C., Bulhoes, L.O.S. *Electrochimica Acta*. **1999**, 44, 4203.
20. Takasu, Y., Murakami, Y. *Electrochimica Acta*. **2000**, 45 (25-26) 4135.
21. Cenkin, V. E., Belevtsev, A. *Effluent and Water Treatment Journal*. **1985**, 243-247.
22. Grimm, J., Bessarabov, D., Maier, W., Storck, S., Sanderson, R.D. *Desalination*. **1998**, 115, 295.
23. Correa-Lozano, B., Comninellis, C., De Bastisti A. *Journal of Electrochem. Society*. **1996**, 143 (1) 203.
24. Comnellis, C., Nerini, A. *Journal of Applied Electrochemistry*. **1995**, 25, 23.

25. Awad, Y.M., Abuzaid, N.S. *Separation Science and Technology*. **1999**, 34 (4) 699.
26. Bock, C., MacDougall, B. *Journal of Electroanalytical Chemistry*. **2000**, 491, 48.
27. Azzam, M.O., Al-Tarazi, M., Tahboub, Y. *Journal of Hazardous Materials B*. **2000**, 75, 99.
28. Comninellis, C. *Electrochimica Acta*. **1994**, 39 (11-12), 1857
29. . Trasatti, S. *Electrodes of Conductive Metallic Oxides: Part A*, Elsevier Scientific Publishing, New York, 1980.
30. Paseka, I. *Applied Catalysis A: General*. **2001**, 207, 257.
31. Livage, J. *Sol-Gel Processes, Current opinion in Solid State and Material Science*. 2 (1997) 132.
32. Chaleton, J.P., Terrier, C., Bernstein, E., Berjoan, R., Roger J.A. *Thin Solid Films*. **1994**, 247 (1), 162.
33. Brinker, C.J., Hurd, A.J., Schunk P.R., Frye G.C., Ashley, C.S. *Journal of Non-Crystalline Solids*. **1992**, 147-148, 424.
34. Brinker, C.J., Scherer, G.W. *Sol-gel Science: The Physics and Chemistry of Sol-gel Processing*, Academic Press, California, USA, 1990.
35. Smyth, D.M. *Solid State Ionics*. **2000**, 129, 5.
36. Juttner, K., Galla, U., Schmieder, H. *Electrochimica Acta*. **2000**, 45, 2575.

37. Seung-Hee Nam, Ho-Gi Kim, *Journal of Applied Physics*. **1992**, 72 (7), 2895.
38. Fröhlich, K.; Machajdik, D.; Rosova, A.; Vavra, I.; Weis, F.; Bochu, B.; Senateur, J. P. *Thin Solid Films*. **1995**, 260, 187.
39. Hiratani, M.; Tarutani, Y.; Fukazawa, T.; Okamoto, M., Takagi, K. *Thin Solid Films*. **1993**, 227, 100.
40. Trasatti, S. *Electrochimica Acta*. **1991**, 36 (2), 225.
41. Trasatti, S. *International Journal of Hydrogen Energy*. **1995**, 20 (10), 835.
42. Correa-Lozano, B., Comninellis, C. *Journal of Applied Electrochemistry*. **1996**, 26, 683.
43. Roginskaya, Y.E., Morozova, O.V. *Electrochimica Acta*. **1995**, 40 (7), 817.
44. Mallick, K. K; Hartridge, A., Woodhead, J. L., Bhattachanga, A. K. *Journal of Material. Science*. **1996**, 31, 267.
45. Beudale, P., Venigalla, S.; Ambrose, J. R., Verink, E. D. Jr., Adair, J. H. *Journal of Am. Ceram. Society*. **1993**, 76 (10), 2619.
46. Greef, R., Peat, R.M., Peter, L.M., Pletcher, D., Robinson, J. *Instrumental methods in Electrochemistry*, Ellis Horwood, Chichester, 1985.
47. Tamura, H., Mita, K., Tanaka, A., Ito, M. *Journal of Colloid and Interface Science*. **2001**, 243, 202.

48. Zemski, K.A., Justes, D.R., Castleman Jr. A.W. *Journal of Physical Chemistry B*. **2002**, 106, 6136.
49. Livage, J. *Encyclopedia of Inorganic Chemistry*; King; R. B., Ed.; John Wiley and Sons, Chichester, 1994, p 3836.
50. Kamalasanan, M. N., Kumar, N. D., Chandra, S. *Journal of Applied Physics*. **1993**, 74 (1), 679.

2

Background

2.1 Background information

The laboratory for electrochemistry at Stellenbosch University has been investigating the preparation and characterization of mixed metal oxides for some time. Earlier work concentrated on the preparation of mixed metal titanates [1, 2]. Lately, the laboratory is concentrating on the preparation of mixed metal stannates for oxidative degradation of organic compounds. This involved the preparation of Sb SnO₂ [3] and Sn ZrO₂, Mn SnO₂ and Pd SnO₂ [4]. Whilst the previous work demonstrated limited degradation of phenol it compared well with the PbO₂ and PtO₂ electrodes currently used.

For this project, precious metal oxides were considered for electrochemical evaluation. Whilst the IrO₂ and RuO₂ electrodes are well known for oxygen evolution reactions, the combination of the mixed metal oxides that were studied and their oxidative application on organic compounds at these surfaces have not been investigated. The studied electrode surfaces were Ti/SnO₂-RuO₂-IrO₂, Ti/Ta₂O₅-IrO₂ and Ti/RhOx-IrO₂.

Generally, the oxidation of phenolic compounds produces unstable phenoxy radicals that can be further oxidized to quinones or can react to form dimers, which readily polymerize into polyaromatic compounds [5, 6]. The phenoxy radicals can interact with each other or with other phenol monomers to give rise to a strongly adherent insulating film that passivates the surface of the working electrode [7].

The latter property has been used for the protective coating of metals in order to solve the problems of corrosion. At the same time intensive studies have been performed in order to protect the electrode surface against passivation or even to remove this adherent polymer film [8, 9]. These processes are important for the treatment of phenolic effluents and have a direct impact on environmental protection.

Numerous treatment techniques have been developed to overcome the problem of surface fouling, particularly in wastewater [5-7]. These include biological, chemical or electrochemical treatment, none of which have completely solved the problems related to this unwanted phenomenon. The electrochemical treatment of the electrode surface has been shown to reduce fouling. For instance, the use of higher applied potentials combined with a lower initial concentration of phenol in acid medium was shown to reduce electrode fouling and increase the amount of oxidized phenol [8].

As a consequence of surface fouling, the activity of noble metal electrodes is shown to be short lived. Platinum is one of the most widely used electrodes in electrochemical applications. It is generally recognized that the oxidation of phenol and other phenolic compounds always produce a very rapid decrease in the oxidation peak during cyclic voltammetry after only the first scan. This step is believed to generate a rapid passivation of the Pt electrode [10].

However, the electrochemistry of phenol is complex and versatile. Depending on electrode pretreatment and experimental conditions, the reaction mechanisms involve electro-oxidation, polymerization or combustion of phenol.

Electrochemical oxidation of organic compounds to CO₂ can be an effective method of wastewater treatment for industrial effluents. Electrodes used for such applications should ideally exhibit high current efficiency towards organic oxidative incineration in order to be economically attractive for this purpose. They must also withstand the concomitantly harsh electrochemical environment.

2.2 Preparation of mixed metal oxides electrodes

There are a variety of methods available for coating the catalyst supports to obtain dynamically stable anodes or electrodes. These include methods of film preparation such as chemical vapour deposition, reactive sputtering, spray pyrolysis and sol-gel dip-coating [11].

One of the pre-requisites of electro catalysis is a large working surface area [12, 13]. The so-called sol-gel technique was therefore the method of choice that was used in this investigation to prepare oxides for electro catalysis using Ti as a substrate [14]. The dip-coating method has further proved to be well suited for the preparation of defect-free films [14]. This method has major advantages, which include: starting materials of high purity, ease of coating of large and complex shaped substrates and low cost [15, 16].

The surface of the substrate was pre-treated prior to coating for the fabrication of the anodes. Metal oxides can be prepared in various ways, but the most widely used procedure is by the thermal decomposition of appropriate precursors dissolved in suitable solvents and spreading on a Ti support. The nature of the precursor and the temperature of calcination appear to be the primary factors influencing the properties of the resulting oxides [14].

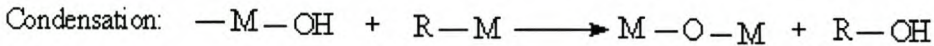
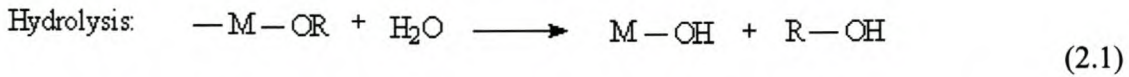
The sol-gel process

Sol-gel chemistry is a versatile tool for the preparation and understanding of catalytic materials. The large variety of synthetic parameters provides control over the structural and chemical properties of catalysts. Sol-gel synthesis offers better control over pore volume, surface area, porosity, and pore size distribution [14]. The process can also facilitate multi-element systems in a single step. It provides a new approach to the preparation of catalysts, membranes, thin layers (catalytic films), etc.

Starting from molecular precursors, an oxide network is obtained by the hydrolysis-polycondensation of alkoxides. The solution chemistry of the alkoxides is investigated; the precursors are commercially available and used in most studies [16]. Sol-gel synthesis involves the formation of a sol, followed by the formation of a gel. A gel is a diphasic material with a solid encapsulating a liquid. These polymerised alkoxides are dried to remove the encapsulated liquid, leaving a porous network [11]. The external surface of the sol-gel catalyst is relatively small compared to the internal surface. Thus, sufficient

diffusion of molecules through the pores of active catalyst centres is crucial and requires a proper design of the pore structure [17].

Sol gel chemistry is based on the hydrolysis of a precursor and the condensation of partially hydrolysed species to form a three-dimensional network. These two reactions can be presented as:



Although reaction 2.1 is a reduced presentation, the complexity thereof makes its simplification necessary. The basic premise is that the sol-gel product depends on the relative rates of hydrolysis and condensation. Controlling these rates can change the characteristics of the product for specific applications. Factors that can also be varied include the acid and water content, the type of solvent precursor, the concentration and temperature.

Dopants are added to a variety of metal oxides in order to modify their properties. In some cases the aim is to create or enhance desirable properties, while in others it is to eliminate or reduce undesirable effects [18]. It is important to recognize that many oxides have useful properties only because of their naturally occurring impurity contents. It will be assumed that oxygen is the only volatile species in the systems under consideration, and that thermodynamic equilibrium involves only equilibration with the ambient oxygen activity. Thus, the cationic concentrations are fixed once the solid solution has been

established, and this may result in super saturation of the dopant concentration at lower temperatures. The effect of dopants on the elemental semiconductors is simple and well understood.

For example, when phosphorus, with its five valence electrons, is substituted for silicon, which has only four, the phosphorus replicates the bonding of the silicon and then has one electron left. This 'extra' electron is only weakly bound to the impurity centre and is thus able to contribute to conduction at normal ambient temperatures. The doping of compounds is somewhat more complex [18].

There are several formal routes that can be taken from the starting point of a host oxide and a dopant oxide to reach the final solid solution and its modified properties. One particularly useful route is to consider the solution of one stoichiometric binary oxide into the lattice of another stoichiometric binary oxide, without loss or gain of oxygen. The resulting single-phase solid solution can be described as a stoichiometric solid solution.

Dopant cations are classified as acceptor centres if their charge is less than that of the cation they replace, and donor centres if they have a greater charge. These labels recognize the fact that the lattice defect that constitutes an acceptor centre can be replaced by holes under oxidizing conditions. The electrons under reducing conditions can replace the lattice defect that compensates for the excess positive charge of a donor centre.

The doping process is governed by factors such as ionic radii and the charge on the defect formed by a given compound. These are the same factors that determine the type of intrinsic ionic disorder favoured by a given compound, and it is reasonable that the charge defect be the same as one of the preferred intrinsic defects [18].

2.3 Characterization techniques

The electro catalytic properties of the metal oxides are mainly related to electronic and geometric factors (intrinsic ionic disorders and preferred intrinsic defects). The electronic factor is related to the chemical composition of the oxide layer and the physical and chemical properties of the constituent oxides (e.g., electronic structure and crystallinity). The geometric factor is directly linked to the morphology of the film. Characterization of the surface properties of electrodes covered with conductive metallic oxide films is therefore of fundamental importance for understanding their electrochemical behaviour.

Characterization techniques have been grouped on the basis of:

- Morphology and physical characteristics
- Surface characteristics
- Bulk characteristics.

2.3.1 *Morphology and physical properties*

Most heterogeneous catalysts are porous solids [19]. The porosity arises from the preparation methods. The porous structure enables the solid to have a total surface area much greater than the external surface area. Knowledge of the morphological parameters is very important to understand the catalyst evolution during the preparation procedure and to give a feedback that will be useful for modifying the method and obtaining the desired results.

(a) Scanning Electron Microscopy (SEM)

Scanning electron microscopy can be used to study the surface morphology of thin films. Essentially, SEM techniques enable both the secondary electron image as well as the elemental image of the region under analysis to be obtained. In many ways SEM techniques are merging with useful spatial resolution using emission electron sources of 50 nm. Such a small and well-defined area of analysis also lends itself to composition depth profiling. This is a particular strength of SEM that is applied to the characterization of a vast range of thin films, multilayer stacks and surface coatings. Electron microscopy is used to study the morphology of catalysts in order to obtain data on the shape, size, homogeneity, presence of amorphous and crystalline regions and their relative distribution, the relative surfaces of different crystalline phases and phase separation.

(b) Atomic Force Microscopy (AFM)

The atomic force microscope (AFM) is being used to solve processing and materials problems in a wide range of technologies, affecting the electronics, telecommunications, biological, chemical, automotive, aerospace, and energy industries. The materials that can be investigated by AFM include thin and thick film coatings, ceramics, composites, glasses, synthetic and biological membranes, metals, polymers, and semiconductors. AFM is used for the study of phenomena such as: abrasion, adhesion, cleaning, corrosion, etching, friction, lubrication, plating, and polishing by using the AFM, it is possible not only to replicate the material surface on the atomic resolution level but also measure forces on the nano-newton scale. Since the advent of AFM, very recent though, the number of publications emanating from the use of this technique has grown at a tremendous rate.

The primary purpose of this instrument is to quantitatively measure surface roughness with a nominal 5 nm lateral and 0.01 nm vertical resolution on all types of samples. Depending on the AFM design, scanners are used to translate either the sample under the cantilever or the cantilever over the sample. By scanning in either way, the local height of the sample is measured. Three dimensional topographical maps of the surface are then constructed by plotting the local sample height versus horizontal probe tip position.

2.3.2 *Surface properties*

The importance of the total surface area measurement has been pointed out [19, 20, and 21]. In acid catalysts, the acid sites not only occupy a small fraction of the surface, but also differ in acid strength and sometimes in nature. To understand how a catalyst works, why a sample gives better performance than others or why activity decays by time, knowledge of the number and the nature of active sites is indispensable.

(a) Rutherford Backscattering Spectroscopy (RBS)

RBS is used to determine the cation stoichiometry and thickness of surfaces. In RBS, a MeV beam of light ions is used as a primary ion source. Measurement of the scattered particles leads to a fully quantitative composition and depth analysis, without the need for reference standards. RBS is a mature technique and easily the most quantitative. It can be used to determine the amount and the distribution of elements in thin layers on substrates. It is also possible to determine the amount and depth of a layer of foreign atoms if the identity of that layer is known, in which case the depth and concentration can be determined.

(b) Particle Induced X-ray Emission (PIXE)

PIXE is an analytical method, which relies on the spectroscopy of characteristic X-rays emitted by the target elements due to the irradiation of a high-energy ion beam (typically 1-2 MeV of H or He). PIXE can identify various constituents in a compound. Since there is little overlapping of the characteristic X-rays for different elements, simultaneous detection of complicated multi element samples is possible. Quantitative analysis is also

possible with the appropriate corrections to absorption and X-ray yields. Trace element analysis using PIXE has a detection limit of the order of magnitude lower than can be attained by X-ray spectrometry techniques using electron excitation. Under favourable conditions, a detection limit of 1 ppm for thin foils and 10 ppm for thick foils can be achieved.

2.3.3 *Bulk properties*

Although the main focus in catalysts characterization is on the surface properties, bulk properties are also important because they determine the nature of surface sites.

(a) Thermal Gravimetric Analysis (TGA)

Thermogravimetry is the measurement of the mass of a sample as the temperature increases. Thermogravimetric analysis provides the change in weight of a sample as a function of temperature. It is a precise quantitative method for determining combustibles, loss of volatiles, curing times, decomposition of hydrates and carbonates, and weight loss changes. Rates of weight loss or gain are easily determined from the thermal gravimetric curves. TGA measures the change in mass of a sample as it is heated, cooled, or held at a constant temperature. The instrument is basically a precisely controlled furnace, combined with a microbalance. TGA's are routinely used to study the quantitative separation of components in a mixture and the decomposition of a material in a given environment.

(b) X-Ray Diffraction (XRD)

XRD is used to determine the phase composition of coatings. X-rays are electromagnetic radiations that have much shorter wavelength, and thus much higher energy, than visible light. In powder diffraction, an incident beam of X-rays interacts with a specimen that is in the form of either a small non-diffracting filament containing bonded powder or polycrystalline fiber of very small grain size. Thus, X-ray diffraction is a technique that can be used for the identification of a crystalline sample, crystal structure and size, crystal lattice parameters or dimensions and crystal orientation determination and refinement, and analysis of a polycrystalline mixture of phases (both quantitatively and qualitatively).

(c) Cyclic Voltammetry (CV)

Voltammetry is an electrochemical technique in which the current at an electrode is monitored as a function of the potential applied to that electrode. The potential is varied in a systematic manner, resulting in a current-potential plot. This plot is called a voltammogram. Any chemical species that is electro active, that is, if it can undergo a redox process, can be analyzed voltammetrically. The electrode can be regarded as a controlling factor for causing chemical species to be oxidized or reduced. When the potential of the electrode is negative it becomes more reducing and when it is positive it becomes more oxidizing.

Cyclic voltammetry (CV) is a versatile electro analytical technique for the study of electro active species. CV monitors redox behaviour of chemical species within a wide potential range. The scan range is narrowed for the study of a particular couple. The

current at the working electrode is monitored as a triangular excitation potential which is applied to the electrode. The resulting voltammogram can be analyzed for fundamental information regarding redox reactions.

Many electrochemical reductions/oxidations generate intermediate species that rapidly reacts with components of the medium. One of the most useful aspects of CV is its application to the qualitative analysis of these chemical reactions that are coupled to the electrode surface reactions. CV is used to determine the redox potential of various donor and acceptor compounds and to investigate the kinetics of electron-transfer reactions at the electrode.

(d) Rotating Disk Electrode (RDE)

RDE is a widely used method for the study of electrode processes at solid electrodes [20]. It can be used to determine the diffusion coefficients and kinetic parameters of the electron-transfer reactions at the electrode. The RDE is constructed from a disk of electrode material embedded in a rod of insulating material (e.g. Teflon). The electrode is attached to a motor and rotated at a certain frequency. The movement of rotation leads to a very well defined solution pattern. The rotating device acts as a pump, pulling the solution upward and then throwing it outward.

The benefits of RDE include:

- It has a diffusion layer with a constant thickness.
- The double-layer charging has a minimal effect on the measurement.

- The theoretical basis of the mass transfer process has been solved and equations are available to relate experimental parameters to the mass transfer of reactants to the electrode surface [21].

(e) Bulk Electrolysis

Electrolysis is the conversion of electrical energy into chemical energy in order to convert compounds by oxidation or reduction, so that products are formed. The bulk electrolysis cell is designed for the complete electrolysis of sample solution. It is typically used for the quantitative analysis of electron transfer per molecule, and the measurement of absolute quantity of the analyte. In this project, bulk electrolysis experiments were conducted in an attempt to break down phenol to less harmful substances or compounds.

References

1. Fourie, J. M. Sc. Thesis. **1996**, University of the Western Cape.
2. Jongwana, T. M. Sc. Thesis. **1999**, University of the Western Cape.
3. Grimm, J., Bessarabov, D., Maier, W., Storck, S., Sanderson, R.D. Desalination. **1998**, 115, 295.
4. Baker, P.G.L. Ph. D. Thesis, **2004**, University of Stellenbosch.
5. Wang, P., Lee, H. Journal of Chromatography A. **1997**, 789, 473.
6. Boudenne, J.L., Cerclier, O., Galea, J., Van der Vlist, E. Applied Catalysis A: General. **1996**, 143:2, 185.
7. Gatrell, M., MacDougall, B. Journal of Electrochemical society. **1998**, 146:9, 3335.
8. Andreescu, S., Andreescu, D., Sadik, O.A. Electrochemistry Communications. **2003**, 5, 681.
9. Bard, A.J, Faulkner, L.R. *Electrochemical Methods: Fundamentals and Applications*, 2nd Ed., Wiley, New York, 2001; Chapter 9.
10. Foti, G., Gandini, D., Comninellis, C., Perret, A., Haenni, W. Electrochem. Solid State Lett. **1999**, 2, 228.
11. Trasatti, S. *Electrodes of Conductive Metallic Oxides: Part A*, Elsevier Scientific Publishing, New York, 1980.
12. Trasatti, S. Electrochimica Acta. **2000**, 45, 2377.
13. Paseka, I. Applied Catalysis A: General. **2001**, 207, 257.

14. Livage, J. Sol-Gel Processes, *Current opinion in Solid State and Material Science*. 2 (1997) 132.
15. Chaleton, J.P., Terrier C., Bernstein, E., Berjoan, R., Roger J.A. *Thin Solid Films*. **1994**, 247 (1), 162.
16. Brinker, C.J., Hurd, A.J., Schunk P.R., Frye G.C., Ashley, C.S. *Journal of Non-Crystalline Solids*. **1992**, 147-148, 424.
17. Brinker, C.J., Scherer, G.W. *Sol-gel Science: The Physics and Chemistry of Sol-gel Processing*, Academic Press, California, USA, 1990.
18. Smyth, D.M. *Solid State Ionics*. **2000**, 129, 5.
19. Juttner, K., Galla, U., Schmieder, H. *Electrochimica Acta*. **2000**, 45, 2575.
20. Seung-Hee Nam, Ho-Gi Kim, *J. Applied Physics*. **1992**, 72 (7), 2895.
21. Greef, R., Peat, R.M., Peter, L.M., Pletcher, D., Robinson, J. *Instrumental methods in Electrochemistry*, Ellis Horwood, Chichester, 1985.

3 Experimental

3.1 Introduction

The mixed metal oxides were prepared by a dip-coating sol-gel technique. The theory behind this technique was given in detail in Chapter 2. Once the mixed metal oxide surfaces were prepared, they were then characterized. TGA was used to determine the temperature at which metal precursors decomposed to form metal oxides. Other characterization techniques used were SEM, AFM and EDX for the general morphology of the thin film electrodes. XRD was used to determine the crystallinity of the coated mixed metal oxides. RBS and PIXE were used to determine the chemical composition and depth profile of the elements. Bulk electrolysis, RDE and cyclic voltammetry were used for electrochemical evaluation of the surfaces and HPLC was used to monitor the breakdown of phenol and the formation of its by-products.

3.2 Preparation of metal oxide electrodes

Coating of Ti surfaces with various metal oxide precursors took place according to a well-defined procedure by Lipp and Pletcher [1]. They identified factors, which control the quality of the electrode coating. Pre-treatment of the surface of the substrate prior to coating is critical for the fabrication of stable electrodes. Hence, shortly before coating the surface, the substrate was etched in boiling 11.5 M HCl for 5 min. After etching, the

substrate was washed well with ultra-pure water and later with absolute ethanol and then dried in air.

The coating films were from the precursors of hydrated SnCl_2 , RuCl_3 , TaCl_5 , RhCl_3 and IrCl_3 dissolved in absolute ethanol [2]. The 50% (mol/mol) of SnO_2 was kept constant and only the mole concentrations of Ru and Ir were varied. The reason behind was that Sn was considered as a matrix for the Ru and Ir oxides. Ru and Ir oxides are known to be oxygen producing [1, 3]. The films were prepared by the dip withdrawal technique, which involves slowly drawing a Ti substrate plate from a solution of the sol consisting of the respective precursors. The compositions of the conducting metal oxides were varied and their stability and electro-catalytic activity were determined by means of cyclic voltammetry, RDE and bulk electrolysis. The various electrodes of varying compositions that were prepared are tabulated in Table 3.1 and their respective annealing temperatures and times are tabulated in Table 3.2.

Table 3.1: Reagent compositions of the prepared metal oxides electrodes (%mol/mol)

Ti/ SnO_2 - RuO_2 - IrO_2			Ti/ Ta_2O_5 - IrO_2		Ti/ RhO_x - IrO_2	
SnO_2	RuO_2	IrO_2	Ta_2O_5	IrO_2	RhO_x	IrO_2
50	10	40	80	20	80	20
50	20	30	60	40	60	40
50	30	20	40	60	40	60
50	40	10	20	80	20	80

Table 3.2: Different metal oxides at their respective annealing temperatures and times

Electrode	Annealing temperature (°C)	Annealing time (h)
Ti/SnO ₂ -RuO ₂ -IrO ₂	400	2
Ti/Ta ₂ O ₅ -IrO ₂	700	1
Ti/RhO _x -IrO ₂	700	2

It has been found that films of 0.05-0.5 μm in thickness can be produced by one dip-coating run, and that repetition of the application leads to thicker coatings [3]. This procedure is also true for the surface coatings prepared in our laboratory. A copper contact was made to the back of the Ti plate by using a Ag epoxy. The back of the electrode and the copper contact was isolated with an inert non-conductive polymer resin. This left an area of 0.9 – 1 cm^2 exposed for electrochemical measurements. All electrodes were annealed at a temperature rate of 1 $^{\circ}\text{C}/\text{min}$, in a tube furnace in an oxygen-rich atmosphere. All these electrodes were evaluated as active surfaces towards the oxidation of phenol and the 50:40:10 % (Sn:Ru:Ir) was found to be the most promising thin film of the four prepared. The reported results in this study are solely based solely on this active surface.

3.3 Ex-situ analysis

3.3.1 (a) TGA analysis of $Ti/SnO_2-RuO_2-IrO_2$ and Ti/RhO_x-IrO_2

The hydrated $SnCl_2$, $RuCl_3$, $IrCl_3$ and $RhCl_3$ precursor solutions were analyzed by TGA. A TGA instrument (Perkin Elmer, Thermal Gravimetric Analyzer 7) was used to monitor the sample weight loss and recorded the temperature at which the metal oxides formed. The procedure for the thermo-analytical experiments was as follows: the precursor was evaporated at 100 °C and the sample was transferred to the TGA cell. The Sn/Ru/Ir precursors were heated to 700 °C using air as the carrier gas. The Rh/Ir precursor solution was heated to 900 °C. All samples were heated at a rate of 10 °C /min.

(b) TGA analysis for $Ti-Ta_2O_5-IrO_2$

The hydrated $TaCl_5$ and $IrCl_3$ precursor solutions were analyzed by TGA. The procedure was as follows: The temperature was kept constant at 400 °C for an hour, and then increased to 900 °C. The Ta/Ir precursor solution heating rate was at 10 °C /min to 900 °C, without a constant temperature of 400 °C. Air was used as the carrier gas.

3.3.2 RBS and PIXE analyses

RBS is relatively a simple technique [4]. It is a technique used to determine the cation stoichiometry and thickness of surfaces. The instrument used for RBS and PIXE analysis was PHI RBS-400 end station with NEC 1 MV accelerator. A beam of a monoenergetic and collimated α - particles (He^{2+}) impinges perpendicularly on a target. Here a 2.0 MeV He^{2+} beam was used. The sample was tilted 10° towards the detector, situated at a

backscattering angle of 165° . The samples were irradiated with a $20 \mu\text{C}$ of He^{2+} . Some of the backscattered particles impinge on the detector, where they generate an electrical signal. This signal is amplified and processed with fast analog or digital electronics. The final stage of the data processing usually has the form of a spectrum, hence the name backscattering spectrometry [4].

Scattering events that take place somewhere between the front and rear surfaces are recorded at some intermediate energies. Since the beam is unattenuated, the scattering probability at any depth is proportional to the number of atoms of a particular kind present there. This is the way a concentration profile of a given element is translated into a signal of corresponding height and decreasing energy in the backscattering spectrum.

The great increase in sensitivity for heavy elements is an asset for the detection of these elements, but with severe limitation for the detection of light elements like carbon, nitrogen and oxygen. Two elements of similar mass cannot be distinguished when they appear together in a sample.

Other analytical tools such as PIXE can resolve this lack of specificity of the signal. PIXE was used to identify various constituents in the coating layer, since there is little overlapping of characteristic X-rays for different elements [5]. The samples were bombarded with protons and the energy of the beam was kept at 3 eV. A selected section of the surface ($5 \mu\text{m} \times 5 \mu\text{m}$) was bombarded with protons and taken to be representative of the total surface composition ($5 \text{mm} \times 5 \text{mm}$). The backscattered energy was recorded

using an X-ray detector. Semi-quantitative on-line imaging was made possible by the use of the GEO-PIXE suite of programmes

3.3.3 SEM, AFM and EDX analyses

The surface morphology of the electrodes was analyzed by elemental X-ray analysis (EDX), SEM and AFM. A Topcon ABT60 Scanning Electron Microscope was used. The SEM pictures were taken at a working distance of 7 mm and an accelerating voltage of 7 kV. For the X-ray analysis, the working distance was 12 mm and the accelerating voltage was 25 kV. The samples were tilted at 30 degrees from the horizontal. Thin films surfaces were cross-sectionally analysed using SEM. The cross sections were obtained as follows: The samples were left in a resin for 24 h in an oven at 60 °C, cut and polished into small pieces and mounted vertically on the stubs.

SEM was used to investigate if the sample has scratches, cavities and other surface non-uniformities (present even if they are in a micron size) that can drastically modify the backscattering spectrum. SEM provides surface topography that lacks in-depth analysis, with little elemental specificity. An EDX (the X-ray analyser) is a link system using AN1000 software. This attachment (EDX) can provide the missing elemental specificity and good lateral resolution.

AFM was used to measure the topography with a force probe. A Topometrix Explorer AFM was used in a contact mode. It operates by measuring attractive or repulsive forces

between a tip of the AFM probe and the sample. In its repulsive ‘contact’ mode, the instrument lightly touches a tip at the end of a leaf spring or ‘cantilever’ to the sample. As a raster-scan moves the tip over the sample, deflection of a laser beam to quadrant detector measures the vertical deflection of the cantilever, which indicates the local sample height. Thus, in contact mode the AFM measures hard sphere repulsion forces between the tip and the sample.

3.3.5 XRD analysis

XRD has been found to be the most useful technique for the determination of crystallographic parameters. XRD measurements identify the crystalline phases of metal oxides present in a thin film [6, 7]. The combination of atomic composition ratios furnished by RBS and the knowledge of diffraction patterns give convincing evidence of the actual nature of the compounds present in the sample.

The thin films were characterized by XRD using a Siemens D8 Advance powder diffractometer with a theta-theta goniometer. The X-ray source was a copper tube and a NaI (Tl) scintillation detector that detects the diffracted beam. The film surface was oriented perpendicular to a plane defined by the X-ray tube, sample holder and detector.

3.3.6 Electrochemical measurements

The surface states of the electrodes were characterized by means of cyclic voltammetry [8], to evaluate the catalytic responses of the electrode surfaces. The voltammetric experiments were carried out with an electrochemical analyzer system, BAS 50W

(Bioanalytical System). A three-electrode system was used. The reference electrode was Ag/AgCl and Pt was the counter electrode. The working electrodes were metal oxides electrodes namely, Ti/SnO₂-RuO₂-IrO₂, Ti/Ta₂O₅-IrO₂ and Ti/RhO_x-IrO₂.

The experiments were carried out at room temperature within a potential window of -1000 mV and 1500 mV, at a scan rate of 100 mV/sec. 3 mM phenol was chosen as the model compound. Solutions were deaerated by bubbling nitrogen gas. Bulk electrolysis experiments were carried out at a constant potential of 1500 mV. The pH of the samples was varied (pH = 2, 7 and 12) and measured by a Metrohm pH meter. Rotating disk electrodes were constructed from disks of electrode materials imbedded in a rod of insulating material (e.g. Teflon). The electrode was attached to a motor and rotated at a certain frequency varying between 0 and 2000 rpm.

All studies were carried out using 0.1 M KCl as the supporting electrolyte, for the basic reason that the medium is neutral, and also, considering its capabilities of reacting with organic compounds. Most of the work has been reported to have been carried out in acid media [3, 4]. The reason why this work was not carried out in acidic media is that acids tend to be harsh and shorten the service life of the electrodes [5].

3.3.7 HPLC analysis

The progress of the electrochemical oxidation of phenol was monitored by HPLC (WatersTM). HPLC as an analytical technique is characterized by high speed and efficiency, and can be coupled to many sensitive and selective detectors [9].

Identification of the by-product compounds of phenol by chromatographic techniques required the availability of commercial standards prior to the use of other analytical techniques, for example NMR, MS, etc. Photodiode array detection has led to considerable improvements in the HPLC analysis of phenolic compounds, as not only the retention time but also the UV spectrum can be used for identification purposes. Quantification also became more exact owing to the simultaneous recording of different wavelengths and the possibility of peak purity checking. There are some instances where UV spectra obtained by diode array detection have been used for the identification of unknown chromatographic peaks by comparison with standards giving the similar spectra.

A variety of compounds are produced during the oxidation of phenol and these have widely varying solubilities, polarities and dissociation constants [10]. Therefore two kinds of HPLC columns were used: The first column was a Luna 5 μ C18 (2), with water/methanol (50:50 v/v) isocratic elution and at a flow rate of 1 ml/min for aromatics. The 10- μ l samples were injected directly into the column. A mixture of water and methanol was used as the mobile phase. It was filtered (<1 μ m pores) and degassed prior

to use. First, the system was flushed with pure methanol, followed by the flushing of the column with methanol/water (50:50, v/v) for 10-20 min. The UV detector was set at wavelengths between 200 and 400 nm.

The second column that was used was a C18 Atlantis column, with a mobile phase of $\text{NaH}_2\text{PO}_4 \cdot \text{H}_2\text{O}$ solution and at a flow rate of 1 ml/min. The specific wavelength set was $\lambda = 210$ nm for detecting organic acids. The results were reproducible. The day-to-day precision of retention times had a 1.2% relative standard deviation.

References

1. Lipp, L., Pletcher, D. *Electrochimica Acta*. **1997**, 42 (7), 1101.
2. Grimm, J., Bessarabov, D., Simon, U., Sanderson, R. *Journal of Applied Electrochemistry*. **2000**, 30, 293.
3. Sakka, S., Kamiya, K., Makita, K., Yamamoto, Y. *Journal of Non-Crystalline Solids*. **1984**, 63, 223.
4. Chu, W., Mayer, J., Nicolet, M. *Backscattering Spectrometry*, Academic Press, New York, 1978.
5. Shaanan, M., Richter, V., Kalish, R. *Nuclear Instruments and Methods in Physics Research B*. **1988**, 35, 319.
6. Lassali, T.A.F., Boodts, J.F.C., Bulhoes, L.O.S. *Electrochimica Acta*. **1999**, 44, 4203.
7. Comninellis, C., Pulgrin, C. *Journal of Applied Electrochemistry*. **1993**, 23, 108.
8. Brett, M.A., Brett, M.O. *Electrochemistry: Principles, Methods and Applications*, Oxford Science Publications, New York, 1993.
9. Wang, P., Lee, H. *Journal of Chromatography A*. **1997**, 789, 473.
10. Boudenne, J.L., Cerclier, O., Galea, J., Van der Vlist, E. *Applied Catalysis A: General*. **1996**, 143 (2), 185.

4

Preparation, characterization and electrochemical evaluation of Ti/SnO₂-RuO₂-IrO₂ thin film as electrode material for the oxidation of phenol

Summary

Titanium substrate was coated with mixed metal oxides of SnO₂, RuO₂ and IrO₂. These coatings were prepared by thermal decomposition of the metal chlorides and alkoxides, and dip-coated on titanium substrates at 400 °C. The surfaces of the thin films were characterized with various surface analytical techniques. The properties of these electrode materials were investigated using TGA, SEM, EDX, AFM, XRD, RBS, PIXE and CV.

It was found that the surface morphology of the thin films had both compact and porous regions. The average area roughness of the surfaces, as determined by AFM, was found to be about 150 nm. Distinct oxides of Sn, Ru, Ir and Ti were identified by XRD. RBS confirmed the depth profile of the elements in the thin film. PIXE was successfully used as an analytical tool to resolve the overlapped peaks of Sn and Ru.

These films act as electro-catalysts for the electro-oxidation of model organic compounds, such as phenol in aqueous potassium chloride media. The electro-catalytic

behaviour is linked to the solid-state properties of the films. The film composed of 40% Ru gave the best catalytic response for the oxidation of phenol. CV measurements indicated a decomposition potential of 200 mV (vs the Ag/AgCl reference electrode) for phenol on the Ti/SnO₂-RuO₂-IrO₂ electrode. Bulk electrolysis proved that Ti/SnO₂-RuO₂-IrO₂ electrode could degrade phenol down to the various carboxylic acids.

4.1 Introduction

Metal oxides and metal oxide mixtures are becoming increasingly important in the chemical industry. Metal-supported mixed oxide thin films have recently become very interesting in various branches of industrial electrochemistry [1]. Transition metal oxides have shown outstanding activity in a variety of electrochemical processes [1]. The discovery of dimensionally stable anodes, DSA-type electrodes, has led to significant improvements in industrial electrochemistry technology, especially in the chlor-alkali industry [2,3]. In addition to the traditional DSA electrodes, which are composed of a binary oxide mixture, modified electrodes composed of ternary oxide mixtures have also recently been investigated and found to have enhanced performance [4].

The development of the use of metal oxides as anodes may lead to the replacement of other kinds of oxygen evolution anodes, such as the Pb-alloy electrodes and Pt-coated Ti electrodes. They are not dimensionally stable [2], their overvoltage for oxygen evolution is very high (~800 mV) and they corrode during the anodic polarization [2].

Thin SnO₂ films provide such benefits as: sufficient optical transparency, high electrical conductivity, excellent chemical and corrosion resistance [4], and properties that satisfy the requirements of a host material in DSA-type electrodes, especially when used in a neutral media such as potassium chloride (KCl).

RuO₂ and IrO₂ have thus far been extensively investigated as anodes for O₂ evolution in acid solutions [4, 5-7]. RuO₂ is more active than IrO₂, while the latter is much more corrosion resistant than the former. RuO₂ and IrO₂ coated Ti electrodes are known to possess high catalytic activity, not only for chlorine evolution but also for oxygen evolution, yet they lack the stability required for practical applications [5]. It has been suggested that the long-term performance of the two-component oxide may be improved by the addition of SnO₂ [6-9].

As characterization of the surface properties of electrodes coated with mixed metal oxides is of fundamental importance to the electrochemical behaviour (refer to chapter 3), a systematic study of the surface characteristics of a range of compositions of mixed metal oxides of SnO₂, RuO₂ and IrO₂ as thin films with electro-catalytic properties was therefore undertaken (see Tables 3.1 and 3.2). The properties of the thin film electrode materials were investigated using CV, SEM, EDX, AFM, XRD, RBS and PIXE.

4.2 Experimental

Experimental procedures are outlined in chapter 3.

4.3 Results and Discussions

4.3.1 Thermo-analytical measurements

Fig. 4.1 shows a typical TGA curve of a coating containing Sn, Ru and Ir precursors separately and a mixture of chloride precursors.

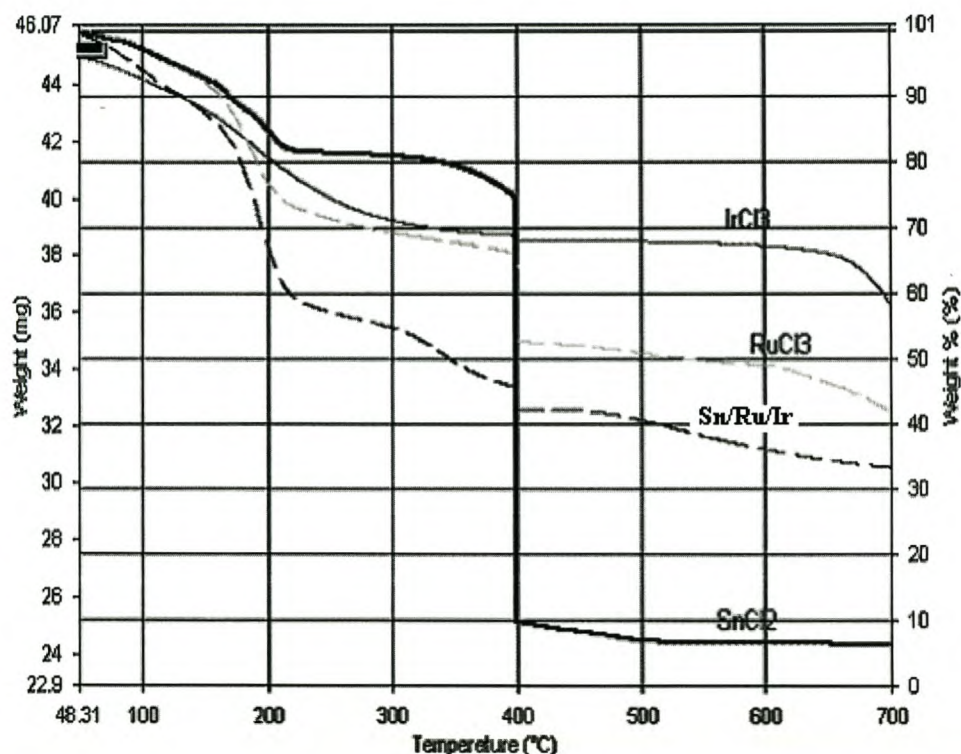


Fig. 4.1 Thermograms of the hydrated precursors of SnCl₂, RuCl₃ and IrCl₃ and the mixture of metal chlorides (Sn/Ru/Ir) with high content of Ru (40%).

The thermogram shows three distinctive stages of thermolysis. First, there is an initial mass loss between 0 °C and 200 °C. The weight loss of Sn/Ru/Ir mixture between these temperatures is about 30%. This is attributed to the evaporation of the free water molecules and the solvent. Then there is another mass loss observed between 200 °C and

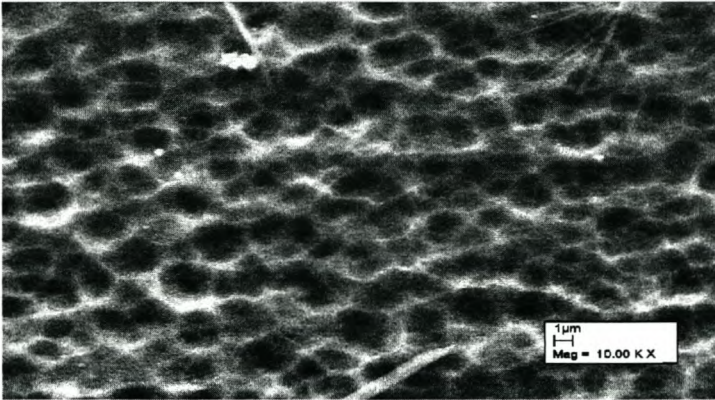
400 °C, and the Sn/Ru/Ir mixture weight loss is about 55%. This is attributed to the decomposition of the metal chloride ions and the formation of oxides. SnCl_2 in particular oxidized drastically at 400 °C to form SnO_2 . The weight loss of SnO_2 at that temperature was about 94%. Less mass variation was observed after the 400 °C isotherm, indicating that at that temperature all the organic and metal chloride residues are eliminated and the respective oxides are formed. Only 32% weight of the original Sn/Ru/Ir mixture was unoxidized.

The thermal curve obtained for a combination of the three metal chlorides (ie. labeled as Sn/Ru/Ir) shows a similar behavioural pattern to that of individual metal chlorides. This is an indication that there might be solubility or polymerization occurring between the three mixed metals, resulting in the thermogram labeled Sn/Ru/Ir in Fig. 4.1. This figure implies that the oxidative decomposition of the individual chlorides in the Sn/Ru/Ir (50:40:10) mixture occurred at the intermediary rate effect. According to Hu et al. [10] this effect is mainly attributed to the formation of solid solution or the initial polymeric gel phase between these metal oxides.

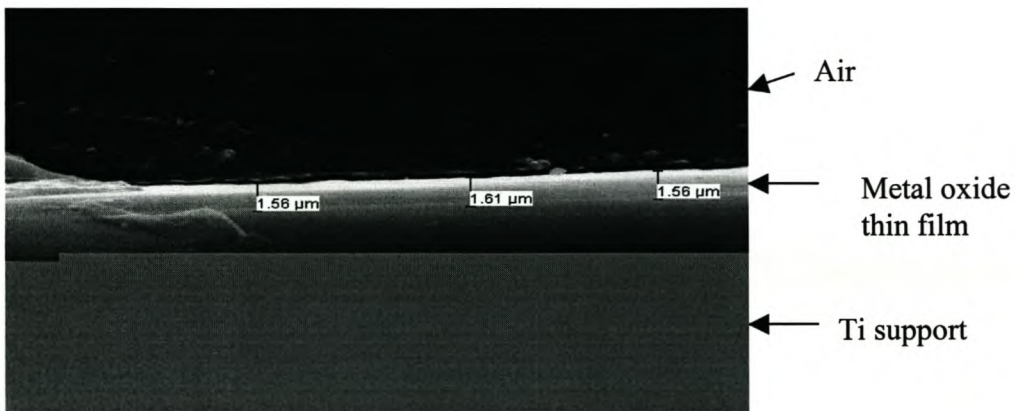
4.3.2 SEM, EDX and AFM analyses

Fig. 4.2 (a) shows a SEM image of the Ti/ SnO_2 - RuO_2 (40)- IrO_2 (10) thin film. The SEM showed that the oxide coatings were showing a rough morphology with a network structure and a porous-like surface. The pore dimensions range between 1.5 - 2 μm in diameter. The surface morphology of the thin film appeared to have both compact and

porous regions. As the Ru content was increased in the coated layer, more pores were seen in the coating on the Ti substrate; hence the formation of TiO_2 was observed. This formation of the TiO_2 was detected by XRD and the depth profile thereof was observed by RBS.



(a)



(b)

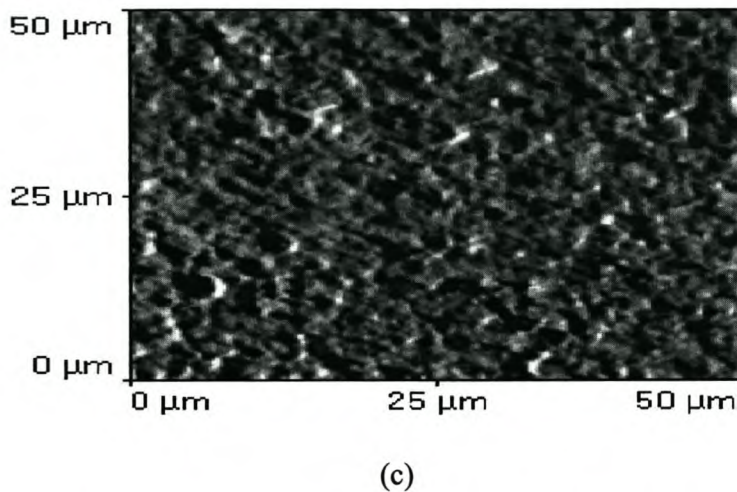


Fig. 4.2 The microstructure of the $\text{Ti/SnO}_2\text{-RuO}_2\text{-IrO}_2$ (50-40-10) electrode. (a) SEM surface image, (b) SEM cross sectional surface image and (c) AFM surface image.

Fig. 4.2 (b) shows a SEM side view of the thin film. Film thickness could be determined from analysis of the SEM cross sectional surface area. The film thickness was estimated to be about $1.6 \mu\text{m}$, which depends on the rate of dip-coating. The side view also indicates the formation of a homogeneous film.

AFM confirmed the roughness of the surface of the electrode, as can be seen in Fig. 4.2(c). The average dimension of the roughness of the surface was found to be about 150 nm. AFM also gave information on the average depth profiles of the pores; this was estimated to be 890 nm. The measurements were taken from the low point (dark spots) on the surface to the high point (light spots) of the film. The depth profiles of the pores and the roughness of the surface gave an indication that the film has a large surface area. A rough surface can be considered advantageous for electro-catalytic applications because of the resulting larger surface area.

4.3.3 XRD measurements

Fig. 4.3 shows an X-ray diffractogram of the Ti/SnO₂-RuO₂-IrO₂ electrode. XRD was used to determine the crystalline nature of the structure of the oxide films coated on the titanium substrate. It was possible to distinctively identify the presence of the crystalline phases of Ti, TiO₂, SnO₂, RuO₂ and IrO₂ in the rutile structure.

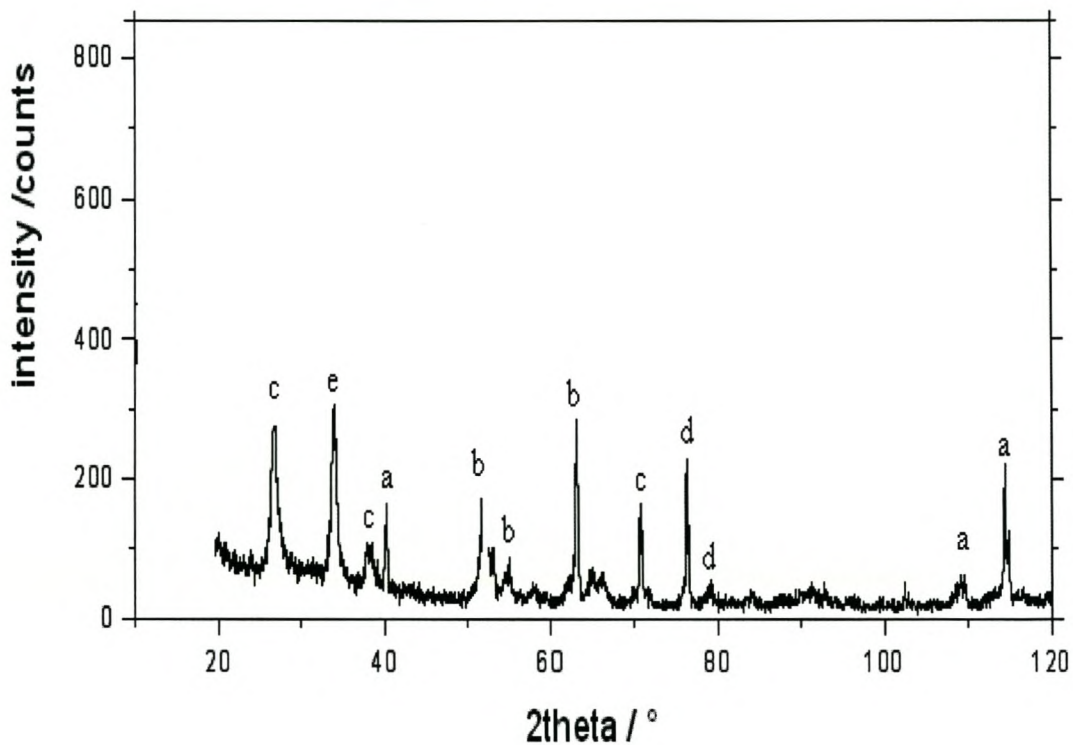


Fig. 4.3 XRD pattern of the Ti/SnO₂-RuO₂-IrO₂ (50-40-10) electrode, (a) Ti, (b) TiO₂, (c) SnO₂, (d) RuO₂, (e) IrO₂.

The oxidized Ti into TiO₂ formed part of the coating layer. The TiO₂ layer formed could not passivate the coating layer because its layer was very thin. The presence of the TiO₂

in the above-mentioned coating layer is explained by the structures and ionic radii of the same magnitude; they could form a substitutional solid solution. Indications are that this postulate agrees with the explanations given during the discussion of the thermo-analytical measurements (section 4.3.1). The unlabeled peaks observed between 80 and 100 (2θ) are attributed to small crystal islands in a semi-crystalline matrix.

4.3.4 RBS and PIXE measurements

The Ti/SnO₂-RuO₂-IrO₂ electrode sample was investigated with RBS and the data (open circles) and simulated spectrum (solid line) are shown in Fig. 4.4. A software package RUMP [17] was used to simulate the spectra. The arrows show at which energy a signal from an element on the electrode surface would be observed; the depth profile of each element is built up of signals lower than this energy. It is clear that there is significant overlap of Sn and Ru peaks between the channels 380 and 420. Nonetheless, a small depth profile of Ir and Sn/Ru can be seen.

The broad shoulder between the Ru and Ti surface positions is indicative of a sample with large differences in thickness over the irradiated spot. This also indicates that the diffusion of the coating layer into the substrate had occurred. A simulated spectrum consistent with the data was obtained by describing the sample as consisting of the Ti substrate covered with a layer of TiO₂ upon which, islands of mixed oxides of non-uniform thickness were formed. PIXE analysis was later performed to resolve the Sn and Ru peaks [Fig. 4.5]. The peaks observed for Fe and Ag are believed to be due to the impurities resulting from these elements. The peaks labeled esc are due to the noise at the beginning of the measurement.

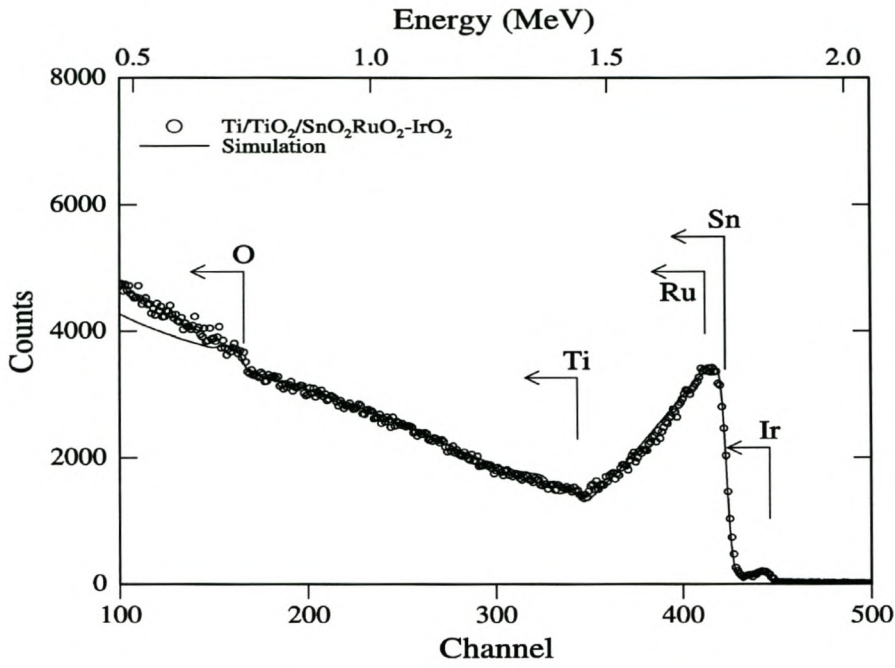


Fig. 4.4 RBS simulated spectrum for the Ti/SnO₂-RuO₂-IrO₂ electrode.

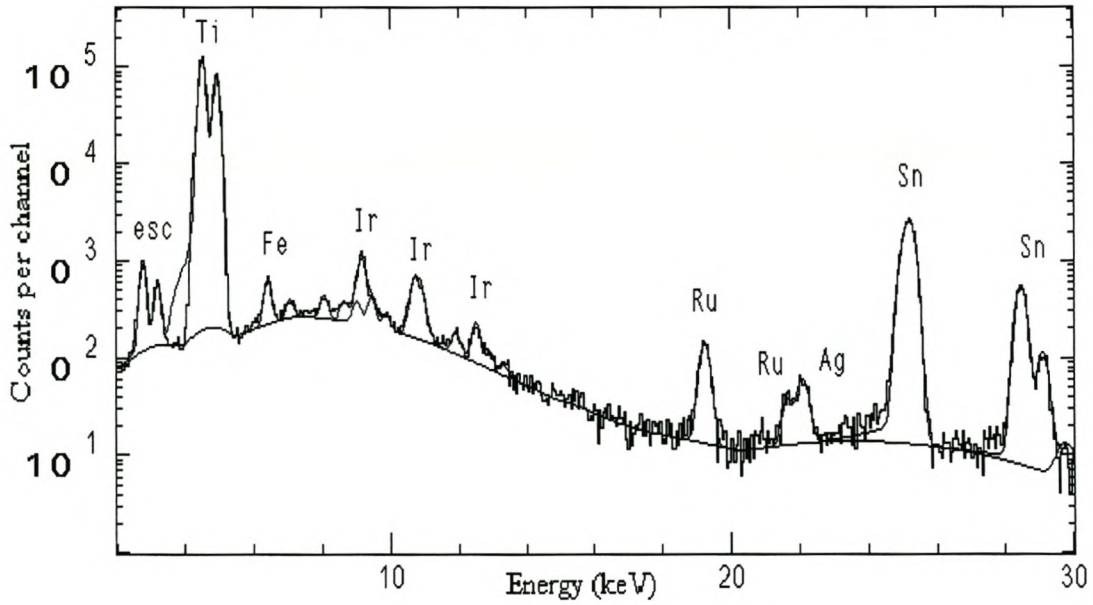


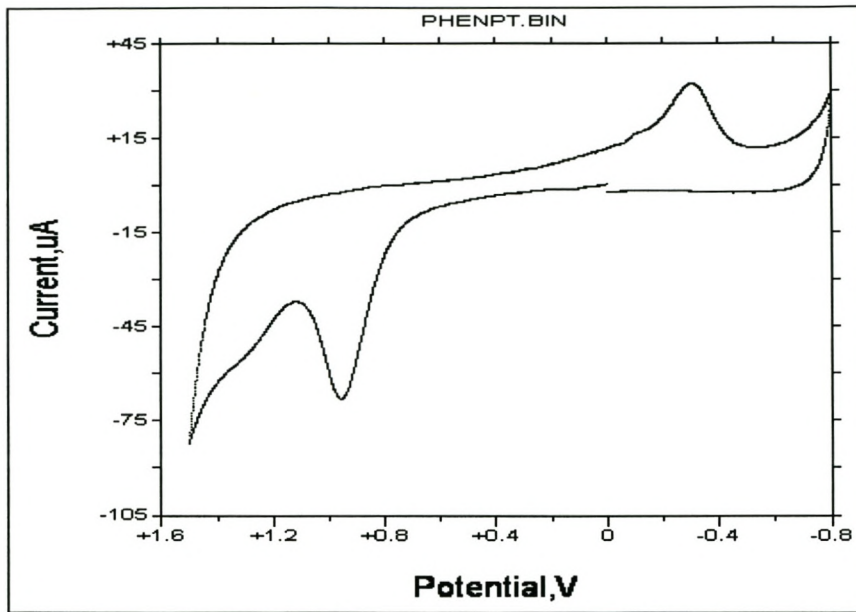
Fig. 4.5 Fitted PIXE spectrum for the Ti/SnO₂-RuO₂-IrO₂ electrode.

4.3.5 *Cyclic voltammetric measurements*

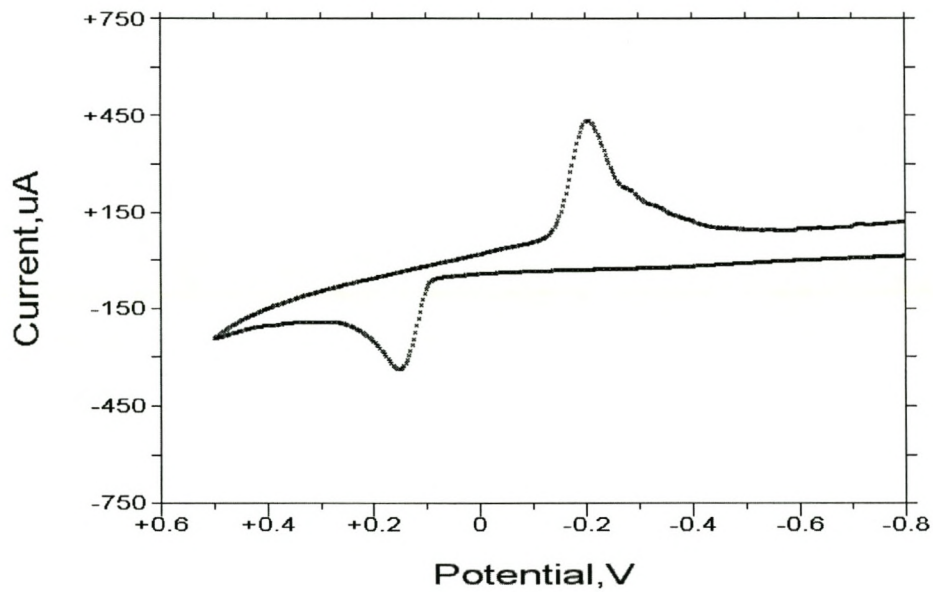
CV was used to evaluate the catalytic response of the electrode surface. Phenol was chosen as the model with which to evaluate the reversibility and kinetics of the thin film surface. Fig. 4.6 (a) and (b) shows the reactions of the oxidation-reduction chemistry of phenol at the platinum and the Ti/SnO₂-RuO₂-IrO₂ electrodes. Various composition concentrations of the conducting oxides were examined. The current/potential curve represented here is that of a thin film having a 40% Ru content. This film showed the optimum performance for the oxidation of phenol. The voltammograms showed a irreversible behaviour for phenol at both the Ti/SnO₂-RuO₂-IrO₂ and Pt electrode surfaces.

The oxidation potential for phenol at a Pt electrode was observed at about 1000 mV vs Ag/AgCl, while at the Ti/SnO₂-RuO₂-IrO₂ electrode, phenol was oxidized at about 200 mV. This oxidation potential of phenol on the Ti/SnO₂-RuO₂-IrO₂ surface is low compared to that observed on the corresponding Pt electrode (see Figs 4.6 (a) and (b)).

This is also lower than the reported oxidation potential of phenol at the Ti/SnO₂-Sb₂O₃ electrode [12]. The catalytic response of Ti/SnO₂-RuO₂-IrO₂ shows promise when compared to that of Pt, because Pt has been widely used as an anode for oxidation applications. The use of the Pt electrode as an anode has serious shortcomings, mainly because oxidation of many organic substrates fails to take place in a potential region where Pt passivation occurs, due to oxide formation [2].



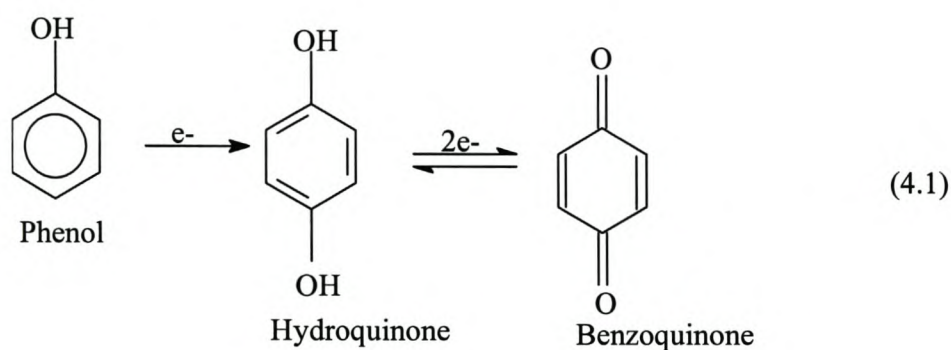
(a)



(b)

Fig. 4.6 Cyclic voltammograms of phenol oxidation at (a) platinum and (b) Ti/SnO₂-RuO₂-IrO₂.

The electrochemical response at the Ti/SnO₂-RuO₂-IrO₂ electrode clearly shows that the oxidation of phenol is irreversible; the reduction peak, of similar magnitude to the oxidation peak appears at a potential of -200 mV. The oxidation of phenol is thought to take place by a three-electron transfer, to form benzoquinone (see Fig. 4.6(b)). However, this is not conclusive unless one can relate the charge Q, to the concentration of phenol. The electron transfer is evidenced by the oxidation peak shown during the oxidation of phenol to quinone (Reaction 4.1).



Previous reports [13-16] on the oxidation of phenol have indicated that the oxidation process is non-reversible. This non-reversibility was largely responsible for the fouling of the electrode surface from the oxidative polymerization of phenol. The irreversible redox behaviour of this couple at this low potential (~200 mV) should therefore significantly decrease the fouling processes associated with the oxidation of phenol.

4.4 Conclusions

The sol-gel process using metal alkoxides has been successfully applied in the preparation of a rutile type $\text{SnO}_2\text{-RuO}_2\text{-IrO}_2$ ternary oxide. TGA results confirmed the loss of free water molecules and the decomposition of the metal chlorides and alkoxides to form oxides. XRD distinctively identified the presence of crystalline structures of Ti, TiO_2 , SnO_2 , RuO_2 and IrO_2 in the rutile phase. The surface activity is largely determined by the morphology of the surface. The $\text{Ti/SnO}_2\text{-RuO}_2\text{-IrO}_2$ electrode had a high surface roughness, with a thickness of about 1.6 μm . This is considered an advantage for electrocatalytic applications.

The $\text{Ti/SnO}_2\text{-RuO}_2\text{-IrO}_2$ electrode was proven to be the catalytic surface for oxidizing phenol under electrochemical conditions. From the available literature, it is believed that these metal oxides combinations have never been reported before. Also, the catalytic response to the oxidation and reduction of phenol at a potential lower than that for Pt electrode, is also new. A coating layer containing 40% Ru was the doping concentration that gave the best catalytic response for the redox electrochemistry of phenol. This latter electrode showed potential as an anode material, to substitute the widely used Pt for the electro-oxidation of organic compounds in aqueous media.

REFERENCES

1. Kodintsev, I.M., Trassati, S. *Electrochimica Acta*. **1994**, 39 (11-12), 1803.
2. Comninellis, C., Vercesi, G.P. *Journal of Applied Electrochemistry*. **1991**, 21, 335.
3. Lassali, T.A.F., Boodts, J.F.C., Bulhoes, L.O.S. *Journal of Non-Crystalline Solids*. **2000**, 273, 129.
4. Shieh, D.T., Hwang, B.J. *Electrochimica Acta*. **1993**, 38, 15, 2239.
5. Iwakura, C., Sakamoto, K. *Journal of Electrochemical Society*. **1985**, 132, 10, 2420.
6. Angelinetta, C., Trassati, S. *Materials Chemistry and Physics*. **1989**, 22, 231.
7. Angelinetta, C., Trassati, S. *Journal of Electroanalytical Chemistry*. **1986**, 214, 535.
8. Onuchukwu, A.I., Trassati, S. *Journal of Applied Electrochemistry*. **1991**, 21, 858.
9. Lassali, T.A.F., Boodts, J.F.C., Bulhoes, L.O.S. *Electrochimica Acta*. **1999**, 44, 4203.
10. Hu, J., Zhang, J., Cao, C. *Thermochimica Acta*. **2003**, 403, 257.
11. Sakka, S., Kamiya, K., Makita, K., Yamamoto, Y. *Journal of Non-Crystalline Solids*. **1984**, 63, 223.
12. Grimm, J., Bessarabov, D., Simon, U., Sanderson, R. *Journal of Applied Electrochemistry*. **2000**, 30, 293.
13. Grimm, J., Bessarabov, D., Maier, W., Storck, S., Sanderson, R. *Desalination*. **1998**, 115, 295.

14. Comninellis, C., Pulgrin, C. *Journal of Applied Electrochemistry*. **1993**, 23, 108.
15. Bock, C., MacDougall, B. *Journal of Electroanalytical Chemistry*. **2000**, 491, 48.
16. Comninellis, C. *Electrochimica Acta*. **1994**, 39, (11-12), 1857.
17. Doolittle, L.R. *Nuclear Instruments and Methods, B*. **1985**, 9, 344.
18. Fiamegos, Y., Stalikas, C., Pilidis, G. *Analytica Chimica Acta*. **2002**, 467 (1-2), 105.
19. Wang, P., Lee, H. *Journal of Chromatography A*. **1997**, 789, 473.
20. Boudenne, J.L., Cerclier, O., Galea, J., Van der Vlist, E. *Applied Catalysis A: General*. **1996**, 143 (2), 185.
21. Christoskova, S., Stoyanova, M., Georgioeva, M. *Applied Catalysis A: General*. **2001**, 208, 243.
22. Santos, A., Yustos, P., Quintanilla, A., Rodriguez, S., Garcia-Ochoa, F. *Applied Catalysis B: Environmental*. **2002**, 39, 97.
23. Feng Y.J., Li, X.Y. *Water Research*. **2003**, 37, 2399.
24. Azzam, M.O., Tahboub, Y., Altarazi, M. *Trans Ichem. B*. **1999**, 77, 219.
25. Azzam, M.O., Tahboub, Y., Altarazi, M. *Journal of Hazardous Materials, B*. **2000**, 75, 99.

5

Preparation, characterization and electrochemical valuation of binary oxide electrode $\text{Ti}/\text{IrO}_2\text{-Ta}_2\text{O}_5$ for the oxidation of phenol

Summary

Iridium and tantalum oxides were thermally prepared from a sol-gel solution on titanium substrates, forming $\text{IrO}_2\text{-Ta}_2\text{O}_5$ layers. The thermal analytical formation of IrO_2 and Ta_2O_5 mixed oxides from chloride precursors was studied by TGA. SEM, EDX, AFM, XRD, RBS and PIXE investigated the surface morphology and microstructure of the layers. The reactivity of the $\text{IrO}_2\text{-Ta}_2\text{O}_5$ films was electrochemically evaluated using CV. CV showed a significant reduction of the over-potential for the oxidation of phenol.

5.1 Introduction

Metal oxide coatings consisting of iridium and tantalum oxides, thermally prepared on a titanium substrate have received much attention as the most widely used catalyst for oxygen evolution in industrial electroplating processes [1]. Tantalum oxide has been reported to remarkably enhance catalytic activity and selectivity and to prolong catalyst life when a small amount of oxide was added to known catalysts [2].

The IrO₂-Ta₂O₅ coated electrode is electrochemically stable since the electro-conducting IrO₂ is stabilized by Ta₂O₅ [3]. The high stability of this binary mixture can be attributed to the formation of an IrO₂ based solid solution with a tantalum component. This type of electrode exhibits high electrocatalysis activity for oxygen evolution [4].

In commercial electrogalvanising lines (EGLs), the application of the Ti/IrO₂-Ta₂O₅ electrode has increased, replacing other kinds of oxygen evolution anodes such as the Pb-alloy electrode and platinum-coated titanium electrodes [1, 5, 6]. There are some disadvantages associated with the use of lead anodes [7]. They are not dimensionally stable, the over-voltage for oxygen evolution is very high (~800 mV) and they corrode during anodic polarization. Several workers [8, 9] have studied the use of dimensionally stable anodes (DSAs) for oxygen evolution in acid solutions, because of their low oxygen over-voltage and inert properties.

An iridium oxide-based anode exhibits a low oxygen over-potential, low consumption rate of the catalyst and low contamination into the electrolyte. The catalytic layer of this type of anode is usually a Ti substrate coated with iridium oxide and tantalum oxide [6]. The IrO₂-Ta₂O₅ coating is reported to have excellent catalytic and corrosion resistance properties [1]. For example, a lifetime of more than 10 000 h was demonstrated under severe operation conditions of 100 A dm⁻² and 333 K in practical use [1]. Based on accelerated electrolysis tests at a current density of 2 A cm⁻², the real service life of a Ti/IrO₂-Ta₂O₅ anode has been estimated to be from 5 to 10 years [10]. In this work, IrO₂-Ta₂O₅ was prepared to act as a DSA for the electro-oxidation of organics in aqueous media. Characterization of such an electrode is a prerequisite to the fundamental

understanding of its electrochemical behaviour as related to its physical and chemical properties [11].

5.2 Experimental

All the experimental procedures are outlined in chapter 3.

5.3 Results and discussion

5.3.1 *Thermo-analytical measurements*

Thermograms of hydrated iridium chloride, tantalum chloride and Ta/Ir mixed precursors are shown in Fig. 5.1. These results are in agreement with the results reported by Kristof et al. [12], that below 100 °C the residual solvent (absolute ethanol) and crystallization water are released. In the mass loss stage between 200 and 400 °C, chlorinated species evolve and their liberation continues up to 550 °C. The Ta/Ir precursor that was held for 1 h at 400 °C showed that more weight loss was observed compared to Ta/Ir precursor without a hold at 400 °C. The reason for this observation is that more of chlorides of the Ta ions are oxidized at this temperature. So, keeping the precursor sample on hold at that temperature gave it enough time for more decomposition.

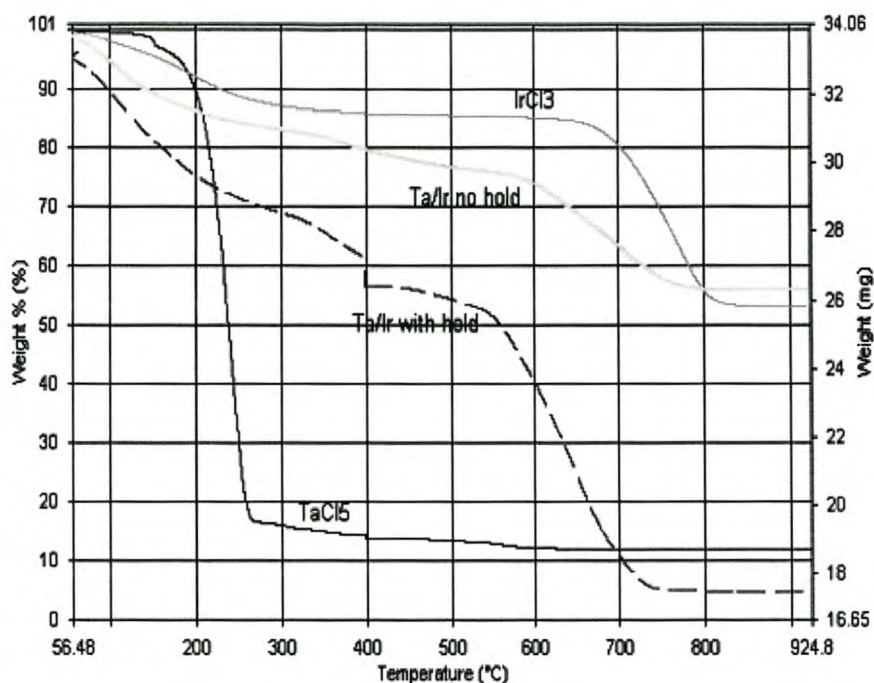


Fig. 5.1 Thermograms for the TaCl₅, IrCl₃ precursors and Ta/Ir (20:80) mixed precursors.

About 84% weight of hydrated TaCl₅ was found to have oxidized at ~250 °C, and about 48% of the hydrated IrCl₃ decomposed at 800 °C. The Ta/Ir mixed solution thermogram showed an initial weight loss between 100 and 400 °C. This is attributed to the decomposition of the hydrated TaCl₅ and the formation of β -Ta₂O₅. The second weight loss occurred between 550 and 720 °C. The Ta/Ir mixture without 10 min. hold at 400 °C was found to have oxidized and only 56% weight was unoxidized. This weight loss is attributed to the decomposition of hydrated iridium chloride.

It is difficult to postulate the reaction products in each of the temperature regions because of the complicated interaction between the Ir and Ta chlorides in the thermal analysis process (see Fig. 5.1). Generally, the value of the weight loss for Ta was larger than that

of Ir over a wide temperature range. This means that Ir inhibited the oxidation of the Ta as weight loss was much lower as it moved to higher temperatures. This intermediary effect is mainly caused by the formation of a solid solution between Ir and Ta oxides [13].

The $\text{TaCl}_5 (x\text{H}_2\text{O})$ and $\text{IrCl}_3 (x\text{H}_2\text{O})$ thermal analysis results were consistent with the results reported by Hu et al. [13]. Above $700\text{ }^\circ\text{C}$ the respective oxides were formed; a minimal amount of Ta_2O_5 remained with more of the IrO_2 formed. The crystalline reflections of rutile-structured IrO_2 on a Ti substrate were also detected by XRD. No mass variation was observed after the $700\text{ }^\circ\text{C}$ isotherm, indicating that at that temperature all the organic and chloride residues had been eliminated and the respective oxides had formed.

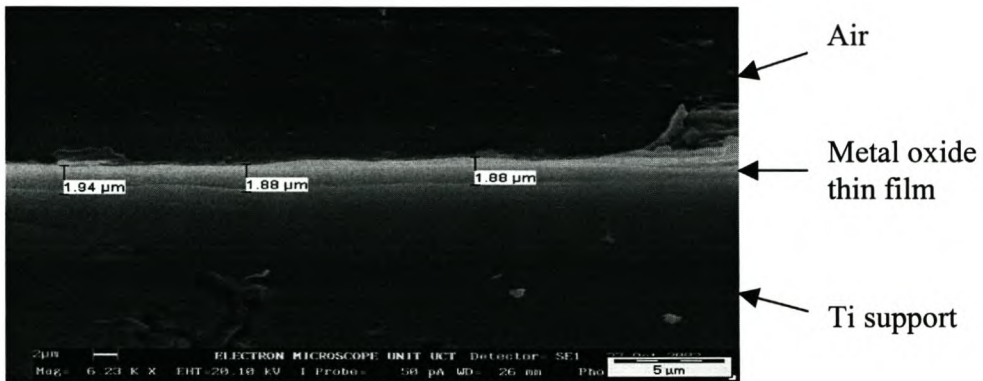
5.3.2 SEM, EDX, AFM and XRD analyses

The surface morphology of a coating layer $\text{Ti/Ta}_2\text{O}_5\text{-IrO}_2$ was examined by SEM and AFM. Fig. 5.2 shows the microstructure of the $\text{Ti/IrO}_2\text{-Ta}_2\text{O}_5$ electrode. The micrograph showed a heterogeneous cracked morphology consisting of flat, smooth areas and agglomerated particles formed on smooth areas. These aggregated particles were attributed to IrO_2 and the flat area to the combination of both tantalum and iridium oxides, as determined by elemental X-ray analysis (EDX).

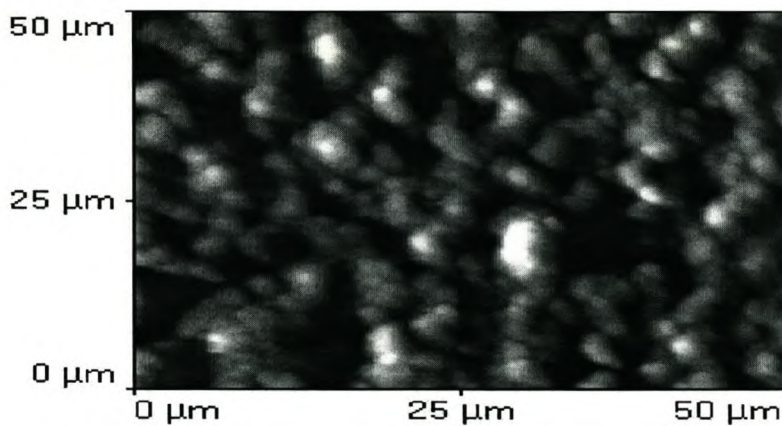
The above mentioned results are also consistent with the view point of Roginskaya et al, [14] who reported, based on the SEM analysis of $\text{Ti/Ta}_2\text{O}_5\text{-IrO}_2$ surface, that the boundaries of IrO_2 crystallites are modified by Ta_2O_5 in mixed oxides.



(a)



(b)



(c)

Fig.5.2 The microstructure of a Ti/IrO₂-Ta₂O₅ electrode. (a) SEM surface image, (b) SEM cross sectional surface image and (c) AFM surface image.

The finer the crystallites of IrO_2 , the greater the contribution of Ta_2O_5 modification to the mixed modified phase. The Ta component has a significant effect on the crystallization dynamics of the IrO_2 crystallite phase as indicated by SEM, TGA and XRD results. Previous work [4, 15, and 16] indicates that the crystallite size of the pure IrO_2 increased with the annealing temperature. This indicates the possibilities of metal oxides rearrangement at higher temperatures, which includes metal oxide separations into separate crystalline domains.

SEM provides surface topography that lacks in-depth analysis, with little elemental specificity. The drawback of the electron microscope results is that the X-ray signal reflects the average composition over large depths, compared to the resolution of the depth of a backscattering spectrum (Fig. 5.4). Therefore the sample was cross-sectionally examined to look at a side view of the thin film. Results of the SEM cross sectional surface area analysis estimated the film thickness to be about $1.9 \mu\text{m}$ (Fig. 5.2b).

The AFM images were taken over $10 \mu\text{m}$ scan size areas. Results confirmed the roughness of the surface. The average dimension of the roughness was estimated to be about 380 nm. The presence of pores on the surface of the electrode was also observed. The average depth of the pores was found to be about 1100 nm.

XRD clearly indicated the presence of IrO_2 , Ta_2O_5 , TiO_2 and Ti, as can be seen in Fig. 5.3. Tantalum oxide was crystallized to the $\beta\text{-Ta}_2\text{O}_5$ phase and the IrO_2 rutile-shape type was in a tetragonal structure. At 80% Ir content, the crystallite phase in the mixture existed

entirely as the rutile phase. These results indicated that the crystallization of Ta_2O_5 is affected by the IrO_2 component. XRD results are in agreement with the results reported by Roginskaya et al. [14] and Hu et al. [13]. They also pointed out that in the binary oxides the β -phase is a solid solution of IrO_2 in $\beta\text{-Ta}_2\text{O}_5$, and, furthermore that it is possible that the Ta component can penetrate into the IrO_2 rutile crystal by solubilization. Because the ion radii of Ta^{IV} , Ta^{V} and Ta^{IV} are extremely close (0.74, 0.72 and 0.71 Å, respectively), it is not difficult for Ir and Ta compounds to form solid solution. The rutile lattice is deformed and the cell volume increases due to access of the larger ion of the Ta component.

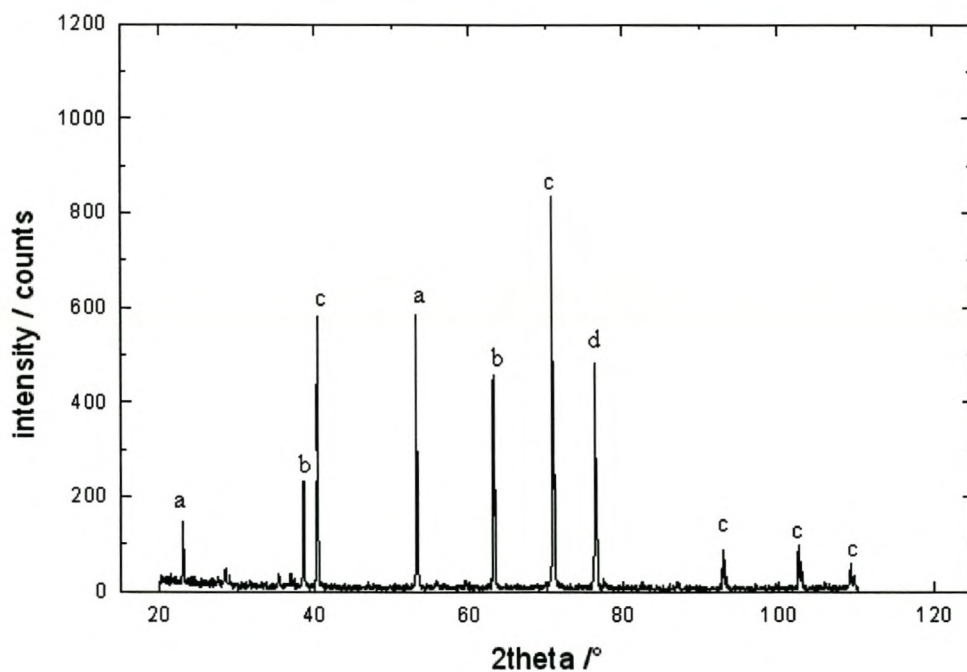


Fig. 5.3 XRD patterns of $\text{Ti/Ta}_2\text{O}_5\cdot\text{IrO}_2$ electrode; (a) Ta_2O_5 , (b) IrO_2 (c) Ti and (d) TiO_2 .

5.3.3 RBS and PIXE measurements

In the RBS spectrum of a Ti/Ta₂O₅-IrO₂ sample (Fig. 5.4), the energy at which elements will be observed when they are on the surface, are indicated by the vertical lines of the arrows shown. The signals at the lower energies (or channels) to the left of these positions arise from backscattering events deeper in the sample and thus represent a depth scale that correlates to deeper positions within the sample with lower energies.

RBS does not have the mass resolution capability to distinguish between Ta and Ir, as they are both at the surface of the Ti/Ta₂O₅-IrO₂ electrode. In RBS simulations (RUMP) [17, 18], only Ta was therefore used, although it was known that Ir was present, as indicated by XRD and EDX results (section 5.3.2). From the RBS spectrum (Fig. 5.4) it was deduced that the sample could be simply described as a pure Ti substrate into which some Ta/Ir had diffused. This indicates that a Ti substrate is covered by a thin layer containing the elements Ta, Ir, Ti and O.

The first layer of Ti/Ta₂O₅-IrO₂ consisted of a mixture of Ta/Ir and Ti (from TiO₂), the Ta signal of which was visible between channels 420 – 440. RBS showed that the Ta concentration was not constant over this layer. Near the surface the composition of Ta was 30% while at the back of the layer the composition was 10%.

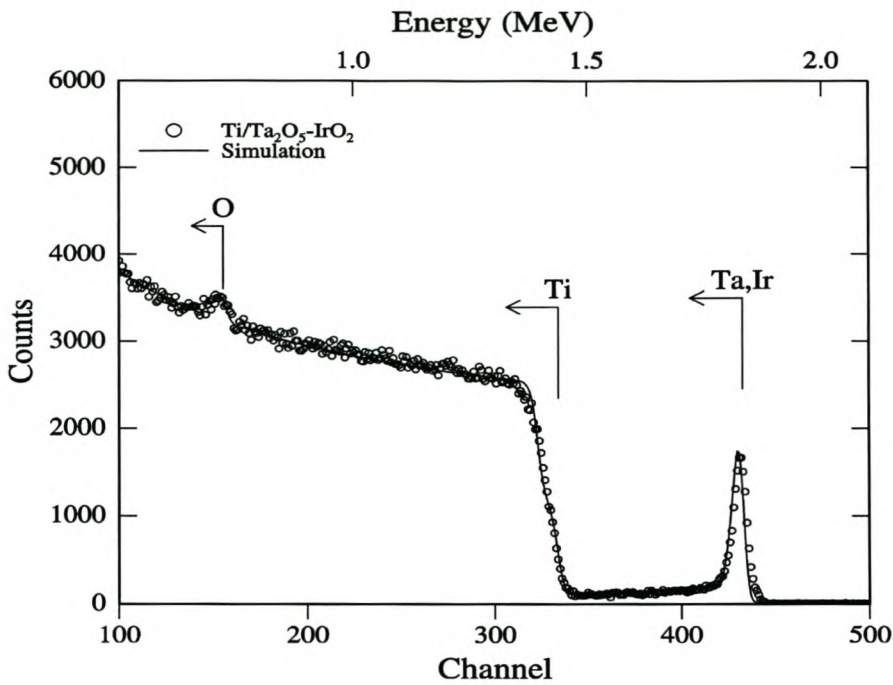


Fig. 5.4 RBS simulated spectrum of a Ti/Ta₂O₅-IrO₂ electrode.

The Ta present at the beginning of the layer decreased rapidly, to a depth of one micron towards the Ti. The interdiffused Ta and Ir signal is clearly seen in Fig. 5.4 as the contribution ranging from channels 340 to 420. The RBS spectrum was consistent with the heterogeneous composition of the coating layer. The peaks of the coating layer (Ta/Ir) overlapped and RBS could not specifically resolve the component elements, because of their closeness in mass numbers. To determine the ratio of Ta to Ir in this layer of Ta₂O₅-IrO₂, the PIXE technique was used. Fig. 5.5 shows that both Ta and Ir can clearly be resolved. Compositional analysis shows the ratio of Ta:Ir to be 3:4.

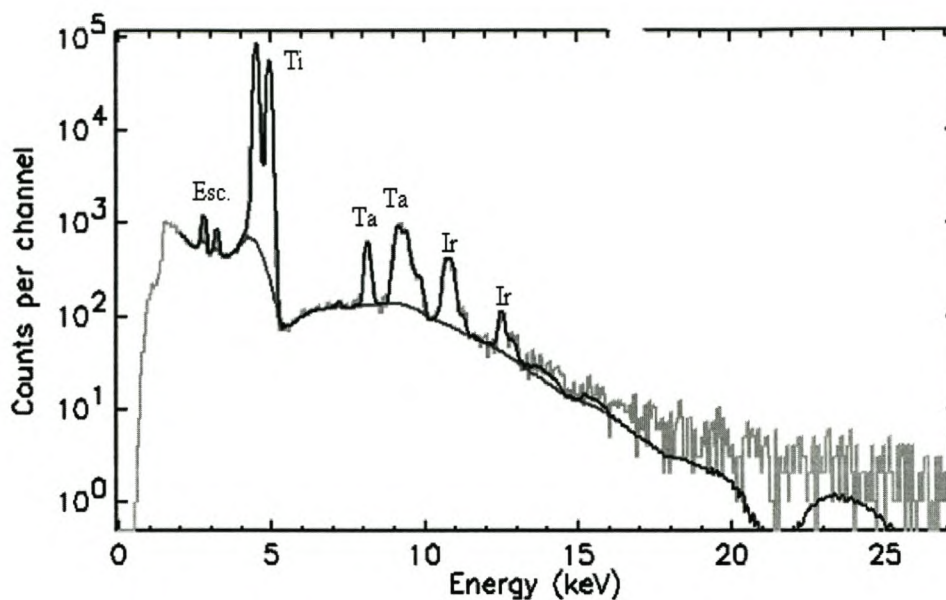


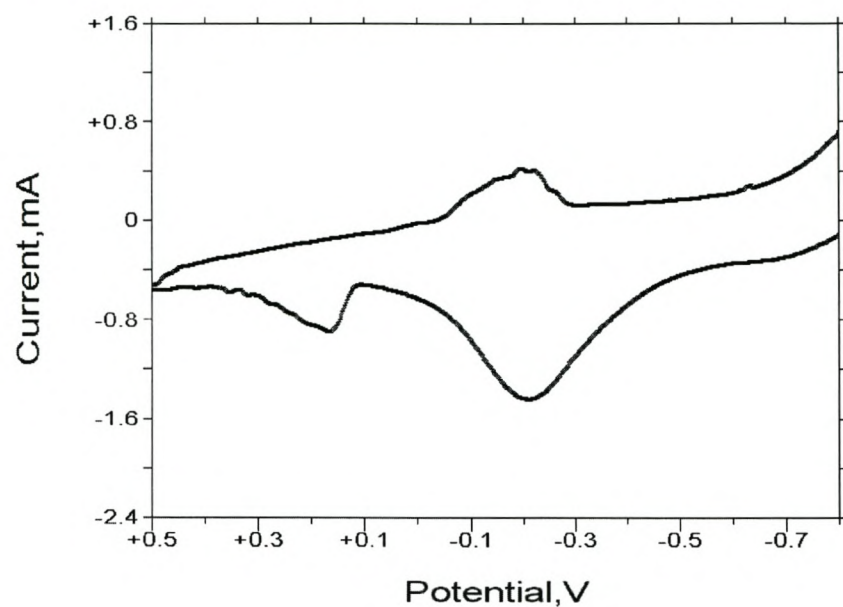
Fig. 5.5 Fitted PIXE spectrum of a Ti/Ta₂O₅-IrO₂ electrode.

5.3.4 Cyclic voltammetric measurements

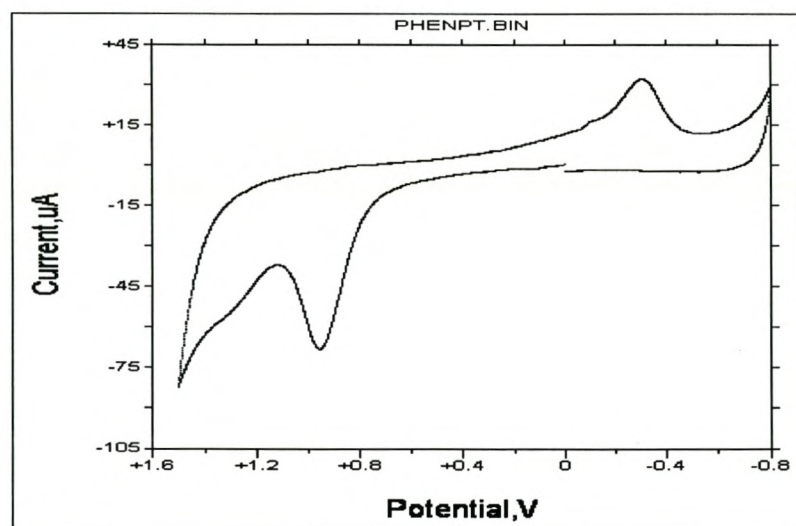
Phenol was chosen to be the model compound for the catalytic activity of Ti/IrO₂-Ta₂O₅ electrode. The cyclic voltammograms of phenol at Ti/IrO₂-Ta₂O₅ and Pt electrodes were recorded. The reference electrode used was Ag/AgCl. Fig. 5.6 shows the comparison in performance between the working electrodes, Ti/IrO₂-Ta₂O₅ and platinum. The cyclic voltammogram in Fig. 5.6 (a) showed the redox process demonstrated the irreversible behaviour. The redox peak occurred at 200 mV vs Ag/AgCl.

The performance of Ti/ Ta₂O₅-IrO₂ was compared to that of the Pt because Pt has been widely used as an anode for oxidation applications. The oxidation potential of phenol was

low (200 mV) compared to that of the Pt electrode, which was at 950 mV vs Ag/AgCl. This indicated that the $\text{Ta}_2\text{O}_5\text{-IrO}_2$ layer had significantly lowered the over-potential for the oxidation of phenol.



(a)



(b)

Fig. 5.6 Cyclic voltammograms of phenol at (a) $\text{Ti/Ta}_2\text{O}_5\text{-IrO}_2$ and (b) Pt electrodes.

5.4 Conclusions

Characterization of the binary oxide electrode Ti/IrO₂-Ta₂O₅ revealed that the IrO₂ and Ta₂O₅ mixed oxide coating layer was heterogeneous with minor cracks. This structure gave rise to a high surface area. The surface morphology and the structure of the coating are important factors affecting the electrocatalytic activity of the thin film. As a result of the crystallization of the Ir and Ta oxides, especially from the solid solution phase during the thermal analysis of mixed chloride precursors, the oxidative dissociation of the IrCl₃ and TaCl₅ mixture into crystalline domains was facilitated.

The IrO₂-Ta₂O₅ (80:20) mixed oxide coating, accompanied by solubility between the two oxides and the crystal grains of the oxides, exhibited the best anodic and electrocatalytic activity. These properties are essential for successful industrial applications. The optimum concentration ratio for the oxidation of organic compounds was 20:80 (Ta:Ir). Indications are that the Ti/IrO₂-Ta₂O₅ electrode is a potential electrochemically active catalyst for the oxidation of phenol. This electrode lowers the overpotential for phenol oxidation.

References

1. Otagawa, R., Morimitsu, M., Matsunaga, M. *Electrochimica Acta*. **1998**, 44, 1509.
2. Otagawa, R., Soda, K., Yamauchi, S., Nagatoishi, Y., Morimitsu, M., Matsunaga, M. *Denki Kagaku*. **1997**, 65 (12), 987.
3. Morimitsu, M., Otagawa, R., Matsunaga, M. *Electrochimica Acta*. **2000**, 46, 401.
4. Murakami, Y., Tsuchiya, S., Yahikozawa, K., Takasu, Y. *Electrochimica Acta*. **1994**, 39 (5), 651.
5. Vercesi, G., Salamin, J., Comninellis, C. *Electrochimica Acta*. **1991**, 36 (5-6), 991.
6. Murakami, Y., Tsuchiya, S., Yahikozawa, K., Takasu, Y. *Electrochimica Acta*. **1994**, 39 (5), 651.
7. Nijjer, S., Thonstad, J., Haarberg, G. *Electrochimica Acta*. **2001**, 46, 3503.
8. Mraz, R., Krysa, J. *Journal of Electrochemistry*. **1994**, 24, 1262.
9. Ushikubo, T. *Catalysis Today*. **2000**, 57, 331.
10. Lassali, T., Boodts, J., Bulhoes, L. *Electrochimica Acta*. **1999**, 44, 4203.
11. Comninellis, C., Vercesi, G. *Journal of Applied Electrochemistry*. **1991**, 21, 335.
12. Kristof, J., Szilagyi, T., Horvath, E., DeBattisti, A. *Thermochimica Acta*. **2004**, 413, 93.

13. Hu, J., Zhang, J., Cao, C. *Thermochimica Acta*. **2003**, 403, 257.
14. Roginskaya Y.E., Morozova, O.V. *Electrochimica Acta*. **1995**, 40 (7), 817.
15. Wang, T.Y., Xu, L.K., Chen, G.Z. *Acta Metallurgica Sinica*. **2001**, 14 (6), 457.
16. Fiamegos, Y., Stalikas, C., Pilidis, G. *Analytica Chimica Acta*. **2002**, 467 (1-2), 105.
17. Doolittle, L.R., *Nuclear Instr. Methods B*. **1985**, 9, 344.
18. Chu, W.K., Mayer, J.W., Nicolet, M.A. *Backscattering Spectrometry*, Academic Press, New York, 1978.
19. Cardarelli, F., Taxil, P., Savill, A., Comninellis, C., Manoli, G., Leclerc, O. *Journal of Applied Electrochemistry*. **1998**, 28, 245.
20. Trasatti, S. *Electrochimica Acta*. **1991**, 36 (2), 225.
21. Krysa, J., Maixner, J., Mraz, R., Rousar, I. *Journal of Applied Electrochemistry*. **1998**, 28, 369.
22. Roginskaya, Y.E., Morozova, O.V., Loubnin, E.N., Popov, A.V., Ulitina, Y.I., Zhurov, V.V., Ivanov, S.A., Trasatti, S. *Journal of Chemical Society: Faraday Trans*. **1993**, 89 (11), 1707.
23. Rasiyah, P., Tseung, A.C.C. *Journal of Electrochemical Society*. **1984**, 131 (4), 803.
24. Li, Y.J., Chang, C.C., Wen, T.C. *Journal of Applied Electrochemistry*. **1997**, 27, 227.

25. Boudenne, J.L., Cerclier, O., Galea, J., Van der Vlist, E. *Applied Catalysis A: General*. **1996**, 143 (2), 185.
26. Feng, Y.J., Li, X.Y. *Water Research*. **2003**, 37, 2399.
27. Gatrell, M., MacDougall, B. *Journal of Electrochemical society*. **1998**, 146 (9), 3335.
28. Santos, A., Yustos, P., Quintanilla, A., Rodriguez, S., Garcia-Ochoa, F. *Applied Catalysis B: Environmental*. **2002**, 39, 97.

6

Preparation, characterization and electrochemical evaluation of Ti/RhO_x-IrO₂ electrode for the oxidation of phenol

Summary

Ti/RhO_x-IrO₂ films were prepared from the chloride precursors of Rh and Ir using the sol-gel technique. These precursors were annealed at 700 °C. The annealing temperature was determined by thermal gravimetric analysis. The morphology of the film was found to be rough, with a grain-like appearance. The phase composition of these metal oxides was determined by XRD. They were found to have crystalline structures. The rhodium oxide had two-phase formations, RhO₂ and Rh₂O₃, attributed to high calcination temperatures. Cyclic voltammetric measurements were performed for the oxidation of phenol. Two oxidation peaks were observed, at -100 and 300 mV respectively. This was an indication that the prepared surfaces or films were catalytically active towards the oxidation of phenol.

6.1 Introduction

Rhodium and its compounds are superb catalysts for a variety of reactions [1]. The metal catalyses the hydrogenation of unsaturated organic molecules, as well as the dissociation of nitrogen oxide (NO) [2]. In combination with oxide promoters, rhodium directs the hydrogenation of carbon monoxide towards higher alcohols [2]. Coatings of pure Ru and Ir oxides, or doped with Ti and / or Sn oxide, have been intensively investigated [2, 3].

However, investigations concerning other metal oxides of the Pt group elements such as Os, Rh and Pd are scarce. Not much has been published about the electrochemical properties of thermally prepared rhodium oxide [2, 3]. The electrochemical stability of RhO_2 electrodes prepared was investigated by Swette et. al. [4]. The results showed this electrode material to be very stable towards both oxygen evolution and reduction, but neither the electrocatalytic activity nor the Tafel plots were evaluated [2].

Oxygen evolution is one of the most important technological reactions in electrochemistry, taking place at the anode of water electrolyzers, in metal electro-winning processes, in cathodic protection, and in electro-organic reduction. Oxygen evolution is very often the more difficult of the two electrolytic reactions in an electrochemical cell, so that the economy of the entire process is governed by that of the anodic reactions. Oxygen evolution is a critical reaction since it creates very aggressive conditions for the electrode material of an anode. This is particularly true in acid solution, in which the severe conditions are enhanced in applications involving proton conductor solid polymer electrolytes. The latter environment is resisted only by thermal oxides of precious transition metals, which belong to the wide class of dimensionally stable anodes (DSAs) [5].

Studies on the electrochemical properties of Ti/RhO_x electrodes prepared by thermal decomposition of suitable precursors have been conducted by other researchers [6, 7]. It has been found that RhO_x is more active than both RuO_2 as well as IrO_2 for hydrogen evolution in acid solution.

Aramata et. al. [8] studied the influence of Sn-oxide on the electrocatalytic activity of Rh, Ir and Pt-based oxide mixtures. In the case of the Rh-based electrode materials, the introduction of tin oxide in the coating caused a negative effect in the catalytic activity. In this dissertation, studies on Rh oxide doped Ir –oxides were conducted and are reported on here.

6.2 Experimental

The experimental procedures are outlined in chapter 3.

6.3 Results and discussion

6.3.1 Thermal analysis

TGA curves of Ti/RhO_x-IrO₂ electrodes were recorded to establish the temperature range in which the precursor decomposition occurs. With respect to this issue, one must always keep in mind that the decomposition of a solid residue in the powder form is not always comparable to the decomposition of successive layers on a Ti support.

For the starting material of hydrated RhCl₃, the number of the hydration water molecules calculated from the initial weight loss is 3.07. TGA results showed that hydrated RhCl₃ decomposed at rather high temperatures (Fig. 6.1). An increase in calcination temperature increased the active surface area. Increase in calcination temperature resulted in a more complete decomposition of the chloride precursor salts.

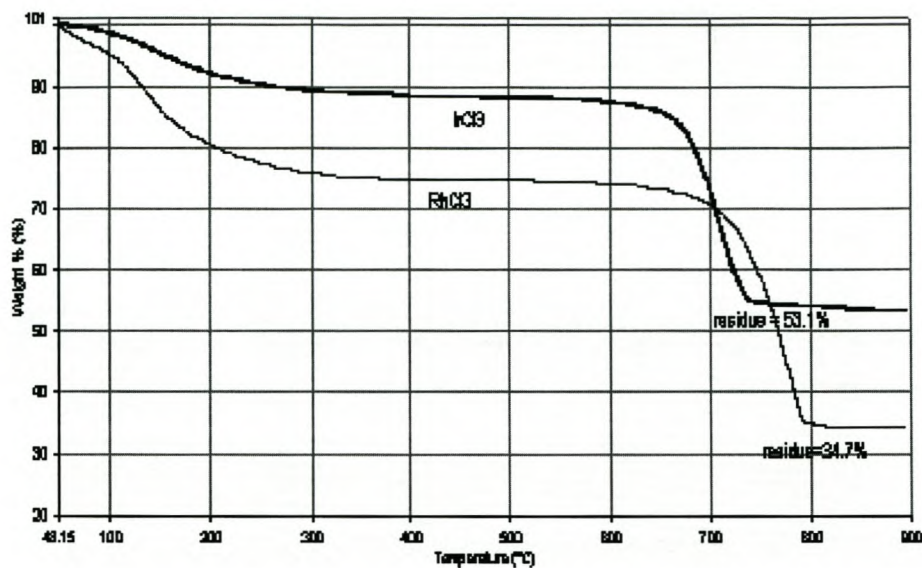


Fig. 6.1: TGA curves of the hydrated RhCl₃ and IrCl₃ respectively.

Representative TGA curves recorded for the evaporation residue of IrCl₃ + RhCl₃ precursor mixtures are shown in Fig. 6.2. It was difficult to identify the individual thermal decomposition steps. A general feature of the TGA curves is the existence of two steps of weight loss, suggesting the first evaporative loss then decomposition and oxidation of the components. It was found that the oxidative decomposition of the mixtures with lower Rh content shifted to lower temperatures. About 60% weight of Rh/Ir (20:80) was found to be decomposed while 40% weight was unoxidized.

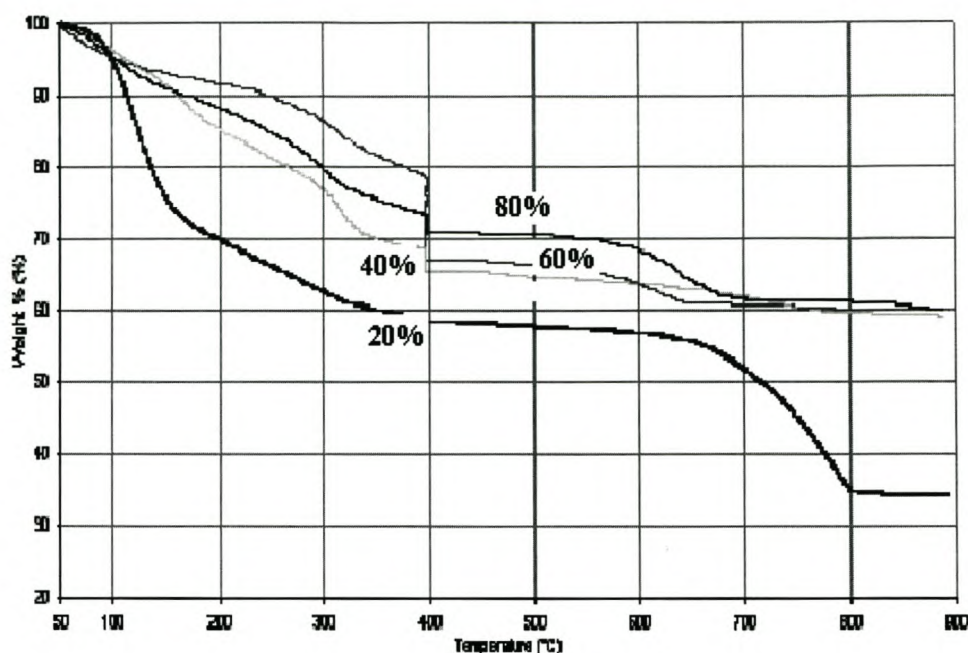
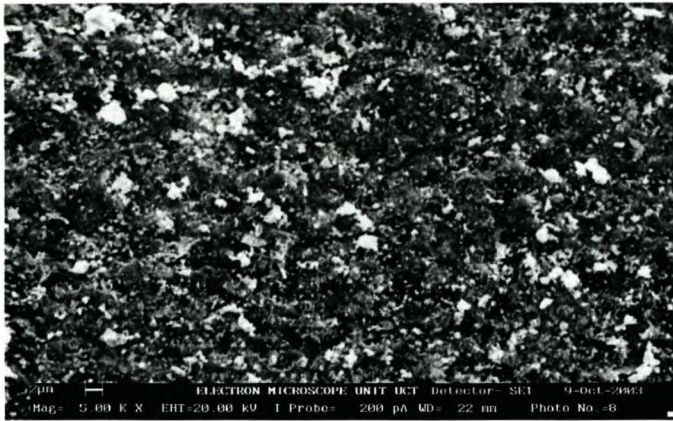


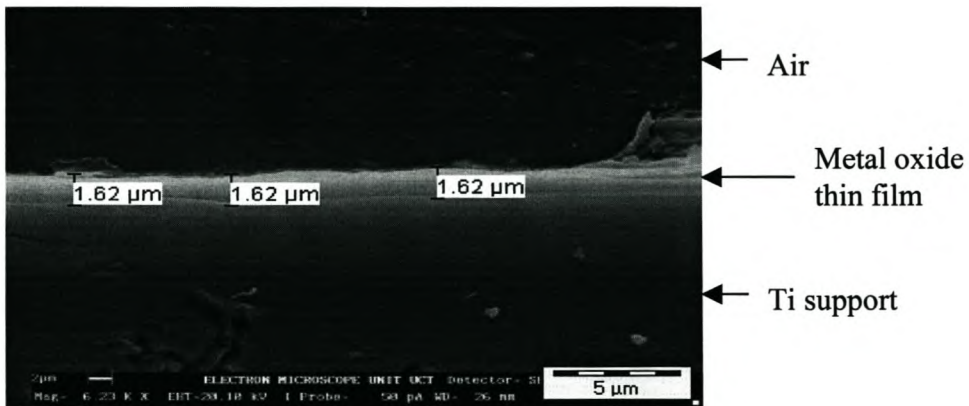
Fig. 6.2: TGA curves of Rh-Ir oxides, as the Ir content was decreased from 80 % to 20%.

6.3.2 Surface Analysis

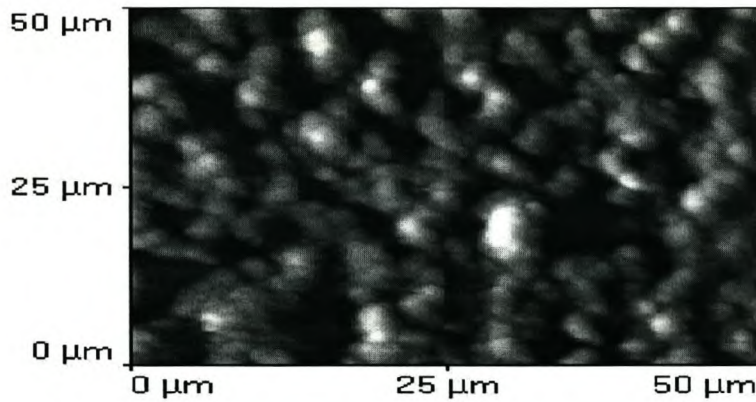
The morphology of the electrode coating strongly depends on the composition of the precursor solution of hydrated RhCl_3 and IrCl_3 and the conditions of preparation. Fig. 6.3 shows SEM micrographs of the $\text{Ti/RhO}_x\text{-IrO}_2$ coating prepared by the sol gel technique. This coating was calcined at 700 °C. The morphology of the coating layer appeared to be uniform. A rough porous coating was observed. This observation was confirmed by the AFM results, which showed that as the Rh content increased, the area roughness in terms of average peak height differences increased.



(a)



(b)



(c)

Fig. 6.3 The microstructure of a Ti/RhO_x-IrO₂ electrode. (a) SEM surface image, (b) SEM cross sectional surface image and (c) AFM surface image.

EDX revealed that the active coating layer is predominantly Ir and poor in Rh content as expected. It also indicated that the crevices were rich in TiO_2 and poor in both Rh and Ir content. The results obtained here confirmed the results reported by Roginkaya et.al. [7] where a low Ti content was found in the valleys. Because of the high calcination temperature, the oxidation of Ti support resulted in TiO_2 migration towards near-to-the-surface regions of the RhO_x/Ir -oxide coating.

The presence of rutile TiO_2 was confirmed by XRD measurements. The thickness of the coating layer was also determined by SEM analysis of a surface cross-sectional area. It was found that the thickness of the coated film was about $1.62 \mu\text{m}$.

XRD showed the crystalline structures of the coated metal oxides (Fig. 6.4). It also indicated the presence of TiO_2 in the rutile phase, which is agreement with results obtained from EDX. The oxides were isostructural and adopted a disordered rutile-type structure. The rutile structure is adopted by a large number of binary MO_2 , and ternary $\text{MM}'\text{O}_4$ oxides [3, 7].

Rutile-type oxides exhibit a diverse range of electronic and magnetic properties that are sensitive to the precise structure of the material [7, 8]. Despite the crystallographic simplicity of the rutile structure, numerous attempts to rigorously explain structural variations in rutile type oxides have not been successful, nor has it been possible to predict the precise structural features of rutiles.

The XRD results of $\text{Ti/RhO}_x\text{-IrO}_2$ indicated that mixed phases of rhodium oxides were observed; the rhodium seems to enter the rutile structure as Rh^{4+} tetragonal RhO_2 and the rhombohedral Rh_2O_3 . The two-phase formation of rhodium is attributed to the high calcination temperatures.

Iridium oxide was observed to be tetragonal in structure as IrO_2 . The mixed phases of the rhodium oxides found agreed with the results obtained by De Campos, et al. [3] which showed, using XRD that the decomposition of the precursor containing RhO_2 which is partially transformed to Rh_2O_3 when higher calcinations temperatures are employed. No chlorides from the precursors were observed by XRD, indicating that there was a complete conversion of chlorides to oxides at $700\text{ }^\circ\text{C}$. These results correlate well with the results obtained from TGA.

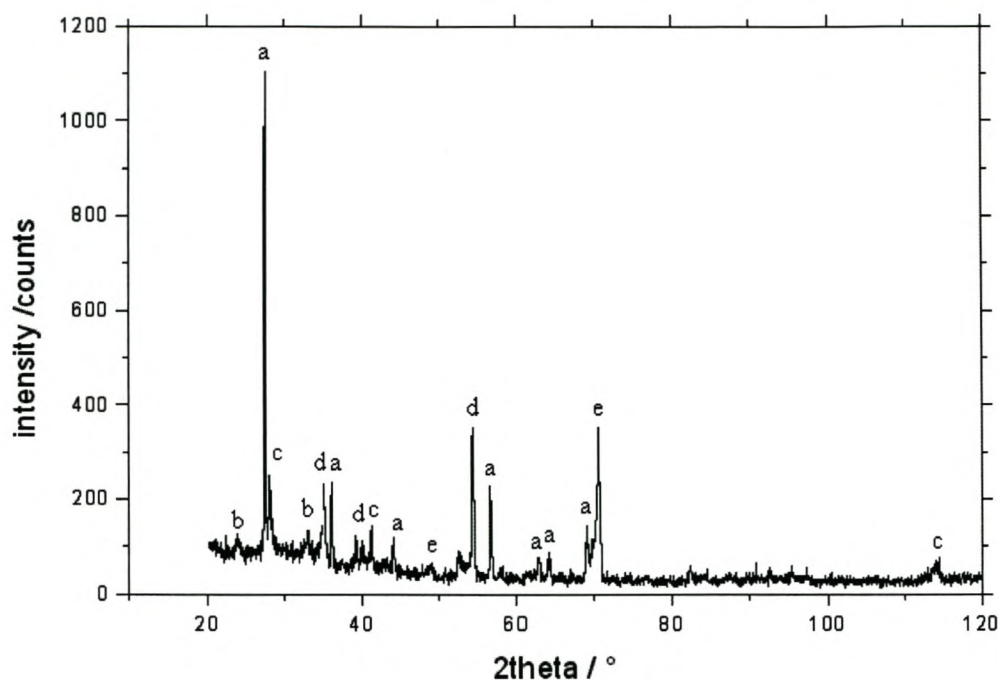


Fig. 6.4 XRD patterns of a Ti/RhO_x-IrO₂ electrode (a) TiO₂, (b) Rh₂O₃, (c) IrO₂, (d) RhO₂ and (e) Ti.

6.3.3 RBS measurements

In the RBS spectrum of a Ti/RhO_x-IrO₂ sample (Fig. 6.5), the energy at which elements will be observed when they are on the surface, are indicated by the vertical lines of the arrows. The signals from lower energies (or channels) to the left of these positions are from backscattering events deeper into the sample and thus represent a depth scale that correlates deeper positions in the sample with lower energies.

RBS results distinctively showed three layers of the metal precursors loaded on titanium substrate. RBS simulations (RUMP) used Rh and Ir since their presence had also been

confirmed by other techniques, such as XRD and EDX. From the RBS spectrum it was deduced that the sample could be simply described as a pure Ti substrate onto which some Rh/Ir had been coated.

The first layer consisted of Ir and Rh, of which the Ir signal was visible at an energy level of 2.3 MeV and Rh was found at 2.1 MeV. The RBS results showed that the concentration of these metals was not constant over this layer. There is an indication that these metals diffused into the substrate.

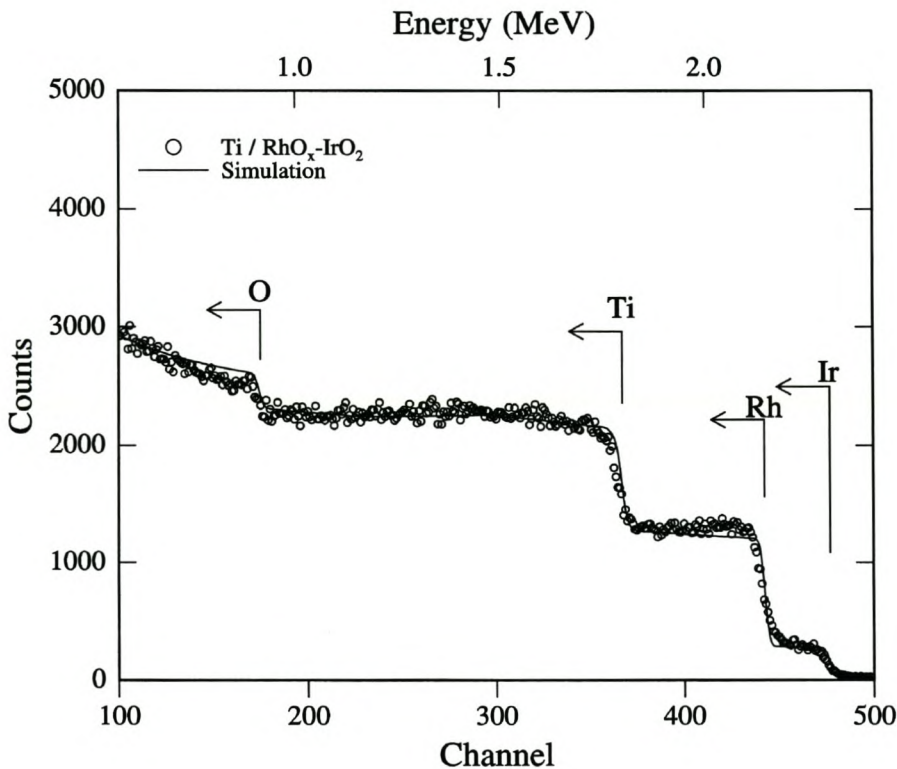


Fig. 6.5 RBS simulated spectrum of a Ti/RhO_x-IrO₂ electrode.

6.3.4 Cyclic voltammetric measurements

A cyclic voltammogram for the oxidation of phenol was recorded in the potential range of -1200 to 1600 mV vs. Ag/AgCl. Cyclic voltammetry in a limited potential range to obtain the electrochemical spectrum of the surface and related surface change is shown in Fig. 6.6. The peak observed at 1200 mV is associated with oxygen evolution. The phenol oxidation peak was observed at the potential of 200 mV. The peak observed at -200 mV was attributed to the hydrogen evolution.

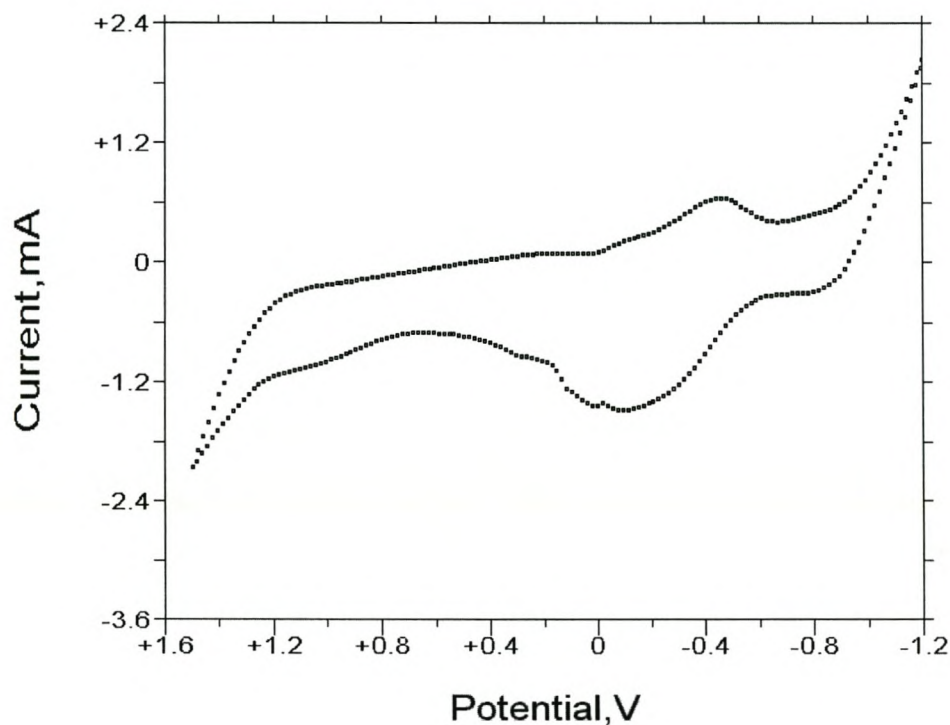


Fig. 6.6 Cyclic voltammograms of phenol at a Ti/RhO_x-IrO₂ electrode.

6.4 Conclusions

The morphology of the Ti/RhO_x-IrO₂ electrode was homogenous, porous and rough with minor cracks, characteristic of the thermally prepared oxide layers [3]. These surfaces were prepared by dissolving hydrated RhCl₃ and IrCl₃ in absolute ethanol, dip-coating and annealing the substrate and coating at 700 °C. XRD results show that crystalline phases of these metal oxides were formed. RBS results confirmed the presence of Rh and Ir in the surface layers of Ti/RhO_x-IrO₂. Cyclic voltammetry showed the potential at which phenol was oxidized, and indicated that the prepared surfaces were catalytically active.

References

1. Tomczak, D.C., Lei, G.D., Schunemann, V., Trevino, H., Sachtler, W.M.H. *Microporous Materials*. **1996**, 5, 263.
2. Baranova, E., Foti, G., Comninellis, C. *Electrochemistry Communications*. **2004**, 6, 389.
3. De Campos, P.M., Benedetti, A.V., Faria, L.A., Cardoso, V., Boodts, J.F.C. *Electrochimica Acta*. **2002**, 47, 1283.
4. Swette, L., LaConti, B., McCatty, A. *Journal of Power Sources*. **1994**, 47 (3), 343.
5. de Souza, A., Arashiro, E., Golveia, H., Lassali, T. *Electrochimica Acta*. **2004**, 49, 2013.
6. Trasatti, S. *Electrochimica Acta*. **2000**, 45, 2377.
7. Roginskaya, Y.E., Morozova, O.V., Kaplan, G.I., Shifrina, R.R., Smirnov, M., Trasatti, S. *Electrochimica Acta*. **1993**, 38, 2435.
8. Aromata, A., Toyomisha, I., Enyo, M. *Electrochimica Acta*. **1992**, 37 (8), 1317.
9. Hrussanova, A., Guerrini, E., Trasatti, S. *Journal of Electroanalytical Chemistry*. **2004**, 564, 151.
10. Wang, H., Yan, M., Jiang, Z. *Thin solid Films*. **2001**, 401, 211.
11. Gottesfeld, S. *Journal of Electrochem. Society*. **1980**, 127, 272.
12. Janssen, M.M.P., Moolhuysen, J. *Electrochimica Acta*. **1976**, 21, 861.

7

Further mechanistic study of the mixed metal oxides surfaces using rotating disk electrode (RDE)

Summary

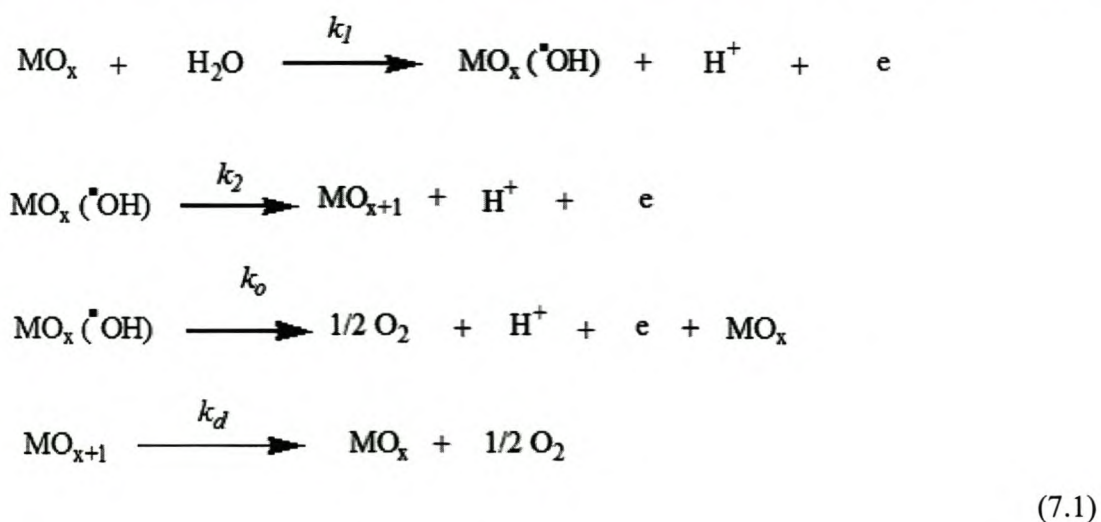
Rotating disk electrode (RDE) was used to determine the kinetic parameters of the electron-transfer reaction involving phenol at the Ti/SnO₂-RuO₂-IrO₂, Ti/Ta₂O₅-IrO₂ and Ti/RhO_x-IrO₂ electrodes. According to the Levich equation, current is directly proportional to the square root of the rotation speed. As the rotation speed increased, the oxidation peaks for phenol are separated, indicating independent electron transfer processes. The rate at which the oxidation of phenol occurred at different oxide surfaces was determined.

The oxidation rate of phenol was found to depend on the nature of the anode material. It was also found that the oxidation rate not only depended on the chemical composition of the anode, but also on morphology of the prepared oxide surfaces as is dependent on preparation procedure.

7.1 Introduction

The determination and characterization of phenolic compounds have received a considerable amount of attention due to their importance in food, environmental and industrial processes [1-2]. Although the electrochemistry of phenol and phenolic compounds has been studied extensively, certain mechanistic aspects have not been explored fully [3-8].

Not much has been done in the way of examining the stages of the oxidation of phenol and the relative efficiency of different materials to the kinetic steps involved in the conversion to CO₂. Active electrode materials such as noble metals and intermediate metal oxides such as IrO₂ will go to more oxidized states by inducing anodic conditions [6-10]. It is found that they can oxidize solution species only by direct electrochemical oxidation or by subsequent transfer of the bound oxygen to the solution species. Formation of hydroxyl radicals (see reaction in 7.1) on the surface of some electrode materials has been demonstrated by in situ studies involving spin-trapping reagents [7].



In this chapter the electrochemical oxidation of organic compound phenol at precious metal oxide electrodes is described. Phenol was selected as a model compound since it is known to undergo oxidation to p-benzoquinone. The benzoquinone can be further oxidized to form carboxylic acids. Benzoquinone is also capable of being reversibly reduced to form hydroquinone.

7.1.1 The RDE technique

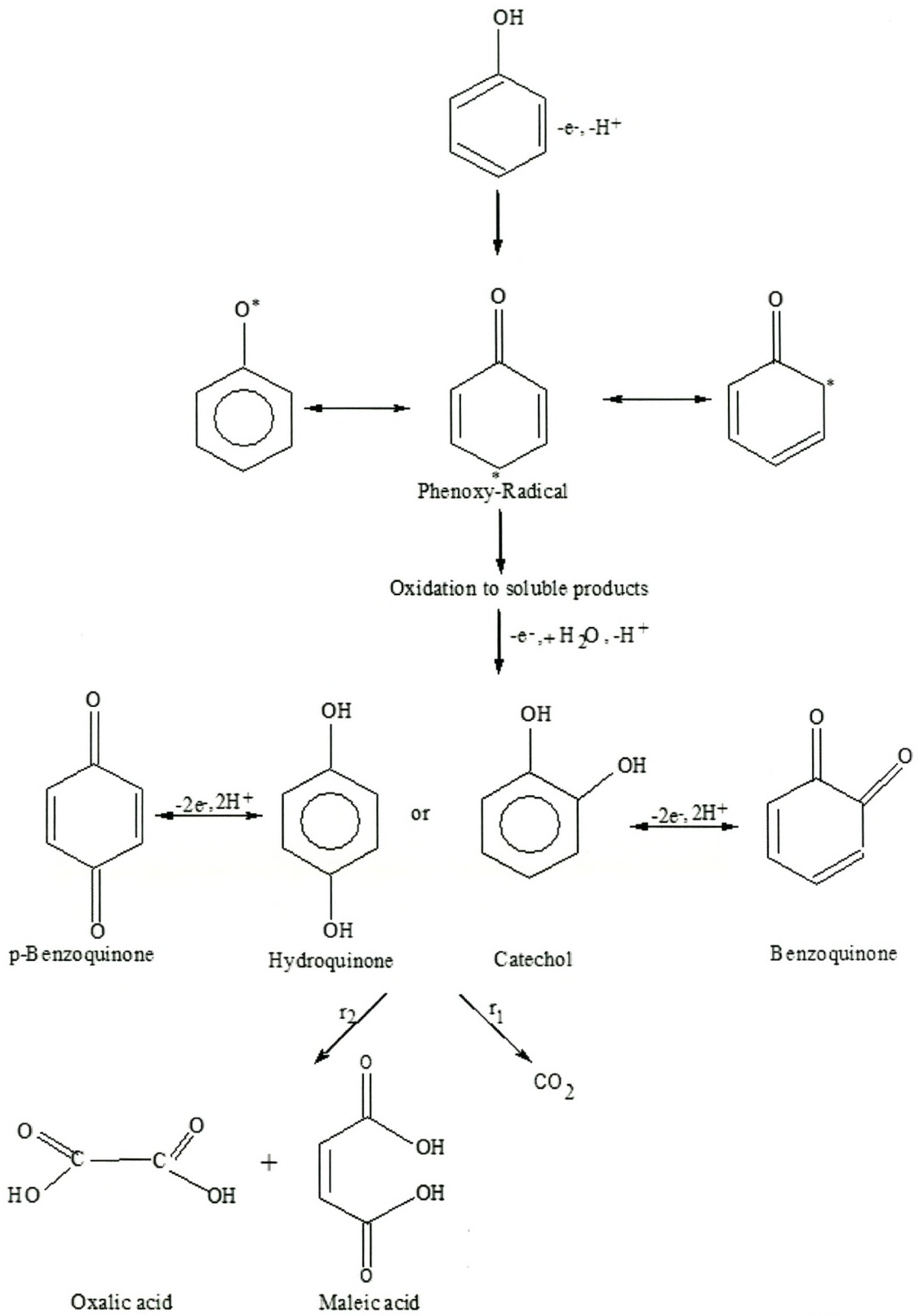
Transport of the reacting species to the surface of electrodes occurs both by convection and diffusion. One advantage of using RDE is to determine the fact that the mass transport is uniform, so that the surface concentration of any reacting species is constant over the working surface of the electrode [5, 11-12].

Several electrochemical techniques have been developed in which forced convection is induced in the cell [5]. These hydrodynamic techniques can be sub-divided into two categories: (i) those in which the electrode induces flow in the cell via its motion (e.g., a rotating disk electrode) and (ii) those in which the electrode is stationary and flow is forced over the electrode surface (e.g., wall jet electrode). For this study the rotating disk electrode was chosen in preference to the wall jet electrode because it is easy and cost effective to design a rotating disk for metal oxides. RDE experiments were performed with Ti/SnO₂-RuO₂-IrO₂, Ti-Ta₂O₅-IrO₂ and Ti/RhO_x-IrO₂ thin film electrodes.

Hydrodynamic methods are employed in electrochemical systems because they increase the rate of mass transport to the electrode surface beyond what is typically observed under conditions where transport is governed solely by diffusion. The consequent enhancement in the mass transport rate leads to a greater range of kinetic parameters, i.e. charge-transfer kinetics being measured. A further advantage of inducing hydrodynamic flow in an electrochemical cell is the fast onset of a steady state response, which significantly reduces the contribution of transient effects such as double layer charging on the measured response.

7.1.2 *Phenol oxidation*

The rotating disk electrode technique was used in this study to characterize the behaviour of phenol at precious metal oxide electrodes. Phenol is oxidized to form quinone in a two-electron reaction. Under severe anodic conditions, quinone can be oxidized to maleic acid and other compounds that are not electrochemically reducible at the potentials for quinone reduction [4, 13-14], and ultimately to CO₂. Thus the detection of quinone can be used to monitor the extent of reaction and the subsequent disappearance of quinone via reaction (7.2) and final pathways to complete incineration [14-16]. Reaction 7.2 shows the general schematic diagram for the oxidation of phenol down to the acids.



(7.2)

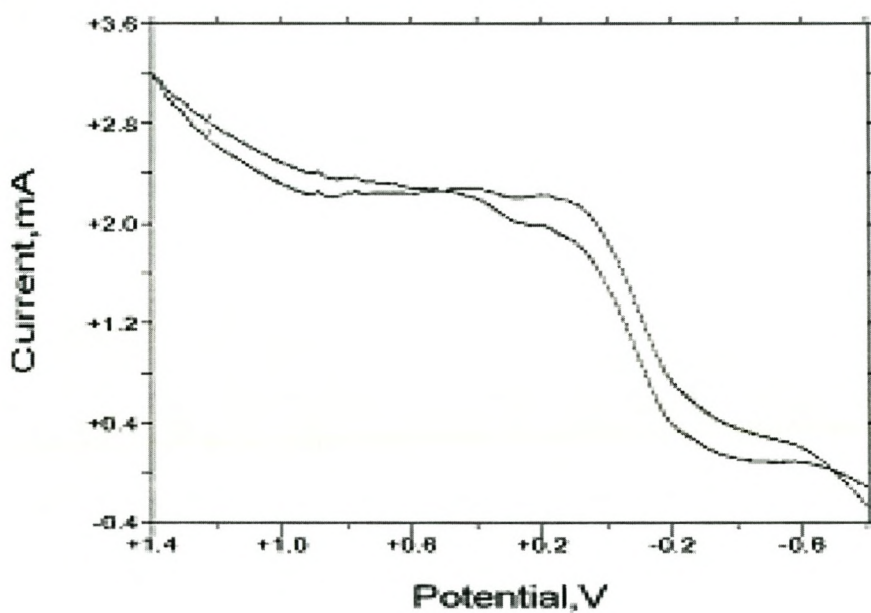
7.2 Experimental

Experimental procedure is outlined in Chapter 3.

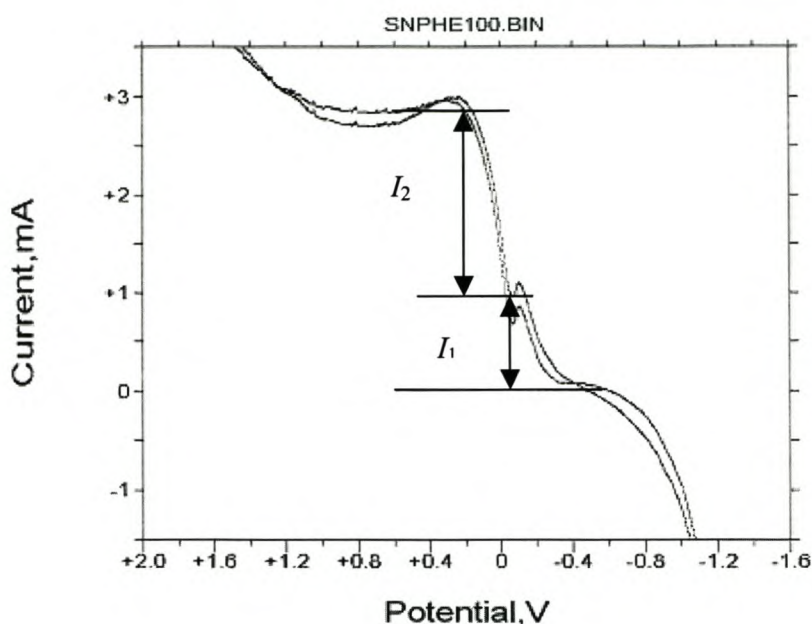
7.3 Results and discussion

RDE voltammogram of 3 mM phenol were performed using the Ti/SnO₂-RuO₂-IrO₂, Ti/Ta₂O₅-IrO₂ and Ti/RhO_x-IrO₂ electrodes to illustrate the nature of the oxidation of phenol to quinone.

(a) *Discussion of the oxidation of phenol at the Sn/Ru/Ir system using RDE*



(a)



(b)

Fig.7.1: RDE voltammograms of phenol at Sn/Ru/Ir oxide electrode (a) under diffusion controlled conditions and (b) at a rotation speed of 1000 rpm.

The RDE curve (Fig. 7.1 (a)) under diffusion-controlled conditions shows the oxidation peak of phenol at 200 mV. These results are in agreement with the cyclic voltammogram (Fig. 4.6 (b)) shown in section 4.3.5 of a typical cyclic voltammogram scanned between -600 mV and 1400 mV, under diffusion controlled conditions, with a prominent oxidation peak for the conversion of phenol to quinone at about 200 mV, and a reduction peak of quinone to hydroquinone at about -200 mV. The re-oxidation of hydroquinone to quinone could not be observed because of mass transfer limitations.

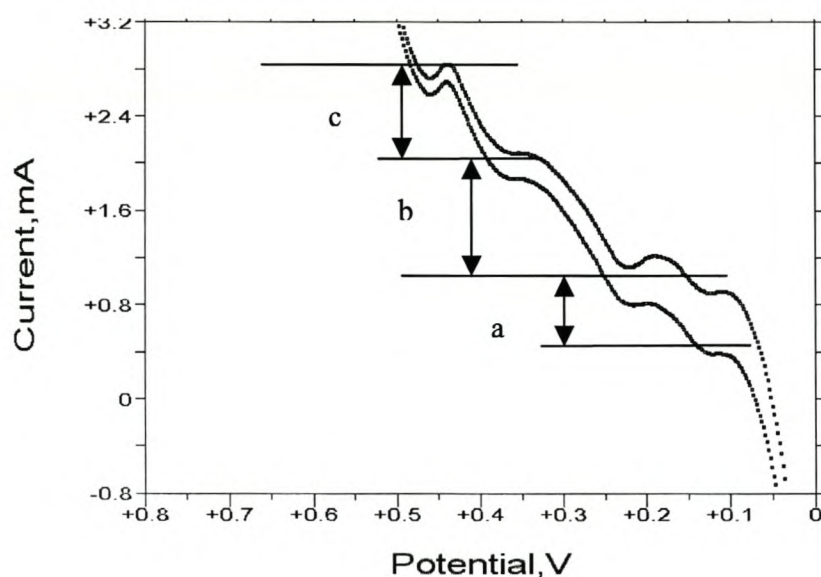
However, as the rotation speed was increased during the RDE experiments, the oxidation peak of phenol observed at 200 mV became separated (see Fig. 7.1 (b)). The splitting of

the oxidation peak is also observed in a Levich plot (Fig. 7.4) where I_{lim} is plotted against the $\omega^{1/2}$. The splitting of the oxidation peak is attributed to the multiple electron transfer responsible for the conversion of phenol to quinone. The first oxidation peak was observed at -100 mV and the second one at 200 mV. It is thought that this split signifies the initial electron oxidation of phenol, followed by a two-electron oxidation of the product to form benzoquinone.

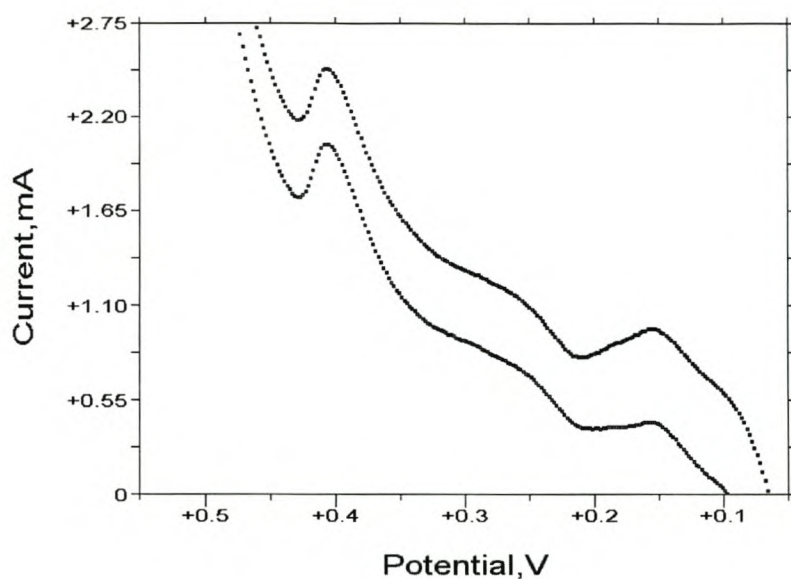
$$I_1 = \frac{1}{2} (I_2) \quad (7.3)$$

The height of the first and the second peaks is in a ratio of 1:2, supporting this hypothesis (see equation 7.3). At rest or low rotation speed, this is not seen. The separation of the oxidation peak of phenol for the Sn/Ru/Ir system could only be observed at higher rotation speeds of about 300 rpm or more.

(b) *Discussion of the oxidation of phenol at the Ta/Ir system using RDE*



(a)



(b)

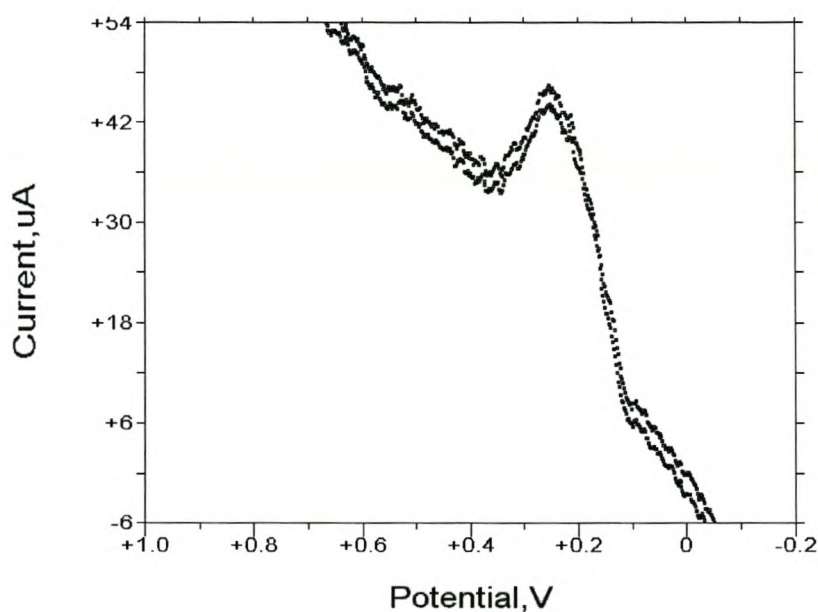
Fig.7.2: RDE voltammograms of phenol at Ta/Ir oxide electrode (a) under diffusion controlled conditions and (b) at a rotation speed of 1000 rpm.

Fig. 7.2 shows the RDE curves for the Ta/Ir system at both the low and high rotation speed. At low rotation speed the three distinctive peaks are observed at ~ 100 , 200 , 300 and 450 mV in Fig. 7.2 (a). These peaks indicated the three distinctive processes that could be attributed to the formation of namely, the oxidation of phenol to phenoxy radical, phenoxy radical to quinone and quinone to hydroquinone. The RDE results observed during the diffusion-controlled conditions differ from the results obtained from cyclic voltammetry (Fig. 5.6 (a)) of this particular system. The cyclic voltammogram of this system showed the oxidation of phenol at the oxidation potential of ~ 200 mV. The other peak that was observed at the potential of ~ 200 mV was due to the hydrogen gas

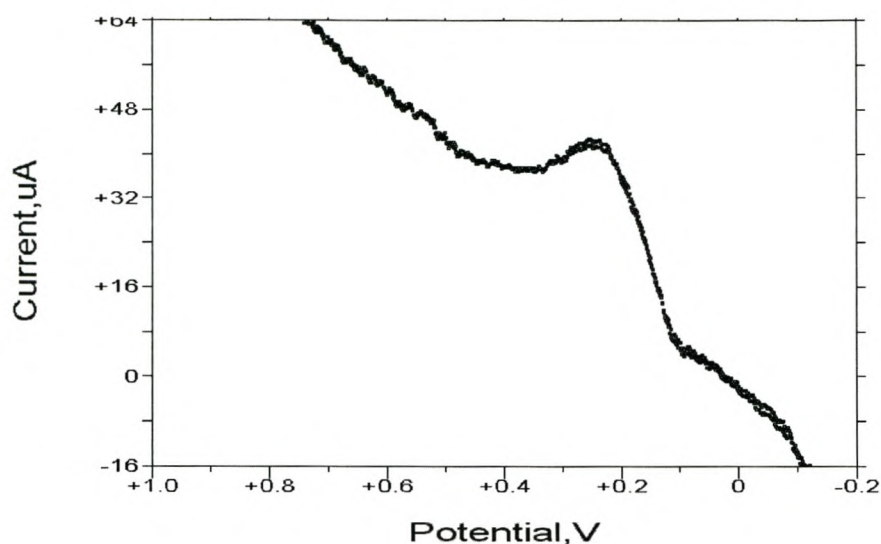
evolved. No peak was observed at ~ 300 mV as indicated by the RDE curve at low rotation speed.

As the speed of the rotating disk electrode increased, only two peaks were observed at the oxidation potential of ~ 200 and 450 mV. The peaks labeled (a) and (b) observed in Fig. 7.2 (a) were merged. This observation was attributed to the disappearance of the phenoxy radical and the oxidation of phenol to benzoquinone and the oxidation of benzoquinone to hydroquinone. The Levich plot (Fig. 7.5) of this particular system supported the obtained RDE curves by showing two straight lines that converged as a function of the square root of the rotation speed. This observation was attributed to the hydrogen gas interference observed in cyclic voltammogram of this system.

(c) *Discussion of the oxidation of phenol at the Rh/Ir system using RDE*



(a)



(b)

Fig.7.3: RDE voltammograms of phenol at Rh/Ir oxide electrode (a) under diffusion controlled conditions and (b) at a rotation speed of 1000 rpm.

Fig. 7.3 shows the RDE curves for the Rh/Ir system at both the low and high rotation speed. The cyclic voltammogram (Fig. 6.6) and RDE curves showed that the oxidation of phenol for this system was also observed at ~ 200 mV. The peak did not split or merge as the speed of the rotating disk electrode increased, but the decrease in the kinetic current was observed (Fig. 7.6). The RDE results are also in agreement with the Levich plot of this particular system. The cyclic voltammogram showed a peak of the hydrogen gas evolution at a potential of about ~ -200 mV. The decrease in the kinetic current is attributed to the hydrogen gas interference.

The metal oxides electrodes exhibited irreversible behaviour towards multi-electron processes, and the hydroquinone/quinone couple was no exception [6]. The behaviour of the electrodes Ti/SnO₂-RuO₂-IrO₂, Ti/Ta₂O₅-IrO₂ and Ti/RhO_x-IrO₂ towards 3 mM phenol oxidation is shown in Figures 7.4 - 7.6. These electrodes reached limiting currents for phenol at ~200 mV. The limiting current, I_{lim} , arising from convective-diffusive flux induced by a rotating disk electrode has a square root dependence on the rotation frequency ω , as given by Levich equation [6.1]:

$$I_l = 0.62 n F A D^{2/3} \omega^{1/2} \nu^{-1/6} C^* \quad (7.1)$$

where ν is the kinematic viscosity of the aqueous solution, A is the electrode area and n , the number of electrons transferred, D is the diffusion coefficient and C is the concentration of the electroactive species. Figures 7.4 - 7.6 show the plots of the I_{lim} values obtained against $\omega^{1/2}$.

The current-potential characteristics of a redox reaction can thus be measured in the following way: an over-potential η is applied, and the current is measured for various rotation rates ω . From the Levich plot the corresponding kinetic current $j_k(\eta)$ is extrapolated, as shown in Figures 7.4 - 7.6.

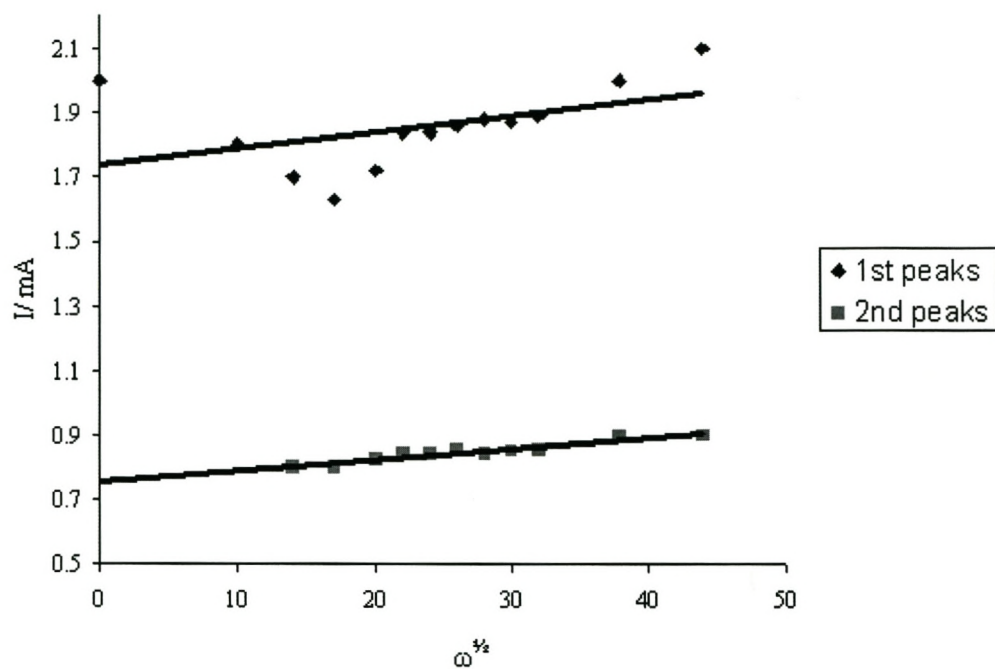


Fig. 7.4 Levich plot for the phenol reaction at Sn-Ru-Ir-oxide electrode.

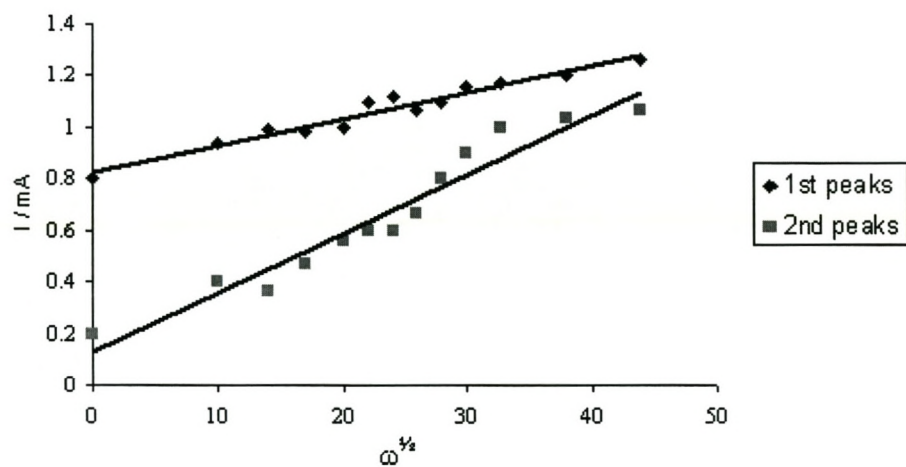


Fig. 7.5 Levich plot for the phenol reaction at Ta/Ir-oxide electrode.

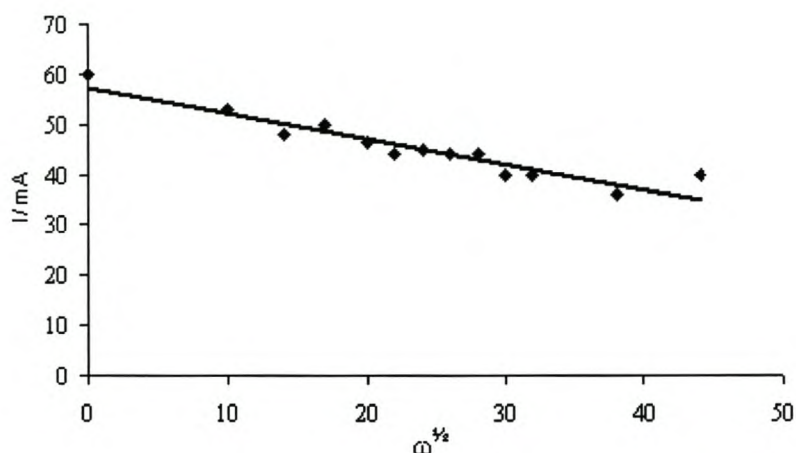


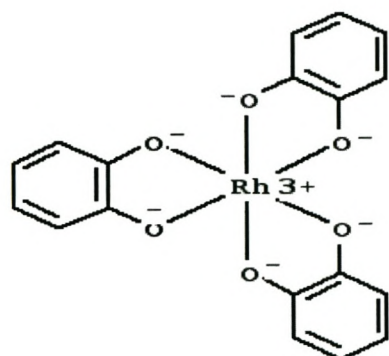
Fig. 7.6 Levich plot for the phenol reaction at Rh/Ir-oxide electrode.

The first and the second peaks shown in the graph represent the oxidation peaks of phenol formed as a function of the rotation speed. For the Sn/Ru/Ir system (Fig. 7.4), initially diffusion is the rate-limiting step. One broad peak is observed when mass transfer is only diffusion controlled. When the rotation speed increases, then the rate of mass transfer becomes fast. The broad peak splits into two as a function of rotation speed. The split of the two broad peaks is due to the two electron transfer that takes place during the phenol oxidation process. The I_{lim} of these peaks increased with an increase in the rotation speed.

This is an extrapolation to infinitely fast mass transport for which surface and bulk concentrations would be equal, and the measured current, J would equal the kinetic current, j_k .

For the Ta/Ir system, the two peaks were observed during diffusion and convection. The I_{lim} increased with an increase in the rotation speed. For the Rh/Ir system, only one peak

was observed. The I_{lim} decreased with an increase in the rotation speed. This indicated that adsorption of the phenol compounds took place on the electrode. This adsorption tended to retard the oxidation process taking place. The Rh/Ir system was prone to adsorption because it had a tendency to form complexes with by-products of phenol. According to the literature reports [17] Rh can easily bond to the strong bases, like phospho and nitro-compounds, and also to the oxy-compounds, for example:



6-hydroxy, tri-phenyl Rhodium (III) complex

7.4 Conclusions

RDE studies showed how precious metal oxide electrodes have their ability to oxidize phenol to less harmful compounds. Rotating disk electrochemistry is a hydrodynamic technique that provided a variable improvement of mass transfer for this reaction. It was found that the reaction of phenol taking place on the electrode depended on the mass transfer rate, ie. the rotation speed of the electrode. Results of RDE experiments showed the various electron transfer processes that are involved in the oxidation of phenol. The one broad oxidation peak for the Sn/Ru/Ir system, observed during diffusion-controlled experiments was split into two in the ratio of 1:2 at a rotation speed of 300 rpm or more. The split signified an initial one-electron oxidation of phenol, followed by a two-electron oxidation of the formed benzoquinone.

References

1. Wang, P., Lee, H. *Journal of Chromatography A*. **1997**, 789, 473.
2. Boudenne, J.L., Cerclier, O., Galea, J., Van der Vlist, E. *Applied Catalysis A: General*. **1996**, 143:2, 185.
3. Gatrell, M., MacDougall, B. *Journal of Electrochemical society*. **1998**, 146:9, 3335.
4. Andreescu, S., Andreescu, D., Sadik, O.A. *Electrochemistry Communications*. **2003**, 5, 681.
5. Bard, A.J, Faulkner, L.R. *Electrochemical Methods: Fundamentals and Applications*, 2nd Ed., Wiley, New York, 2001; Chapter 9.
6. Foti, G., Gandini, D., Comninellis, C., Perret, A., Haenni, W. *Electrochem. Solid State Lett.* **1999**, 2, 228.
7. Comninellis, C., DeBastisti, A. *Journal of Chim. Phys.* **1996**, 93, 673.
8. Bock, C., MacDougall, B. *Journal of Electrochemical Society*. **1996**, 146, 2925.
9. Shopchak, D., Miller, B., Avyigal, Y., Kalish, R. *Journal of Electroanalytical Chemistry*. **2002**, 538-539, 39.
10. Alehashem, S., Chambers, F., Strojek, J., Swain, G.M. *Anal. Chemistry*. **1995**, 67, 2812.
11. Pletcher, D., Walsh F. C. *Industrial Electrochemistry*, 2nd Edition, Chapman and Hall, London, 1990.

12. Brett, M.A., Brett, and M.O. *Electrochemistry: Principles, Methods and Applications*, Oxford Science Publications, 1993.
13. Hawley, D., Adams, R. *Journal of Electroanal. Chemistry*. **1964**, 8, 163.
14. Xu, J., Chen, Q., Swain, G.M. *Anal Chemistry*. **1998**, 70, 3146.
15. Yoo, K., Miller, B., Kalish, R., Shi, X. *Electrochem. Lett.* **1999**, 2, 233.
16. Kralj, B., Dryfe, R.A.W., *Electrochemistry Communications*. **2003**, 5, 325.
17. Trzeciak, A., Ziolkowski, J., Lis, T. *Journal of Organometallic Chemistry*. **1999**, 575 (1), 87.

8

Degradation of phenol by bulk electrolysis in a batch system using metal oxides electrodes

Summary

Phenol is often found in industrial wastewater and is considered a hazardous pollutant. Hence, a systematic study of phenol degradation by the prepared mixed metal oxide electrodes was carried out. Fundamental kinetic data were obtained for the conversion of phenol. The degradation of phenol in aqueous solution and its by-products were investigated by bulk electrolysis and HPLC. Bulk electrolysis experiments were performed at a constant potential of 1500 mV. During electrolysis, phenol was converted to benzoquinone / hydroquinone, which were further oxidized to various carboxylic acids.

8.1 Introduction

Electrochemical oxidation opens up new ways of treating organic compounds. Phenol is considered to be an intermediate product in the oxidation pathway of higher molecular weight aromatic hydrocarbons, thus it is often used as a model compound for advanced wastewater treatments [1, 2]. Several researchers [1-5] have worked on the electrochemical destruction of phenolic wastes, but to date it has not been considered to be commercially viable because of a low phenol reaction rate and/or low removal and destruction efficiency. Others encountered problems of electrode fouling, which also reduced the efficiency of the process [6]. One way in which these problems can be

overcome is to use alloyed electrodes, also labeled promoters, such as Ru, Sn, or Ti with Pt [4]. Comninellis et al. [6] have developed an electrochemical reactor using Ti/IrO₂ and Ti/SnO₂ anodes, which allowed the complete mineralization of phenol and/or benzoquinone.

Generally, the electrochemical oxidation of an organic compound in aqueous solution results from a transfer reaction of one or more oxygen atoms. It is often assumed that the first step of oxygen transfer is the water molecule discharge at one electron, leading to the formation of a hydroxyl radical OH* adsorbed on an active site of the anode surface. The second step is an electrophilic attack of the hydroxyl radical on the organic compound transported from the bulk of the solution. However, on classical anode materials (Au, Pt, C), the oxygen transfer reactions are slow and characterized by low Faradaic yields due to the formation of molecular oxygen. Thus to oxidize an organic compound in an aqueous solution, an anode material with a high oxygen over-potential should be used. Among the materials that meet these criteria are SnO₂, IrO₂, and RuO₂ [7].

Sn, Ru, Ir and Ta-oxides were therefore used to study the feasibility of an electrochemical treatment method.

8.2 Aims

The main aim of this work was first, to study the decomposition of phenol to less harmful products or the total breakdown to carbon dioxide and water at metal oxides electrodes; and secondly, to identify phenol and its broken down components. HPLC was used to follow the decomposition or conversion of phenol and the formation of its by-products.

8.3 Experimental

The experimental procedure for the experiments is outlined in Chapter 3.

8.4 Results and discussion

8.4.1 Phenol determination

The bulk electrolysis experiments were carried out to monitor the performance of the electrode on the degradation of phenol by varying the concentration of the phenol samples. It was therefore easy to point out the effect of concentration on the degradation of phenol as a function of time. The lower the phenol concentration the slower is its degradation. This is because there are competing reactions such as H₂O oxidation taking place, lowering the degradation efficiency of phenol. Decreasing the phenol concentration led to lower energy consumption and therefore less time was required to degrade phenol in solution. Results of HPLC analysis and PDA show that during the oxidation of phenol ($\lambda_{\text{max}} = 254 \text{ nm}$ and 270 nm) some intermediate compounds are being formed: hydroquinone ($\lambda_{\text{max}} = 220 \text{ nm}$ and 290 nm), benzoquinone ($\lambda_{\text{max}} = 270 \text{ nm}$) and catechol ($\lambda_{\text{max}} = 290 \text{ nm}$) (Fig. 8.1). The identification of the indicated intermediate

compounds was achieved by comparing PDA spectra of the model mixture of phenol, hydroquinone, benzoquinone and catechol.

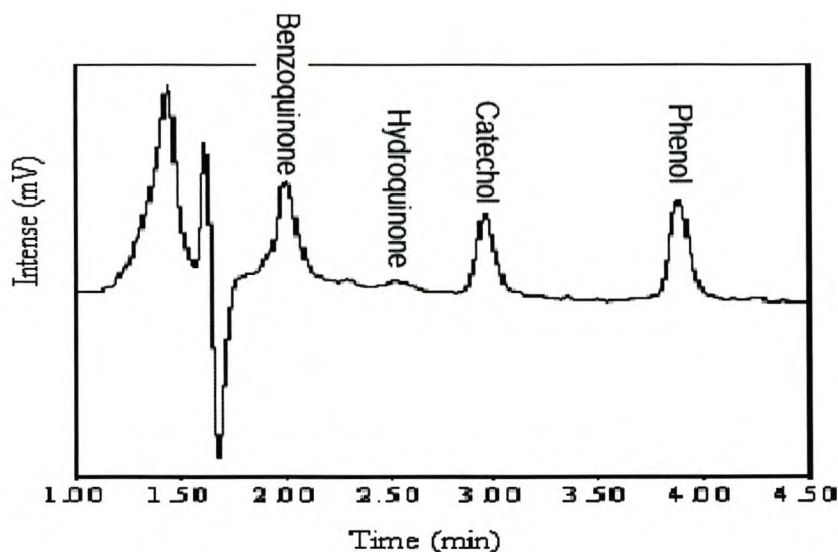


Fig.8.1: HPLC chromatogram showing phenol and its aromatic by-products.

During the HPLC analysis, phenol yielded intermediate ring compounds such as catechol, hydroquinone, p-benzoquinone and acids such as malonic, malic and oxalic. Figures 8.2 to 8.4 show how the aromatic ring intermediate compounds and the organic acids were formed and oxidized.

The Sn/Ru/Ir system showed that as phenol gets degraded with time, the aromatic compounds are formed at 2 hours, with a simultaneous formation of carboxylic acids at lower concentrations compared to aromatic compounds. The concentration of the aromatic compounds increased and reached a maximum after 4 hours. It then decreased with time and the concentration of the carboxylic acids increased and reached a maximum height at 5 hours and then decreased with time.

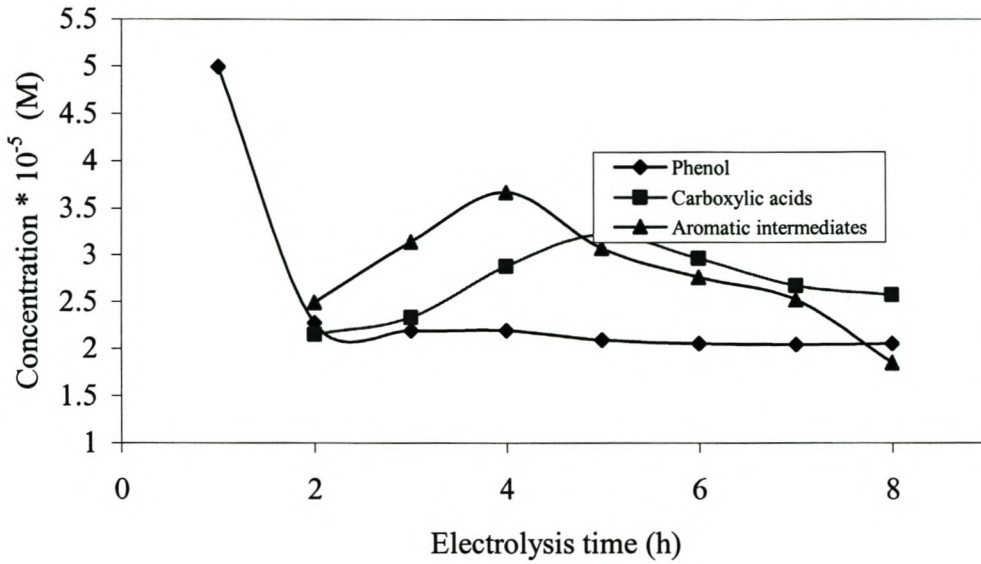


Fig 8.2: The breakdown of phenol into its by-products during electrolysis using Sn/Ru/Ir system as determined by HPLC and PDA.

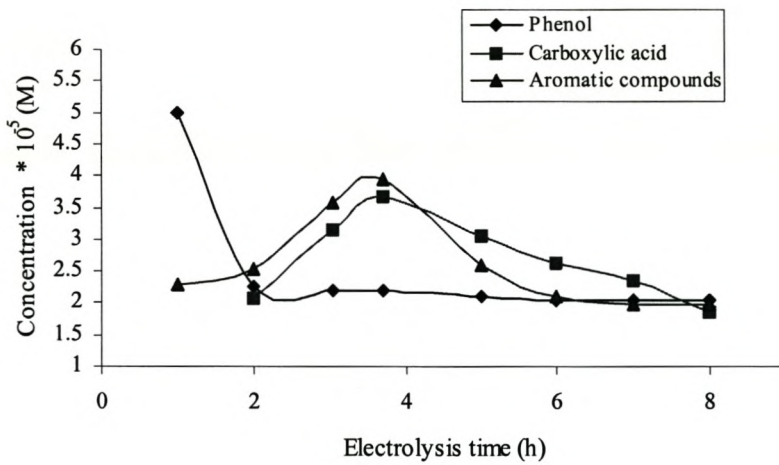


Fig.8.3: The breakdown of phenol into its by-products during electrolysis using Ta/Ir system as determined by HPLC and PDA.

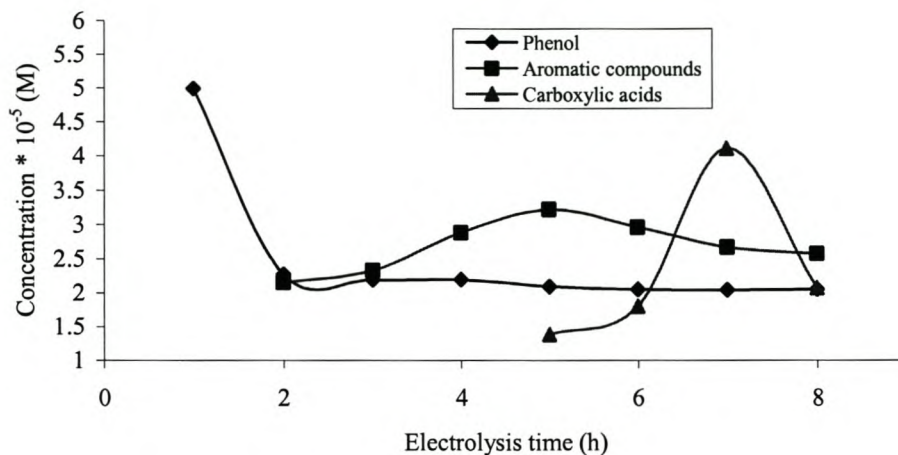


Fig. 8.4: The breakdown of phenol into its by-products during electrolysis using Rh/Ir system as determined by HPLC and PDA.

The Ta/Ir system showed that phenol concentration decreased with time after 1 hour with the simultaneous formation of aromatic compounds at low concentrations. The concentration of the aromatic compounds increased with time with the formation of the carboxylic acids after 2 hours. Both the aromatic compounds and the carboxylic acids reached their maxima at 4 hours, but the concentration of the aromatic compounds decreased drastically afterwards and reached a constant concentration after 6 hours.

The Rh/Ir system showed that as phenol degrades, the aromatic compounds are formed at 2 hours. The concentration of the aromatic compounds increased with time and reached a maximum at 5 hours with a simultaneous formation of carboxylic acids at low

concentrations, about 1.5×10^{-5} M. The concentration of the carboxylic acids increased and reached a maximum at 7 hours then decreased with time.

Figures 8.2 to 8.4 show the degradation curves at the different metal oxide electrodes. Catechol, hydroquinone and benzoquinone amounts increased initially as phenol was oxidized. However, not all (total) phenol concentration was oxidized, about 2.5×10^{-5} M was still left in solution unoxidized. This could be attributed to the adsorption of the phenol by-products on the prepared coatings during the electrolysis process. The aromatic products formed were also subject to oxidation hence their concentration began to decrease with time, as new carboxylic by-products were formed. The concentration of malic acid, malonic and oxalic acid built up slowly and began to decrease after some time. These surfaces demonstrated the capabilities of oxidizing oxalic acid at a potential of 180 mV (see Fig. 8.6). The total organic carbon (TOC) content was however not measured. The redox behaviour of oxalic acid is shown in Fig. 8.6. It shows that oxalic acid is active on the metal oxide surface within the potential range 600 to -600 mV. It is thus not inconceivable that oxalic acid is oxidized once it is formed as a by-product of the phenol oxidation.

8.4.2 *Organic acids determination*

The statutory method for the determination of oxalic acid, malonic acid and malic acid is ion exchange chromatography. The disadvantages associated with using this method are the use of a strongly cation exchanger which has a lower exchange capacity, the long time required for equilibrium to be reached, separation and re-equilibrium. Reverse phase

HPLC has become more popular for analysing certain mixtures of organic acids because of its simplicity, rapidity and stability of the method [8-10].

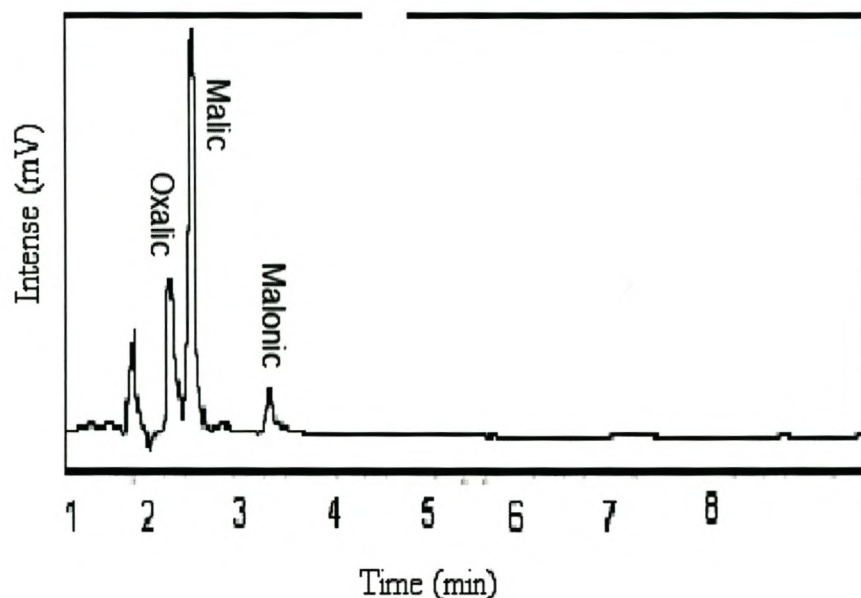


Fig. 8.5: HPLC chromatogram for the carboxylic acids formed as by-products of phenol oxidation.

According to Shui et. al. [11], oxalic acid has a tendency of appearing before the eluent not only because of its lack of hydrophobic groups but also due to its dissociation at pH 2.10 – 2.15. Phosphoric and sulphuric acids are the most commonly used ion-suppressants for the determination of organic acids on the C18 column by the reversed phase HPLC [12].

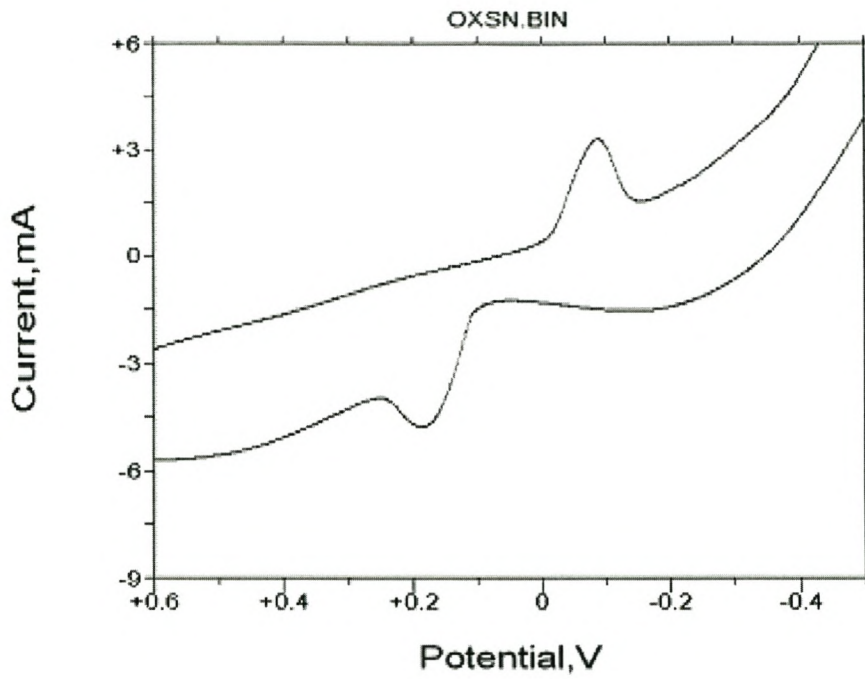


Fig. 8.6: Cyclic voltammogram of oxalic acid at the Ti/SnO₂-RuO₂-IrO₂ electrode.

Fig. 8.5 shows the carboxylic acids as by-products of phenol degradation. The first (unmarked) peak is the injection peak. Results from this investigation showed that using phosphoric acid as an ion suppressant, oxalic acid elutes immediately after the injection peak when the pH is 2.1.

8.5 Proposed pathway of the electrochemical oxidation of phenol

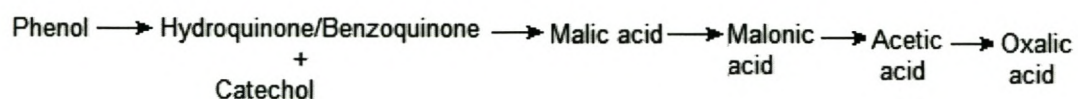
The mechanism of electrochemical oxidation of phenol has been studied by various researchers [1, 3, 5, 13-15]. It is generally known that phenol oxidation starts with one electron transfer, leading to a phenoxy radical reaction. It is further known that some possible reactions of phenoxy radical relate to radical-radial coupling, radical disproportionation, radical elimination or radical oxidation to cation, and then followed by benzoquinone formation [13]. It is possible that intermediate species in aqueous phenol solution are formed before the detection of benzoquinone and are not detected because of their instability.

Most researchers believe that benzoquinone/hydroquinone is an important intermediate, and that the benzoquinone degrades to form various carboxylic acids [16-18]. Different researchers have proposed the formations of various carboxylic acids under various experimental conditions [19-22]. The process of carboxylic acid degradation was more complicated than benzoquinone formation. There are several suggested mechanisms for benzoquinone degradation. If benzoquinone is absorbed onto the electrode surface and gives an electron, an adsorbed OH radical will attack the benzoquinone. When this process repeats itself at the para position, the aromatic ring could be opened, resulting in the formation of malic or maleic acid and other small organic acids, such as oxalic and malonic acids. In this work it has been found that the intermediate malic acid was reduced to malonic, acetic, oxalic and formic acids by anode oxidation.

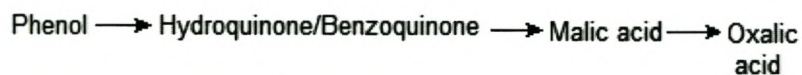
Different reaction pathways for phenol were observed for different metal oxides thin coated films. These pathways are supported by the HPLC studies referred to earlier in the chapter.

1. The Sn /Ru /Ir system

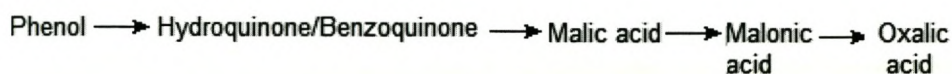
In basic medium



In acidic medium

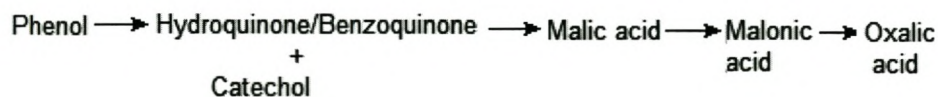


In neutral medium



2. The Ta /Ir system

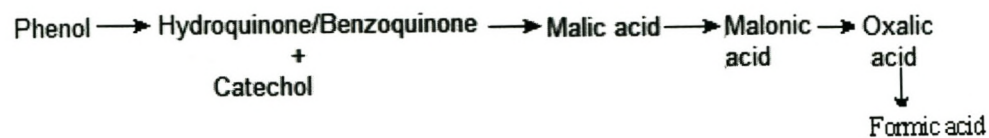
In basic medium



In acidic medium

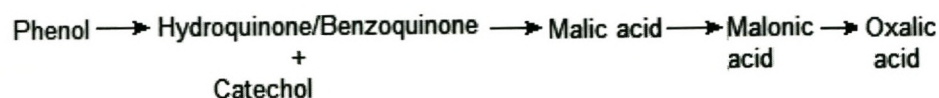


In neutral medium



3. The Rh /Ir system

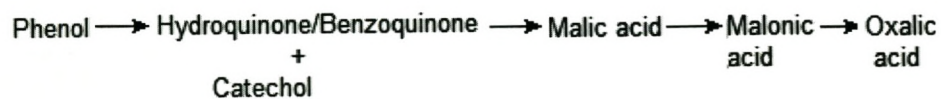
In basic medium



In acidic medium



In neutral medium



8.6 Kinetic studies

The activities of the catalytic systems were evaluated both on the basis of phenol removal efficiency, as well as the rate constants (k) (hour^{-1}) determined in accordance with the kinetic equation of the first order reactions.

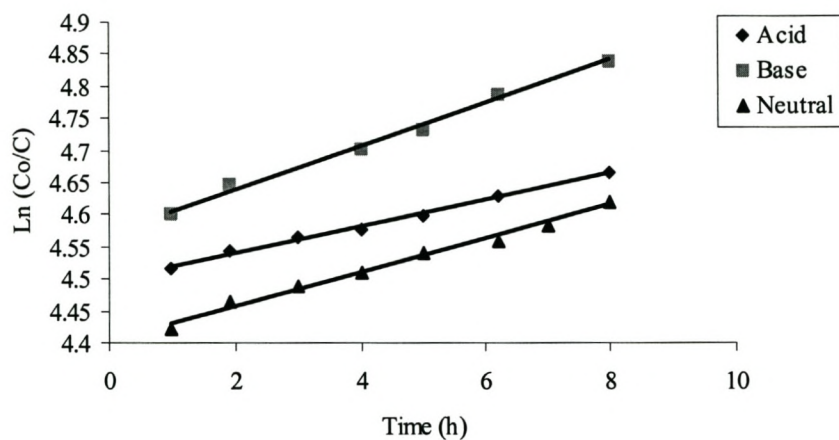


Fig. 8.7: The plot of $\ln(C_0/C)$ as a function of time using different pH media for the Sn/Ru/Ir system, where C is the final and C_0 is the initial concentration.

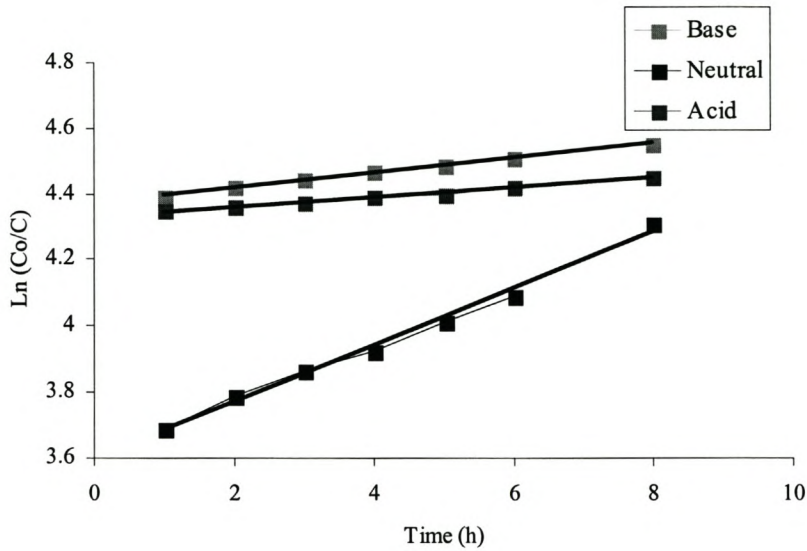


Fig. 8.8: The plot of $\ln(Co/C)$ as a function of time using different pH media for Ta/Ir system, where C is the final and Co is the initial concentration.

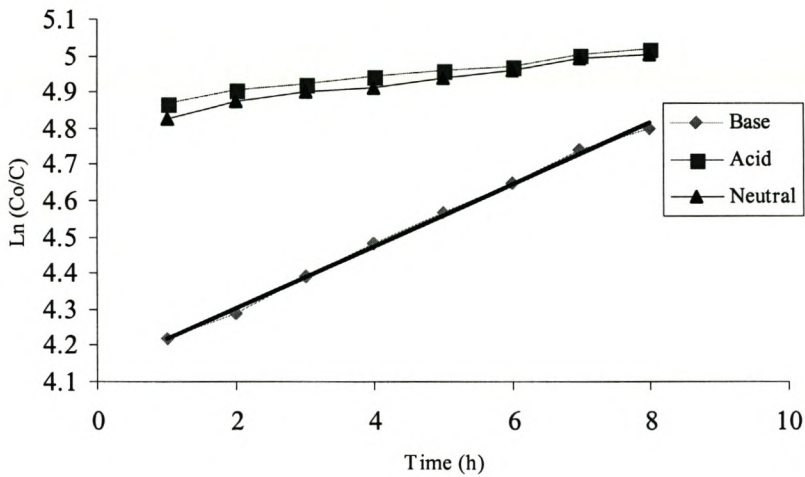


Fig. 8.9: The plot of $\ln(Co/C)$ as a function of time using different pH media for the Rh/Ir system, where C is the final and Co is the initial concentration.

Results of the kinetic investigations to the oxidation of phenol at various metal oxide electrodes are represented in Figures 8.7 to 8.9. The plots of $\ln (C_0/C)$ versus time represent a straight line for the studied samples. On this basis, it may be assumed that the catalytic oxidation of phenol using Ti/Sn-Ru-Ir oxide electrodes proceeds in accordance with the pseudo-first order kinetics with respect to the phenol concentration [18, 23-29]. The slopes of these curves upon linear regression are equal to the first order rate constants and the estimated values of constants are represented in Table 8.1.

Table 8.1: The % of removal/ conversion and rate constants of the phenol oxidation process on the studied films/surfaces at various pHs.

Type of electrodes	pH values	Phenol removal efficiency (%)	Rate constants (k/h)
Sn/Ru/Ir oxide	2	99	0.0101
	7	99	0.0266
	12	99.2	0.0322
Ta/Ir	2	98.8	0.0145
	7	98.6	0.0856
	12	98.9	0.0226
Rh/Ir	2	99.1	0.0202
	7	99.1	0.0244
	12	99.3	0.0870

The influences of pH and the initial phenol concentration on the oxidation of phenol were investigated. Highest rates of oxidations were achieved at pH 12. The transfer of the oxygen atom occurred through the intermediary of hydroxyl radicals adsorbed on the active sites of the anode.

8.7 Conclusions

The metal oxide materials used in this project are good electronic conductors at anode potentials. They also have high surface roughness and some internal porosity, which is equivalent to a large number of electro-active sites; hence, these oxides exhibit a high electro-catalytic activity for the oxygen evolution per geometrical oxide. This is reflected in the results, indicating the performance of these oxides towards phenol removal efficiency.

Electrochemical oxidation using these electrodes was successfully used for treating aqueous phenol solutions. The pathways of the electrochemical oxidation of phenol were proposed for different metal oxide electrodes prepared. An almost total mineralization was obtained. HPLC results showed that phenol yielded intermediate ring compounds such as hydroquinone, benzoquinone, catechol and carboxylic acids such as malic, malonic, acetic, oxalic and formic. Kinetic studies of these metal oxide electrodes were also investigated. The removal or conversion efficiency of the phenol oxidation was found to be more than 90%.

REFERENCES

1. Santos, A., Yustos, P., Quintanilla, A., Rodriguez, S., Garcia-Ochoa, F. *Applied Catalysis B: Environmental*. **2002**, 39, 97.
2. Chen, J., Preston, B., Zimmerman, M. *Journal Chromatography A*. **1997**, 781, 205.
3. Sharifian, H., Kirk, D. W. *Journal of Electrochemical Society*. **1986**, 133:5, 921.
4. Gatrell, M., MacDougall, B. *Journal of Electrochemical Society*. **1998**, 146:9, 3335.
5. Boudenne, J.L., Cerclier, O., Galea, J., Van der Vlist, E. *Applied Catalysis A: General*. **1996**, 143:2, 185.
6. Comninellis C., Vercesi G.P. *Journal of Applied Electrochemistry*. **1991**, 21, 335.
7. Comninellis, C. *Electrochimica Acta*. **1994**, 39:11-12, 1857.
8. Wang, P., Lee, H. *Journal of Chromatography A*. **1997**, 789, 473.
9. Lian, H.Z., Mao, L., Ye, X.L., Miao, J. *Journal of Pharmaceutical and Biomedical Analysis*. **1999**, 19, 621.
10. Fiamegos, Y., Stalikas, C., Pilidis, G., *Analytica Chimica Acta*. **2002**, 467:1-2, 105.
11. Shui, G., Leong, L. *Journal of Chromatography A*. **2002**, 977, 89.

12. Christoskova, S., Stoyanova, M., Georgioeva, M. *Applied Catalysis A: General*. **2001**, 208, 243.
13. Carnizares, P., Diaz, M., Dominquez, J.A., Garcia-Gomez, J., Rodrigo, M.A. *Industrial Eng. Chem. Res.* **2002**, 41, 4187.
14. Azzam, M.O., Tahboub, Y., Altarazi, M. *Trans Ichem. B.* **1999**, 77, 219.
15. Azzam, M.O., Tahboub, Y., Altarazi, M. *Journal of Hazardous Materials, B.* **2000**, 75, 99.
16. Tahar, N.B., Savall, A., *Journal of Applied Electrochemistry.* **1999**, 29, 277.
17. Chailapakul, O., Popa, E., Tai, H., Sarada, B., Tryk, D., Fujishima, A. *Electrochemistry Communications.* **2000**, 2, 422.
18. Chen, J., Eberlein, L., Langford, C., *Journal of photochemistry and photobiology A: Chemistry.* **2002**, 148, 183.
19. Bock, C., MacDougall, B. *Electrochimica Acta.* **2002**, 47, 3361.
20. Korbarti, B., Tanyolac, A. *Water Research.* **2003**, 37, 1505.
21. Castillo, M., Barcelo, D. *Analytica Chimica Acta.* **2001**, 426, 253.
22. Zhao, L., Lee, H. *Journal of Chromatography A.* **2001**, 931, 95.
23. Fiehn, O., Jekel, M. *Journal of Chromatography A.* **1997**, 769, 189.
24. Gomis, D., Palomino, N., Alonso, J. *Analytica Chimica Acta.* **2001**, 426, 111.
25. Fockedey, E., Van Lierde, A. *Water Research.* **2002**, 36, 4169.

26. Bartolome, B., Bengoechea, M., Galvez, M., Perez-Ilzarbe, F., Hernandez, T., Estrella, I., Gomez-Cordoves, C. *Journal of Chromatography A*. **1993**, 119.
27. Bock, C., Mac Dougall, B., *Journal of Electrochemical society*. **1999**, 146:8, 2925.
28. Feng, Y.J., Li, X.Y. *Water Research*. **2003**, 37, 2399.
29. Comninellis, C. *Electrochimica Acta*. **1994**, 39, 11-12, 1857.

9 Conclusions and Recommendations for Further Studies

DSA-type electrodes, made with titanium as base metal and coated with platinum group metal catalysts are well known and widely used as anodes. The focus of this study was to consider the preparation, characterization and electrochemical evaluation of transition metal oxides because of their ability to influence oxidation/reduction reactions. The sol-gel method was used to manufacture mixed-oxide films on metallic substrates in a controlled manner and to eliminate the presence of residual chloride.

The following metal oxide surfaces were prepared: Ti/SnO₂-RuO₂-IrO₂, Ti/Ta₂O₅-IrO₂ and Ti/RhO_x-IrO₂. The characterization of the mixed-metal oxide films developed was performed by means of several complementary analytical methods, both surface and bulk sensitive. These included SEM, AFM, EDX, XRD, RBS, PIXE and electrochemical measurements such as CV, RDE and bulk electrolysis. The most important results can be summarized in conclusion as follows:

- ✓ According to SEM micrographs, all oxide layers exhibited a rough and porous morphology, showing a large active surface area. This was influenced by the calcination temperature. The film thickness corresponding to a given loading

supplied important indirect information on the porosity of the films. All the films prepared had a thickness of about 2 μm .

- ✓ XRD studies have shown that the metal oxides films formed crystalline phases. The dispersed rutile phases found in the IrO_2 - Ta_2O_5 films resembled the solid solutions formed. The high stability of this binary mixture was attributed to the formation of IrO_2 -based solid solution with a tantalum component. The electrochemical active surface area increased when the Ta_2O_5 was added to the pure IrO_2 . Therefore, this type of electrode exhibited high electrocatalysis activity for O_2 evolution.

- ✓ Cyclic voltammetry, as determined by the activity of the catalytic film towards combustion, was indicated by the presence/appearance of the oxidation and reduction peaks of phenol. The cyclic voltammograms showed a quasi-reversible behaviour. The voltammogram for SnO_2 - RuO_2 - IrO_2 film indicated a decomposition potential of 200 mV vs Ag/AgCl.

- ✓ RDE was used to examine the various stages of oxidation of model organic compound phenol and the relative efficiency of different thin films materials to the kinetic steps involved in the conversion of phenol to carboxylic acids. RDE improved mass transfer for this reaction. The dependence of the reaction taking place on the electrode rotation speed was observed. The kinetic studies were

found to proceed in accordance with the pseudo-first order kinetics with respect to phenol concentration.

Bulk electrolysis was used to electro-oxidize phenol at a constant potential of 1500 mV. HPLC was used to monitor the breakdown of phenol. Phenol was found to be electrochemically degraded on the Ti/SnO₂-RuO₂-IrO₂, Ti-Ta₂O₅-IrO₂ and Ti/RhO_x-IrO₂ electrode surfaces at a potential less than 1000 mV. Pathways of electrochemical degradation of phenol were suggested, which included the formation of benzoquinone and further oxidation of benzoquinone to various carboxylic acids.

Shortcomings and Recommendations

Surface experimental techniques that provide information on the atomic structure and composition of surfaces, often present limitations in their ability to directly probe structure-reactivity relationship due to the variety of coordination sites present on the surfaces. The surface structure of bulk transition metal oxides can be envisioned as a collection of clusters of varying sizes and structures. Hence in order to address these concerns the following approaches and techniques are recommended.

- As a complementary approach, the difficulty presented by surface in-homogeneity in understanding surface-reactivity relationships can be overcome by examining the reactivity of gas-phase transition metal oxide clusters; such a study needs to be undertaken.

- Use of a continuous flow-through tubular reactor is recommended to further investigate the stability of the films so that the efficiencies of these oxides in terms of the oxidation of phenols can be examined more fully.

- The developed films need to be tested with actual wastewater samples to evaluate the potential of this technique for the treatment of effluent streams in actual industrial settings.